

INFORMATION TO USERS

This manuscript has been reproduced from the microfilm master. UMI films the text directly from the original or copy submitted. Thus, some thesis and dissertation copies are in typewriter face, while others may be from any type of computer printer.

The quality of this reproduction is dependent upon the quality of the copy submitted. Broken or indistinct print, colored or poor quality illustrations and photographs, print bleedthrough, substandard margins, and improper alignment can adversely affect reproduction.

In the unlikely event that the author did not send UMI a complete manuscript and there are missing pages, these will be noted. Also, if unauthorized copyright material had to be removed, a note will indicate the deletion.

Oversize materials (e.g., maps, drawings, charts) are reproduced by sectioning the original, beginning at the upper left-hand corner and continuing from left to right in equal sections with small overlaps.

Photographs included in the original manuscript have been reproduced xerographically in this copy. Higher quality 6" x 9" black and white photographic prints are available for any photographs or illustrations appearing in this copy for an additional charge. Contact UMI directly to order.

**Bell & Howell Information and Learning
300 North Zeeb Road, Ann Arbor, MI 48106-1346 USA
800-521-0600**

UMI[®]

**THE GEOLOGY, PETROLOGY, GEOCHEMISTRY AND
PLATINUM-GROUP ELEMENT-GOLD-COPPER-NICKEL ORE ASSEMBLAGE
OF THE ROBY ZONE, LAC DES ILES MAFIC-ULTRAMAFIC COMPLEX,
NORTHWESTERN ONTARIO**

BY

MICHAEL JULIEN MICHAUD ©

**A THESIS SUBMITTED IN PARTIAL FULFILLMENT OF THE
REQUIREMENTS FOR THE DEGREE OF MASTER OF SCIENCE**

**LAKEHEAD UNIVERSITY
THUNDER BAY, ONTARIO
CANADA**

NOVEMBER, 1998



**National Library
of Canada**

**Acquisitions and
Bibliographic Services**

**395 Wellington Street
Ottawa ON K1A 0N4
Canada**

**Bibliothèque nationale
du Canada**

**Acquisitions et
services bibliographiques**

**395, rue Wellington
Ottawa ON K1A 0N4
Canada**

Your file Votre référence

Our file Notre référence

The author has granted a non-exclusive licence allowing the National Library of Canada to reproduce, loan, distribute or sell copies of this thesis in microform, paper or electronic formats.

The author retains ownership of the copyright in this thesis. Neither the thesis nor substantial extracts from it may be printed or otherwise reproduced without the author's permission.

L'auteur a accordé une licence non exclusive permettant à la Bibliothèque nationale du Canada de reproduire, prêter, distribuer ou vendre des copies de cette thèse sous la forme de microfiche/film, de reproduction sur papier ou sur format électronique.

L'auteur conserve la propriété du droit d'auteur qui protège cette thèse. Ni la thèse ni des extraits substantiels de celle-ci ne doivent être imprimés ou autrement reproduits sans son autorisation.

0-612-52068-4

Canada

ABSTRACT

The Archean Lac des Iles Complex is a mafic to ultramafic intrusion emplaced into gneissic tonalite. The Lac des Iles Complex is the largest of several mafic to ultramafic intrusions that form a circular outcrop pattern approximately 30 kilometers in diameter. The Lac des Iles Complex is composed of two ultramafic intrusions exposed at Lac des Iles and a gabbroic intrusion located south of the lake. The gabbroic rocks contain the economically significant Roby Zone PGE-Au-Cu-Ni deposit.

The Roby Zone deposit is composed of two texturally- and compositionally-distinct portions. The northern portion of the deposit is composed of a relatively unaltered layered gabbroic sequence consisting of leucogabbro, gabbronorite, gabbro and clinopyroxenite. Field data, including the orientation and type of geologic contacts, indicate that the layers represent an intrusion of magma into a largely crystallized mush. In-situ fractionation was identified within individual layers. The southern portion of the Roby Zone consists of a lithologically and texturally complex unit containing numerous rounded and angular fragments varying in composition from leucogabbroic to pyroxenitic and grain size ranging from medium-grained to pegmatitic. These rocks have experienced pervasive deuteric alteration that modified the original magmatic textures and compositions. Numerous pegmatitic dikes and patches occur throughout the heterolithic gabbro.

PGE-Au-Cu-Ni mineralization within the northern layered sequence often forms net-textured sulphides and represents primary magmatic mineralization. Within the heterolithic gabbro, PGEs occur as primarily sulphides and tellurides. These PGE minerals occur as blebs within pegmatitic pods and as fine-grained inclusions and streaks within secondary silicates

suggesting that deuteric fluids have concentrated and deposited the metals within the heterolithic gabbro. Within the southern portion of the Roby Zone, higher PGE concentrations are associated with altered areas.

The model for the development of the Roby Zone and its attendant PGE-Au-Cu-Ni mineralization consists of 1) fractionation of tholeiitic magma in lower magma chamber and exsolution of immiscible sulphide liquid with associated PGE-Au-Cu-Ni, 2) intrusion of fractionated magma into Roby Zone and subsequent in-situ fractionation, 3) prior to complete solidification of the layers, a volatile-rich gabbroic magma injected the Roby Zone resulting in brecciation of the layered sequence and formation of the heterolithic gabbro composed of rounded and angular fragments within a gabbroic matrix, 4) partially solidified rounded fragments and partial melting of some of the remaining fragments by the gabbroic magma triggered liquid immiscibility, 5) deuteric fluids percolated through the fragmented gabbroic rocks modifying the original magmatic textures and compositions and concentrated and redeposited metals within the heterolithic gabbro. Subsequent regional deformation tilted the Roby Zone to the east and shearing occurred within a portion of the clinopyroxenite. Late-stage local faulting and hydrothermal fluids further modified the original magmatic textures, compositions and PGE-Au-Cu-Ni mineralization.

ACKNOWLEDGEMENTS

I would like to thank Dr. Stephen Kissin, my advisor, for his invaluable advice, editing skills and patience during the course of this study.

I would also like to thank a number of faculty and staff from Lakehead University, including Dr. M.M. Kehlenbeck, who reviewed the structural geology of the Roby Zone, A.D.

Mackenzie of the Lakehead University Instrument Laboratory who provided instruction of the operation of the scanning electron microscope, Anne Hammond and Reino Viitala in sample preparation, who prepared all of the thin sections and polished thin sections during this study.

I would also like to extend thanks to Lac des Iles Mines Ltd who provided the author the time and access to the property and all the necessary data. In addition, Lac des Iles Mines Ltd provided funding for the analytical data.

In addition, I would like to SRK Consulting Ltd., my present employer, particularly Christine Kraatz, for assistance in preparing the figures.

Finally, I would like to thank my wife, Michelle, for her support and patience, even during the birth of our two children, Daniel and Nicole, that without, this task may have never been completed.

TABLE OF CONTENTS

1.0 Introduction	2
1.1 Location and Access	2
1.2 Previous Work	2
1.3 Purpose	5
2.0 Geology	6
2.1 Regional Geology	6
2.2 Geology of the Lac des Iles Complex:	9
2.2.1 Ultramafic Rocks	9
2.2.2 Gabbroic Rocks	11
2.2.3 Structural Geology of the Lac des Iles Complex.....	15
3.0 Geology of the Roby Zone:	16
3.1 Rock Types and Field Relationships.....	19
3.1.1 Leucogabbro (East Gabbro).....	19
3.1.2 Clinopyroxenite	20
3.1.3 Gabbronorite	22
3.1.4 Gabbro.....	25
3.1.5 Coarse-Grained Leucogabbro.....	25
3.1.6 Heterolithic Gabbro	28
3.1.7 Shear Zone	34
3.1.8 Late-Stage Pegmatitic Gabbro Dikes	34
3.1.10 Biotite Dikes	35
3.1.11 Felsic Dikes.....	35
3.1.13 Intrusive Relationships	39

3.2 Alteration and Mineralization	41
3.3 Structural Geology of the Roby Zone.....	43
4.0 Petrography of the Roby Zone	51
4.1 Leucogabbro (East Gabbro)	51
4.2 Clinopyroxenite.....	52
4.3 Gabbronorite	56
4.4 Gabbro	60
4.5 Coarse-Grained Leucogabbro	60
4.6 Heterolithic Gabbro.....	62
4.7 Shear Zone:.....	67
4.8 Late-Stage Pegmatitic Gabbro Dikes.....	69
5.0 Whole Rock Geochemistry.....	71
5.1 Introduction	71
5.2 Major elements.....	71
5.3 Trace Elements	77
5.4 Rare Earth Elements	80
6.0 Silicate Mineral Composition.....	87
6.1 Orthopyroxene.....	87
6.2 Clinopyroxene	92
6.3 Plagioclase	96
6.4 Amphibole	101
6.5 Other Minerals.....	101
7.0 Platinum Group Element Mineralization	104
7.1 Introduction	104
7.2 Sulphide Mineralization.....	105
7.3 Platinum Group Element-Gold-Copper-Nickel Mineralization	105

8.0 Discussion	126
8.1 Introduction	126
8.2 Origin and Relationship of Magma.....	127
8.3 Formation of the Heterolithic Gabbro.....	129
8.4 PGE-Au-Cu-Ni Mineralization in the Roby Zone Deposit.....	133
8.5 Model for the Development of the Roby Zone deposit.....	138
8.6 Summary and Conclusions.....	143
9.0 References	144

APPENDICES

Appendix 1 Sample Location Map

Appendix 2 Whole Rock Analyses

Appendix 3 Mineral Analyses

Appendix 4 Platinum Group Element-Gold Analyses

LIST OF FIGURES

Figure 1.1:	Location Map showing the Lac des Iles Area.....	3
Figure 2.1:	Regional Geology of the Lac des Iles Area (after Sutcliffe, 1986).....	7
Figure 2.2:	Geologic map of the Lac des Iles Complex.....	10
Figure 2.3:	Geologic map of the gabbroic rocks of the Lac des Iles Complex.....	14
Figure 3.1:	Geologic map of the Roby Zone.....	18
Figure 3.2:	Photograph of leucogabbro, or East Gabbro, showing centimeter-scale layering.	19
Figure 3.3:	Photograph of clinopyroxenite in the northern layered sequence showing a dimpled contact.	21
Figure 3.4:	Photograph of clinopyroxenite in the central portion of the Roby Zone containing numerous angular fragments of leucogabbro (East Gabbro).....	21
Figure 3.5:	Photograph of layering within gabbronorite from the northern layered sequence.....	24
Figure 3.6:	Photograph of gabbronorite-leucogabbro contact within the northern layered sequence.....	24
Figure 3.7:	Photograph of a cut surface of gabbro from the northern layered sequence.....	26
Figure 3.8:	Photograph of coarse-grained leucogabbro from the northern layered sequence showing the uniform cumulate texture.....	27
Figure 3.9:	Photograph of coarse-grained leucogabbro.....	27
Figure 3.10:	Photograph showing the textural and compositional variation within the heterolithic gabbro.	31
Figure 3.11:	Photograph showing the textural and compositional variation within the heterolithic gabbro.....	32
Figure 3.12:	Photograph of irregularly shaped gabbronorite section within mafic gabbroic matrix of the heterolithic gabbro.	32
Figure 3.13:	Photograph showing the typical distribution of pegmatoidal gabbroic pods, dikes and layers within the heterolithic gabbro.	33
Figure 3.14:	Photograph showing local layering developed in heterolithic gabbro with the base of the layers defined by large (>5cm.) clinopyroxene	

	grains oriented with their long axes perpendicular to the base of the layer and propagating upwards to the top of the layer.....	33
Figure 3.15:	Photograph of shear zone outcropping in the Roby Zone open pit showing fissile nature of rocks. Photograph taken facing south.....	37
Figure 3.16:	Photograph showing late-stage pegmatitic gabbro dike.....	38
Figure 3.17:	Photograph of late-stage breccia dikes.....	38
Figure 3.18:	Contoured stereonet plot of poles to planar elements.....	45
Figure 3.19:	Contoured stereonet plot of the poles to planar elements within the shear zone.....	46
Figure 3.20:	Photograph showing typical C and S fabric developed in rocks from the shear zone.....	47
Figure 3.21:	Schematic illustration of the development of S and C fabric in ductile shear zones.....	47
Figure 3.22:	Schematic diagram of asymmetric augen structures.....	48
Figure 3.23:	Photograph showing the east-northeast striking faults that have sinistrally offset the clinopyroxenite-leucogabbro contact.....	50
Figure 4.1:	Photomicrograph of clinopyroxenite from the northern layered sequence showing pseudomorphic amphibole, predominantly actinolite, on clinopyroxene cumulate grains.....	54
Figure 4.2:	Photomicrograph of clinopyroxenite from the southern portion of the Roby Zone.....	54
Figure 4.3:	Photomicrograph of clinopyroxenite showing sulphide mineralization.....	55
Figure 4.4:	Photomicrograph of gabbronorite from the northern layered sequence.....	58
Figure 4.5:	Photomicrograph of gabbronorite from the northern layered sequence.....	58
Figure 4.6:	Photomicrograph of fractured orthopyroxene grain.....	59
Figure 4.7:	Photomicrograph of gabbronorite from the northern layered sequence showing the distribution of net-textured sulphides.....	59
Figure 4.8:	Photomicrograph of leucogabbro from within heterolithic gabbro showing the strong pervasive amphibole alteration of clinopyroxene and saussurization of plagioclase feldspar.....	61

Figure 4.9:	Photomicrograph of heterolithic gabbro showing strong pervasive amphibole and chlorite alteration and actinolite pseudomorphing clinopyroxene.....	64
Figure 4.10:	Photograph showing pyrrhotite, pentlandite and chalcopyrite mineralization within the gabbroic matrix of heterolithic gabbro.....	64
Figure 4.11:	Photograph of pyrrhotite, pentlandite, chalcopyrite and pyrite mineralization within pegmatitic gabbro	65
Figure 4.12:	Photomicrograph of sulphide mineralization along a narrow fault within the heterolithic gabbro.....	65
Figure 4.13:	SEM image showing sulphide mineralization within heterolithic gabbro.....	66
Figure 4.14:	Photomicrograph of the shear zone showing the high degree of alteration	68
Figure 4.15:	Photomicrograph of shear zone showing pyrrhotite, pentlandite, chalcopyrite and pyrite mineralization	68
Figure 4.16:	Photograph of cut sample surface of pegmatitic gabbro dike.....	70
Figure 4.17:	Photomicrograph of pegmatitic gabbro dike.....	70
Figure 5.1:	Whole rock major elements in weight percent oxides plotted on AFM diagram.....	75
Figure 5.2:	Whole rock major elements in weight percent oxides plots of MgO versus MnO, FeOT, Al ₂ O ₃ , CaO, TiO ₂ , Na ₂ O and K ₂ O.....	76
Figure 5.3:	Chondrite normalized rare earth element profiles	84
Figure 5.4:	Chondrite normalized rare earth element profiles	85
Figure 5.5:	Chondrite normalized rare earth element profiles	86
Figure 6.1:	Pyroxene triangular plot showing the compositional range of orthopyroxenes from several of the rock types comprising the Roby Zone.....	91
Figure 6.2:	Pyroxene triangular plot showing the compositional range of clinopyroxenes from several of the rock types comprising the Roby Zone.....	95
Figure 6.3:	Feldspar triangular plot showing the compositional range of feldspars from the majority of rock types comprising the Roby Zone.....	100

Figure 6.4:	Amphibole triangular plot showing the compositional range of amphiboles from various rock types comprising the Roby Zone.....	103
Figure 7.1:	Plot showing the range of values and average concentration for Pt, Pd, Cu, Ni, and Au for each of the rock types comprising the Roby Zone.....	107
Figure 7.2:	Log-log plot of Pd versus Pt for each of the rock types comprising the Roby Zone.....	112
Figure 7.3:	Normal-log plot of Pd/Pt versus Pd for each of the rock types comprising the Roby Zone.....	113
Figure 7.4:	Log-log plots of a) Pd/Ir versus Pd, b) Pt/Ir versus Pt, and c) Au/Ir versus Au.....	114
Figure 7.5:	Log-log plots a) and b) showing correlation between Pt, Pd and chalcophile elements for each of the rock types comprising the Roby Zone.....	117
Figure 7.5:	Log-log plots c) and d) showing correlation between Pt, Pd and chalcophile elements for each of the rock types comprising the Roby Zone.....	118
Figure 7.5:	Log-log plots e) and f) showing correlation between Pt, Pd and chalcophile elements for each of the rock types comprising the Roby Zone.....	119
Figure 7.5:	Log-log plots g) and h) showing correlation between Pt, Pd and chalcophile elements for each of the rock types comprising the Roby Zone.....	120
Figure 7.6:	Plot of Cu/(Cu+Ni) versus Pt/(Pt+Pd) for rocks of the Roby Zone.....	121
Figure 7.7:	Comparison of average PGE and Au values for each of the rock types comprising the Roby Zone. The data has been recalculated to 100% sulphide, then chondrite-normalized based on methodology of Naldrett (1981).....	124
Figure 7.8:	Comparison of average PGE and Au values for the Roby Zone and other PGE deposits.....	125
Figure 8.1:	Schematic cross-section showing the different stages of development of the formation of the Roby Zone PGE mineralization.....	142

LIST OF TABLES

Table 6.1:	Representative Compositions of Orthopyroxenes from the Roby Zone	90
Table 6.2:	Representative Compositions of Clinopyroxenes from the Roby Zone.	94
Table 6.3:	Representative Compositions of Feldspars from the Roby Zone	99
Table 6.4:	Representative Compositions of Amphiboles from the Roby Zone	102
Table 7.1:	Correlation coefficients for Pt, Pd, Au, chalcophile elements and sulphur	111

**THE GEOLOGY, PETROLOGY, GEOCHEMISTRY AND
PLATINUM-GROUP ELEMENT-GOLD-COPPER NICKEL MINERALIZATION
OF THE ROBY ZONE, LAC DES ILES MAFIC-ULTRAMAFIC COMPLEX,
NORTHWESTERN ONTARIO**

1.0 Introduction

The Archean Lac des Iles Complex is a mafic to ultramafic intrusive complex surrounded by granites and gneisses of the Wabigoon subprovince of the Superior geologic province. The Lac des Iles Complex is host to the economically significant platinum group element-gold-copper-nickel mineralization of the Roby Zone deposit. The Roby Zone deposit is estimated to contain 8.9 million tons grading 5.8 g/t palladium, 0.34 g/t platinum, 0.30 g/t gold, 0.1% copper and 0.1% nickel (North American Palladium Ltd., 1998).

1.1 Location and Access

The Lac des Iles Complex is exposed at and south of Lac des Iles, located approximately 80 kilometers due north of the City of Thunder Bay, Ontario (Figure 1.1). The complex occurs at latitude 49°10'N and longitude 89°37'W, National Topographic Series Map 52 H/4 NE. The Lac des Iles Complex is accessible from the City of Thunder Bay by travelling 94 kilometers north along Provincial Highway 527 and proceeding west 16 kilometers along a gravel roadway.

1.2 Previous Work

The summary of previous work outlined below was obtained from a number of earlier sources, including Sutcliffe (1986), North American Palladium Ltd. (1997), and Sweeny (1989). The Lac des Iles Complex was first mapped by F. Joliffe of the Geological Survey of Canada during reconnaissance mapping in 1933. In 1963, E.G. Pye of the Ontario Department of Mines completed detailed geologic mapping of the Lac des Iles area at 1:31,680 scale. Exploration interest in the area began in the late 1950s, following airborne geophysical surveys that identified several magnetic anomalies associated with the Lac des Iles Complex. Copper and nickel mineralization was discovered south of Lac des Iles by prospectors G. Moore and W. Baker in 1963. Mining claims over the areas of anomalous mineralization were acquired by Gunnex Limited and subsequently optioned to Anaconda American Brass Limited. Exploration efforts between 1963 and 1966 resulted in the discovery of eight zones containing significant platinum group element mineralization.

LAC DES ILES

Thunder Bay District, Ontario

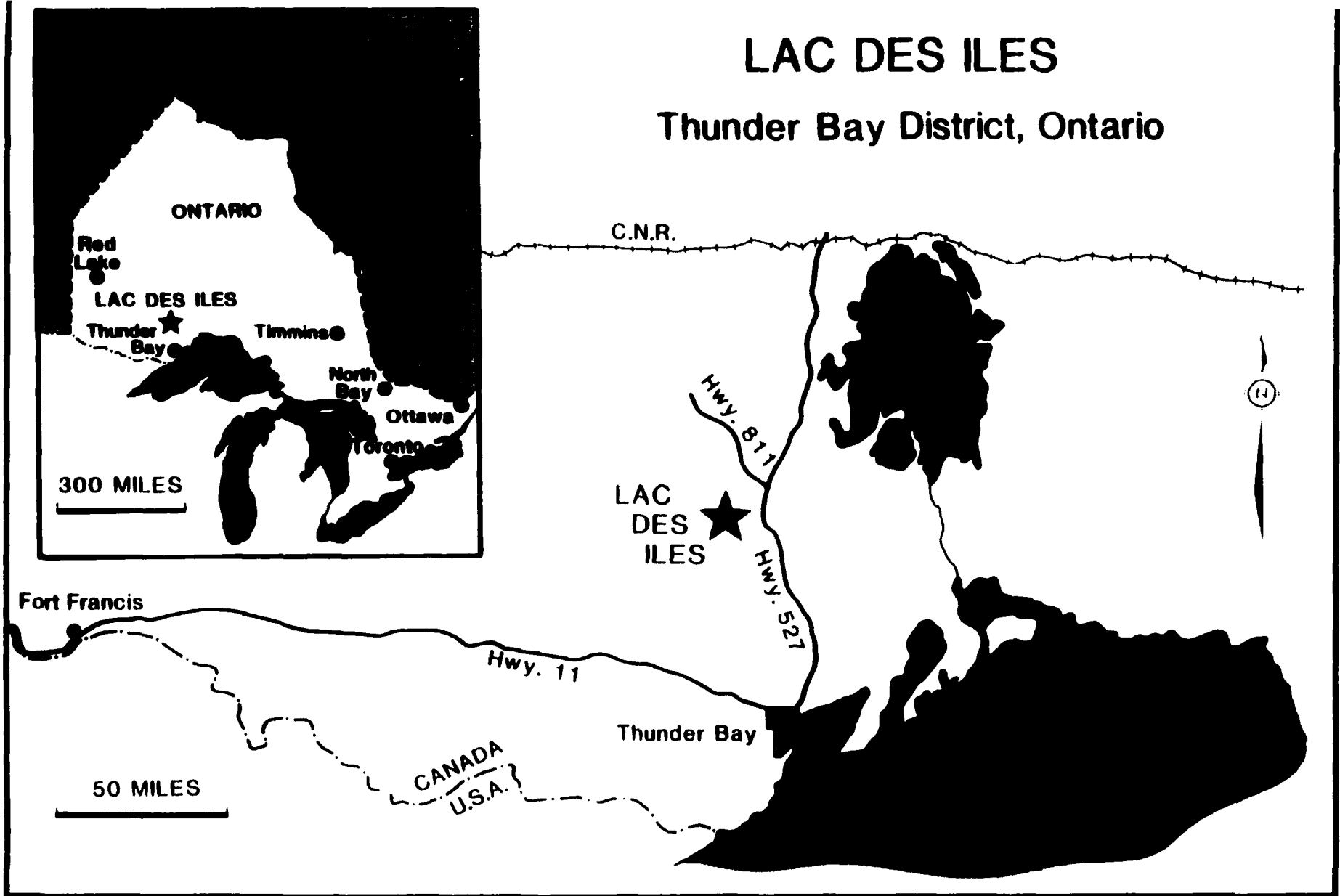


Figure 1.1 Location Map showing Lac des Iles Area.

The mining claims were eventually acquired by Boston Bay Mines Limited in 1974 and subsequently optioned to Texasgulf Canada in 1975. Extensive exploration in 1975 and 1976 resulted in the identification and delineation of the economically significant platinum group element mineralization of the Roby Zone.

In 1986, Madeleine Mines Ltd acquired the mining claims, and after further delineation of the Roby Zone mineralization, constructed a concentrator mill and commenced production in 1990. Production continued for only several months before being halted. Lac des Iles Mines Limited acquired control of the property in 1991, and on November 20, 1993, the Lac des Iles Mine Property was brought into commercial production at a rate of 2,000 tons/day.

Subsequent to 1985, the Ontario Geological Survey has remapped the Lac des Iles Complex on several occasions in an attempt to understand better mafic to ultramafic intrusions and their association with platinum group element mineralization. Previous research was completed by Sutcliffe and Sweeny (1985, 1986), Macdonald (1985, 1986), and Macdonald and Lawson (1987). Additional research studies were undertaken by Fortescue and Webb (1986), Gupta et al. (1986), Palmer (1987), Brugmann and Naldrett (1987, 1990), and Sweeny and Edgar (1990, 1991). Three M.Sc. theses have been completed on the southern gabbroic rocks of the Lac des Iles Complex, including: Guarnera (1967), Dunning (1979), and Sweeny (1989).

1.3 Purpose

The primary objectives of this study are: 1) to map and identify the various intrusive phases comprising the Roby Zone deposit on the basis of their mineralogy, petrography and macroscopic textures; 2) to classify the various intrusive phases and to identify any elemental variation based on mineral composition, whole rock geochemistry and rare earth element abundance; 3) to identify the magmatic processes involved by examining the primary silicates and their relationships between intrusive phases; 4) to identify alteration assemblages and determine the effect of secondary fluids and alteration and their association to the platinum group element mineralization; 5) to identify the process of formation of the heterolithic gabbro and its relationship to the encompassing intrusive phases and 6) to identify the various processes of mineralization based on the relative and absolute concentrations of the platinum group elements, gold, copper and nickel within the intrusive phases.

2.0 Geology

2.1 Regional Geology

The Lac des Iles Complex forms part of an east-northeast trending linear zone of mafic plutons extending from Atikokan to Lake Nipigon (Sutcliffe, 1986). The Lac des Iles Complex occurs within Archean granitoid rocks, consisting of predominantly gneissic tonalites, medium-grained hornblende diorite and quartz diorite (Figure 2.1). The rocks of the Lac des Iles Complex have U-Pb ages of 2,695 to 2,700 Ma (Davis and Edwards, 1986); the encompassing gneissic tonalites have U-Pb ages of 2,716 to 3,000 Ma B.P. (Davis and Jackson, 1988; Davis and Sutcliffe, 1985).

The Lac des Iles Complex is the largest of a series of mafic to ultramafic intrusions confined to a circular outcrop pattern approximately 30 kilometers in diameter (Sutcliffe, 1986). Two younger granitoid phases occur within the circular outcrop pattern, including a foliated biotite-hornblende tonalite and a foliated to massive pluton of granodioritic to granitic composition (Sutcliffe, 1986).

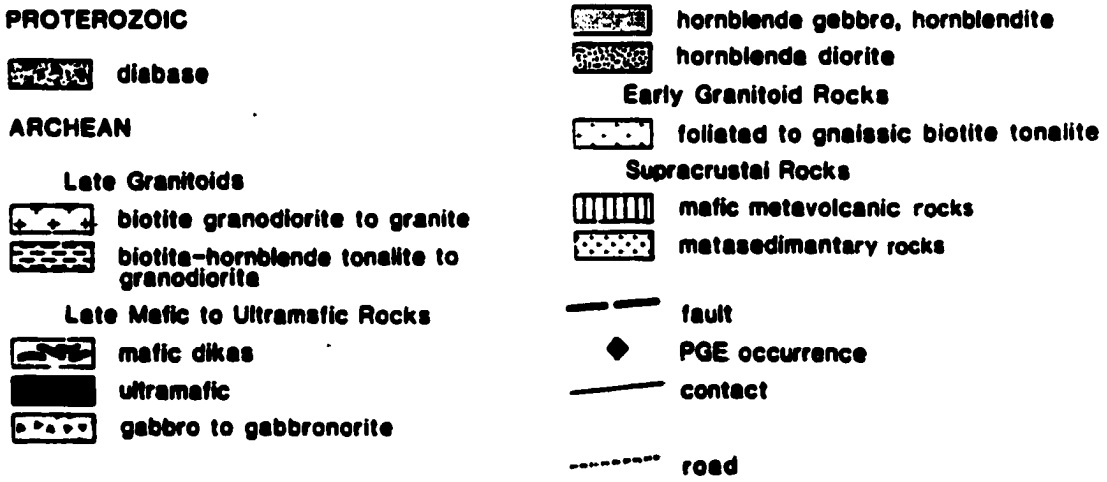
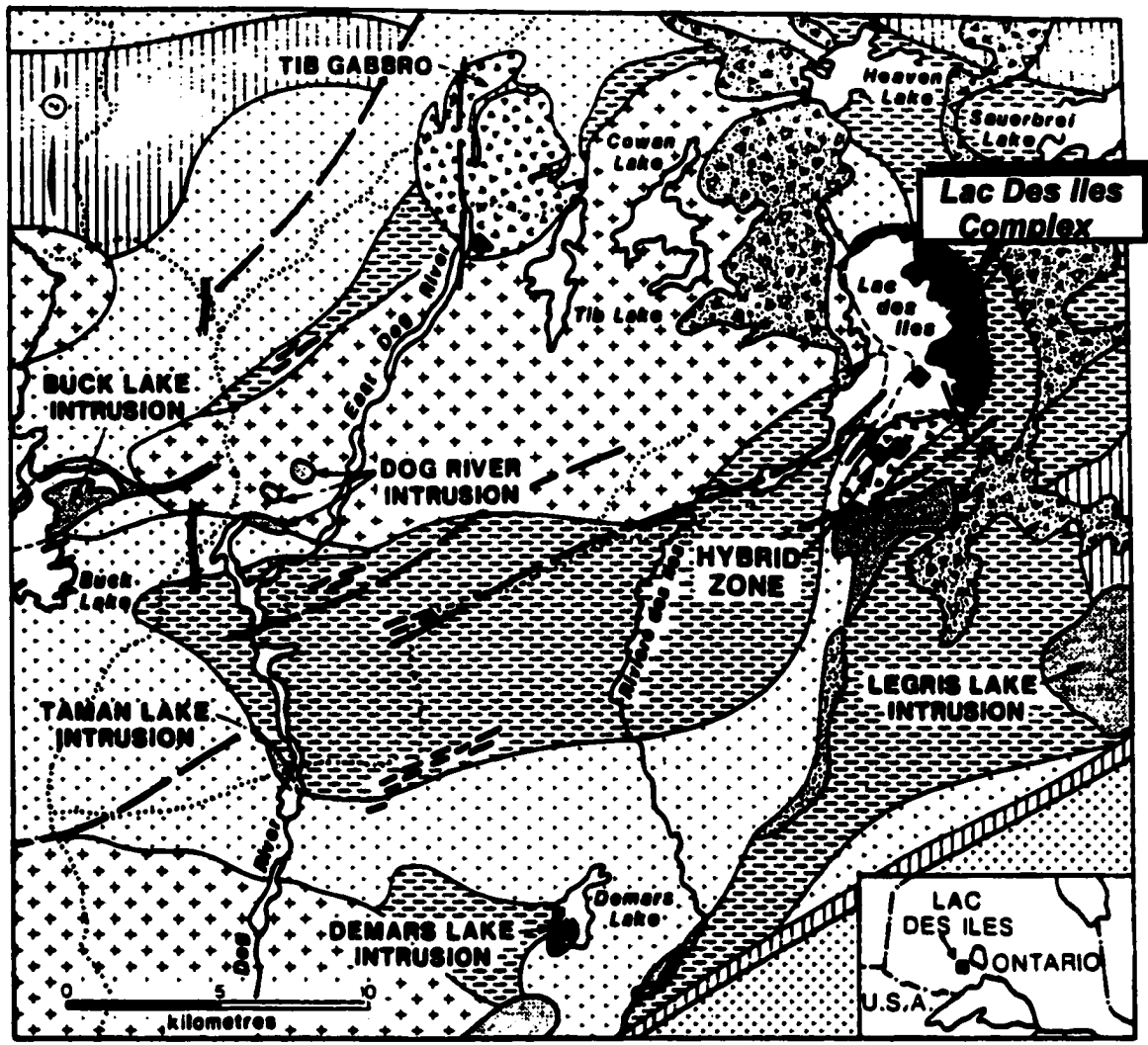


Figure 2.1 Regional Geology of the Lac des Iles Area (after Sutcliffe, 1986)

Other mafic to ultramafic intrusions in the Lac des Iles area include the Tib Lake and Demars Lake Intrusions. The Tib Lake Intrusion is characterized by unaltered rocks possessing well-developed igneous layering. The predominant phases include gabbro, hornblende gabbro, orthopyroxenite and gabbro. Ultramafic cumulates occur as conformable layers that are traceable for tens of meters. Pegmatitic gabbro layers occur as conformable layers but more often as discordant dykes. Platinum group element mineralization is associated with pegmatitic dykes and orthopyroxenite phases (Smith and Sutcliffe, 1986).

The Demars Lake Intrusion is a small elliptical plug consisting of an ultramafic core of websterite with a marginal zone of hornblende gabbro and hornblende pyroxenite (Sutcliffe, 1986). Platinum group element mineralization occurs within the websterite core (Kaye, 1969; Sutcliffe, 1986). Both the Tib Lake and Demars lake intrusions are interpreted as being contemporaneous with the magmatism of the Lac des Iles Complex (Smith and Sutcliffe, 1986). Additional mafic-ultramafic rocks identified in the region are near Wakinoo Lake, Taman Lake, Buck Lake and on the Dog River. Rocks within these regions range in composition from hornblende gabbro to hornblende clinopyroxenite and commonly contain minor sulphide mineralization (Kaye, 1969; Sutcliffe, 1986).

An east-northeast trending volcano-sedimentary greenstone belt is located to the south and east of the Lac des Iles Complex. This belt appears to parallel the boundary between the Wabigoon and Quetico geologic subprovinces. Deformation identified in the greenstone belt consists of folding, faulting and regional metamorphism (Pye, 1968). All of the aforementioned Archean rocks have been intruded by Keweenawan diabase dikes and sills.

2.2 Geology of the Lac des Iles Complex:

The extent and shape of the Lac des Iles complex was originally determined from geologic mapping by Pye (1968), who divided the complex into an ultramafic portion and a gabbroic portion (Figure 2.2). The ultramafic portion was further subdivided into the Northern and Southern Centers, respectively. Geologic mapping of the Lac des Iles Complex was completed by Watkinson and Dunning (1979), Sutcliffe and Sweeny (1986), Macdonald (1985, 1986), and Linhardt and Bues (1987). Gravity studies indicate that the thickest part of the complex is located within the ultramafic rocks (Gupta and Sutcliffe, 1986).

2.2.1 Ultramafic Rocks

The ultramafic rocks of the Lac des Iles Complex consist of two coalescing centers that have been defined on the basis of the distribution of ultramafic lithologies and the attitudes of the igneous layering. The northern ultramafic center is nearly circular in plan with a diameter of approximately four kilometers. The intrusive phases form discontinuous, lensoid- to dish-shaped bodies of various thickness and extent (Linhardt and Bues, 1987). The primary lithologies include dunite, wehrlite, olivine clinopyroxenite, westerite and gabbronorite. The concentric layers have been disrupted by several late-stage magmatic injections, manifested by serpentinite dikes, breccias and local unconformities.

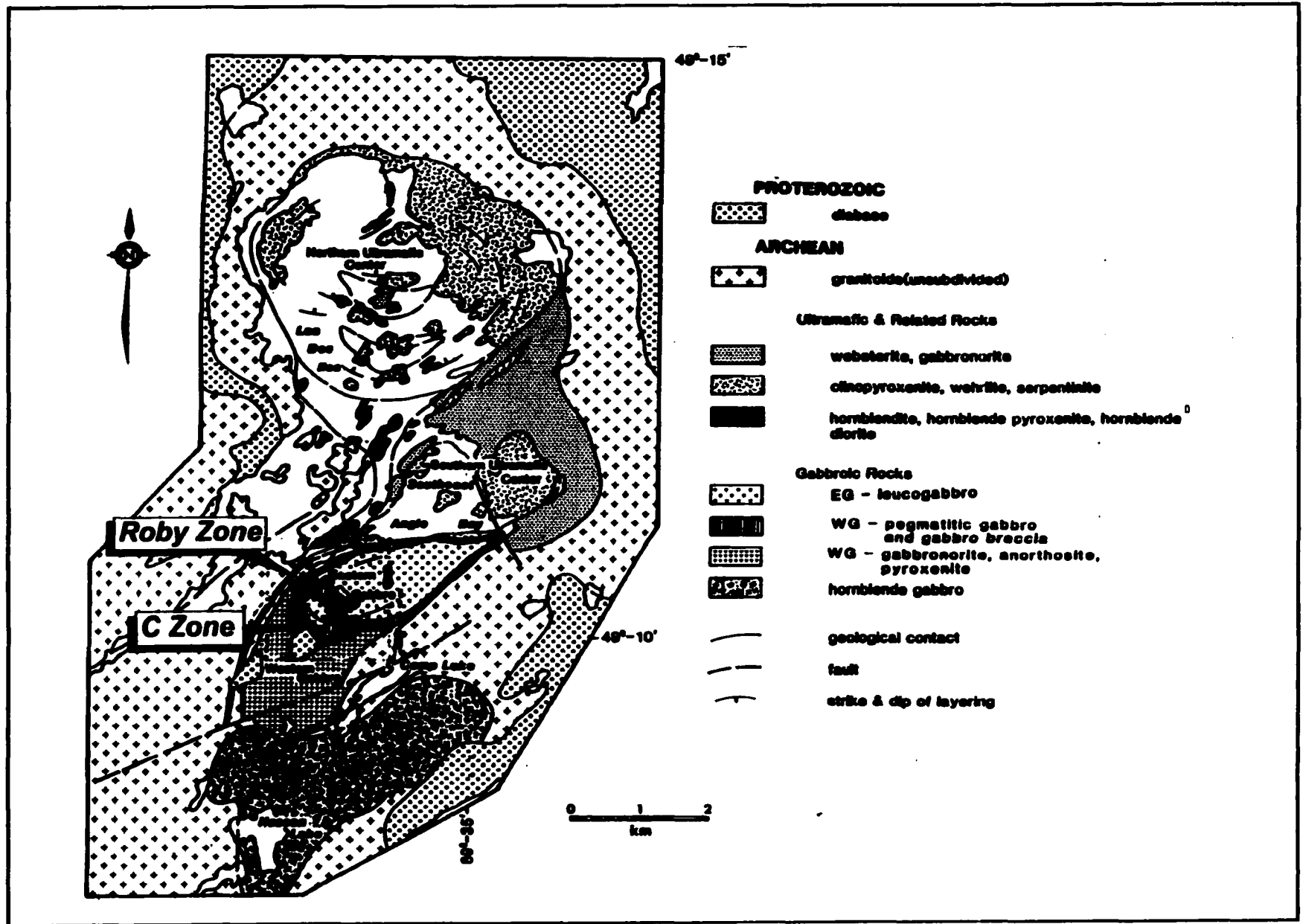


Figure 2.2 Geology of Lac des Iles Complex showing the distribution of ultramafic and gabbroic rocks (after Sutcliffe and Sweeny, 1985)

The southern ultramafic center is elliptical in plan, with an irregularly shaped wehrlite core centered on Southeast Angle Bay of Lac des Iles. The wehrlite core is surrounded by websterite, except along the eastern margin where websterite grades into gabbronorite. The southern center is composed predominantly of massive rocks that lack well-defined igneous layering (Sutcliffe and Sweeny, 1986).

The ultramafic rocks of the Lac des Iles Complex are generally unaltered; however, local uraltic alteration of clinopyroxenes is present. The alteration is concentrated primarily along fractures, although, pervasive alteration has been observed across entire outcrops (Sutcliffe and Sweeny, 1986). The greatest concentration of platinum group elements is associated with websterite and gabbronorite phases that typically contain 2 vol.% sulphides. The sulphide mineralization, which consists primarily of pyrrhotite, pyrite, chalcopyrite and pentlandite, occurs as fine-grained disseminations, occasionally forming a net-texture (Linhardt and Bues, 1987).

2.2.2 Gabbroic Rocks

The majority of the gabbroic rocks of the Lac des Iles Complex are located south of Lac des Iles and form an elliptical shape elongated north-south (Figure 2.2). The gabbroic rocks of the complex consist of a variety of intrusive phases including gabbro, norite, gabbronorite, leucogabbro and a lesser amount of ultramafic rocks. The gabbroic rocks of the complex are host to several zones of significant platinum group element mineralization, including the Roby Zone.

Dunning (1979) subdivided the gabbroic rocks into two major units, the East Gabbro and the West Gabbro. As defined by Dunning (1979), the West Gabbro is composed of interlayered gabbroic, noritic, pyroxenitic and anorthositic rocks with an abundance of pegmatitic phases. The East Gabbro is composed of oxide-rich gabbroic and noritic rocks. The West Gabbro contains a greater amount of gabbro-noritic and noritic rocks, and typically contains less magnetite and more calcium-rich plagioclase feldspar and magnesium-rich orthopyroxene than the East Gabbro. This distinction is significant because the Roby Zone is located near the contact of these two intrusive phases. Many of the layers identified by Dunning are interpreted to be separate intrusive phases (Macdonald, 1985; Sutcliffe and Sweeny, 1986; Sweeny and Edgar, 1987).

Geologic mapping by Sutcliffe and Sweeny (1986) identified leucogabbro as the dominant rock type comprising the East Gabbro. Leucogabbro commonly exhibits an igneous lamination and a weakly developed modal layering. The leucogabbro is pervasively altered, commonly obscuring the primary igneous assemblages. Remapping of the West Gabbro by Sutcliffe and Sweeny (1985) identified numerous intrusive phases of gabbro and gabbro-norite. A hybrid zone, consisting of pegmatitic gabbro, gabbro breccia, gabbro-norite and clinopyroxenite, was observed forming an arc-shaped zone of variable width west of and adjacent to the East Gabbro. Pegmatitic gabbro phases within the hybrid zone occur primarily as inclusions, pegmatoidal segregations and as discordant pegmatite dikes (Sutcliffe and Sweeny, 1986). The Roby Zone and a number of other zones containing significant platinum group element mineralization, are located near the contact between the hybrid zone and the East Gabbro (Figure 2.3).

Sheets and minor discordant dikes of clinopyroxenite and gabbronorite intrude the East Gabbro and West Gabbro. The sheets and dikes contain cumulus orthopyroxene and clinopyroxene and vary from intensely altered to unaltered (Sutcliffe and Sweeny, 1986). Late-stage fine-grained gabbroic dikes intrude the gabbroic rocks locally resulting in an intrusive breccia. The dikes contain numerous angular fragments of gabbroic and tonalitic rocks. Late-stage leucocratic tonalite dikes and veins also cross-cut the gabbroic rocks of the Roby Zone (Sutcliffe and Sweeny, 1986).

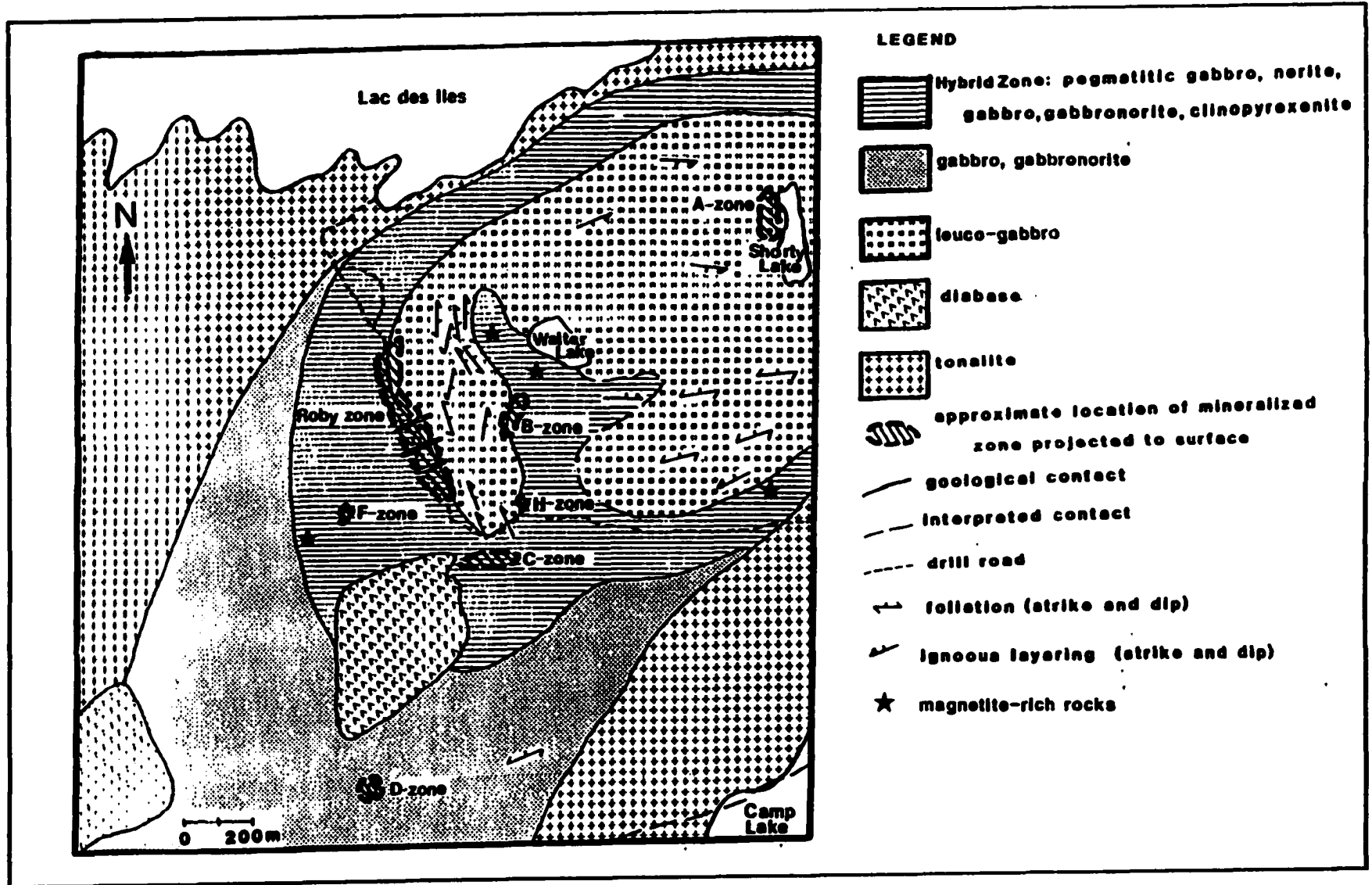


Figure 2.3 Geologic map of the gabbroic portion of the Lac des Iles Complex showing the extent of the hybrid zone and the location of the Roby Zone (after Sutcliffe and Sweeny, 1986). Additional zones containing significant platinum group element mineralization include the A, B, C, D, F, and H zones of previous workers (Pye, 1968; Dunning, 1979).

2.2.3 Structural Geology of the Lac des Iles Complex

The rocks of the Lac des Iles Complex are transected by a number of major fault zones expressed as topographic lineaments, well-developed foliation, mylonitization and fracturing. The fault zones, which are traceable for a distance of over several kilometers, are east-northeast and north-south striking and vertically dipping. Geologic contacts commonly display sinistral displacement across the faults with offsets ranging from several centimeters up to 350 meters (Sweeney, 1989).

The strike of the intrusive layering in the gabbroic rocks parallels the perimeter contact of the Lac des Iles Complex with the granitoids. The layers are steeply dipping towards the center of the intrusion. A weakly developed mineral foliation, defined by an alignment of mineral grains, parallels the contact of the complex (Sutcliffe, 1986).

3.0 Geology of the Roby Zone:

The Roby Zone, which is located near the contact between the West Gabbro and the East Gabbro, extends approximately 600 meters north-northwesterly and is up to 350 meters wide. As part of this study, the bedrock surface was stripped of any overlying overburden and washed with a high-pressure water system. A grid was established over the Roby Zone to provide accurate locations for geologic mapping of the various rock types, textures and geological structures. In addition, drill core from several drill holes was examined to compare with the bedrock mapping. Over 100 thin sections were made from outcrop samples and drill core samples. The majority of rocks comprising the Roby Zone are crystal cumulates and were classified using the IUGS system for plutonic rocks. The classification is based on the relative proportions of plagioclase, orthopyroxene and clinopyroxene, regardless of whether these minerals occurred as cumulus or intercumulus phases.

Detailed geologic mapping of the Roby Zone identified two lithologically and texturally different portions of the deposit (Figure 3.1; Map at back cover). The northern portion is comprised of a layered sequence, including coarse-grained leucogabbro, gabbro, clinopyroxenite and gabbronorite, with a minor amount of pegmatitic gabbroic segregations, patches and discordant dikes. The layers and pods strike north-south and dip 70 degrees to the east. The southern portion of the Roby Zone is composed mostly of a lithologically and texturally complex unit, termed the heterolithic gabbro. The heterolithic gabbro consists of irregularly shaped and sized masses ranging in composition from leucogabbroic to clinopyroxenitic with grain size ranging from medium-grained to pegmatitic. The degree of textural and compositional variation in the heterolithic gabbro gradually decreases to the south and the west.

The northern and southern portions of the Roby Zone are separated by a north-northwest trending, vertically-dipping, 15-meter wide shear zone, defined by a well-developed mylonitic foliation. The shear zone consists of a well-foliated talc-actinolite-chlorite schist. A thin wedge of non-foliated, cumulate clinopyroxenite, up to several meters wide is preserved between the shear zone and the East Gabbro. The north-northeast trending geologic contact between clinopyroxenite and the East Gabbro observed in the northern layered sequence is maintained in the southern portion of the Roby Zone, where it trends north-northwest.

Several east-west trending, vertically dipping pegmatitic gabbro dikes up to several meters wide cross-cut all of the aforementioned intrusive phases of the Roby Zone, with the exception of the East Gabbro. The pegmatitic gabbro dikes transect the western contact of the clinopyroxenite, however, have not been observed in the leucogabbroic rocks east of the clinopyroxenite. Numerous, small-scale, parallel, east-northeast trending sinistral and dextral faults have offset the lithologic contacts up to several meters.

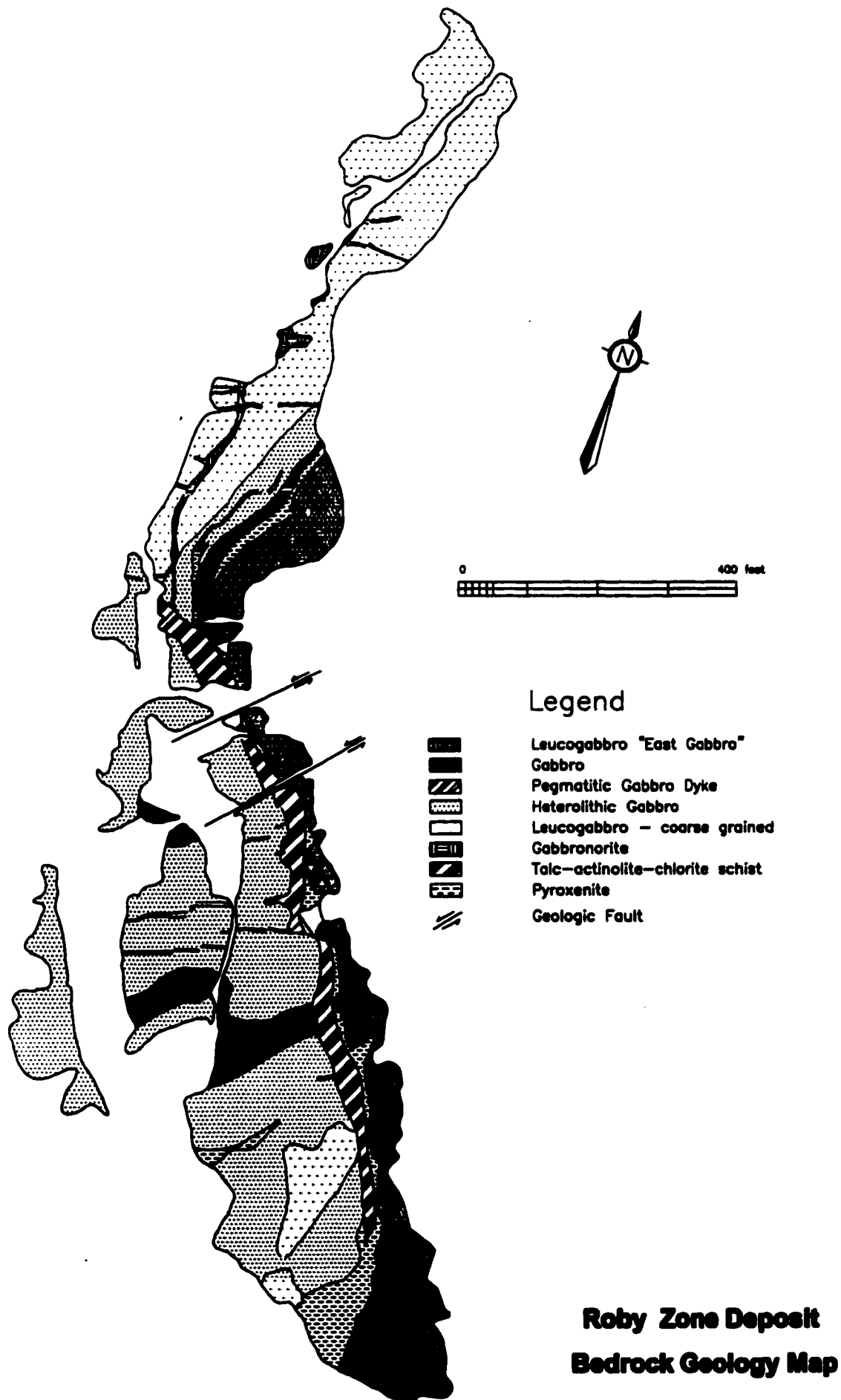


Figure 3.1 Geologic map of the Roby Zone

Reproduced with permission of the copyright owner. Further reproduction prohibited without permission.

3.1 Rock Types and Field Relationships

3.1.1 Leucogabbro (East Gabbro)

A medium grained, relatively uniform leucogabbro, commonly referred to as the East Gabbro, occurs along the eastern extent of the Roby Zone. Although the leucogabbro is isomodal, centimeter-scale rhythmic layering is common and is defined by varying proportions of felspathic and mafic minerals, specifically plagioclase and clinopyroxene (Figure 3.2). The layers, which typically reach widths of up to several centimeters, have gradational contacts. The centimeter-scale layering trends approximately north-northeast and dips steeply to the east. A local, weakly developed mineral foliation parallels the centimeter-scale layering.

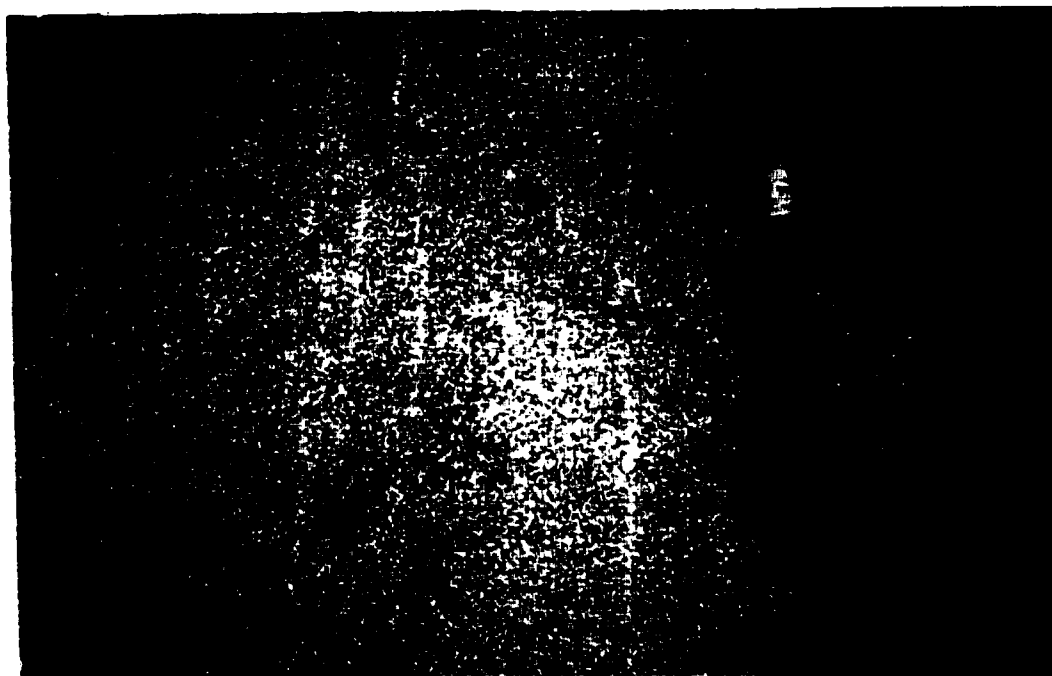


Figure 3.2: Photograph of leucogabbro, or East Gabbro, showing centimeter-scale layering that strikes north-northeast and dips steeply to the east. The centimeter-scale layering is defined by varying proportions of plagioclase feldspar and clinopyroxene grains.

3.1.2 Clinopyroxenite

Clinopyroxenite layering within the northern layered sequence ranges from 2.0 to 9.0 meters in width and occurs along the western extent of the East Gabbro. The clinopyroxenite-East Gabbro contact is sharp and often dimpled. The attitude of the contact parallels the centimeter-scale layering in the East Gabbro (Figure 3.3). This indicates that the intrusive layers co-existed in a fluid/crystal mush state. Occasionally, tongue-shaped lenses and lobes of clinopyroxenite, up to several meters in width, extend eastwards from the clinopyroxenite into the East Gabbro, thus cross-cutting the centimeter-scale layering. The contact of these lobes are sharp, however, the contacts are not chilled. During solidification of the clinopyroxenite, stress applied to the clinopyroxenite layering may have caused lenses of clinopyroxenite to intrude into the adjacent semi-solid gabbro and leucogabbro layers.

In the central portion of the Roby Zone, clinopyroxenite contains numerous angular fragments, up to 25 centimeters in diameter, of leucogabbro and gabbro (Figure 3.4). The presence of angular fragments suggests that the clinopyroxenite layer has intruded the leucogabbro and gabbro layers during a forceful event, thus producing fragmentation of the adjacent layers. This indicates that leucogabbro, gabbro and clinopyroxenite co-existed at varying degrees of solidification along the contact. Size-graded layering has been observed in outcrop and in drill core. The increasing grain size towards the west indicates that the stratigraphic top to the igneous layering is to the east, towards the center of the intrusion.

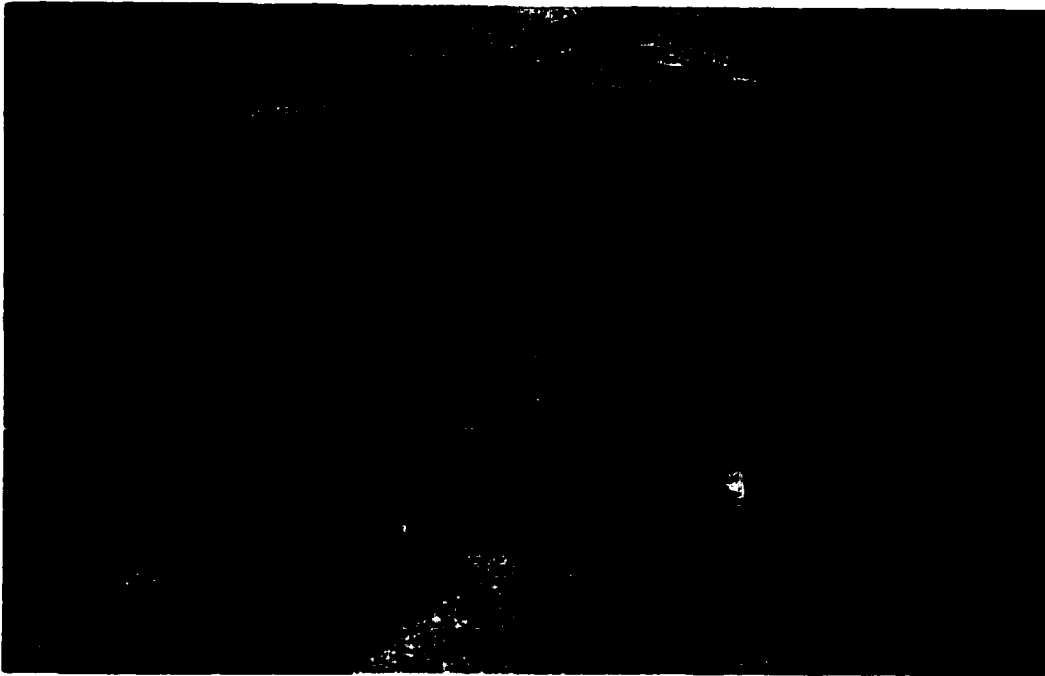


Figure 3.3: Photograph of clinopyroxenite in the northern layered sequence showing a dimpled contact, suggesting the co-existence of clinopyroxenite and leucogabbro in a fluid/crystal mush state.

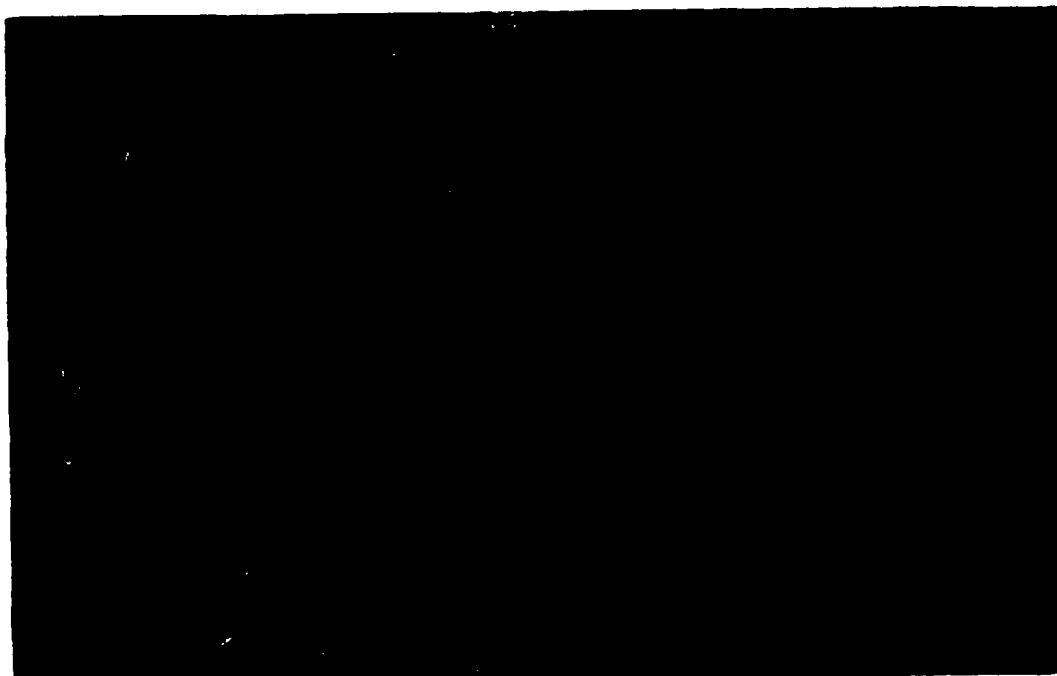


Figure 3.4: Photograph of clinopyroxenite in the central portion of the Roby Zone containing numerous angular fragments of leucogabbro (East Gabbro).

3.1.3 Gabbronorite

Gabbronorite in the northern layered sequence occurs as a massive to rhythmically layered unit up to 2.5 meters wide (Figure 3.5). The layer often pinches and swells along strike ranging from 0.5 to 2.5 meters in width. Gabbronorite forms a sharp contact with the enclosing coarse-grained leucogabbro (Figure 3.6). There is an abrupt change in the modal mineralogy of the cumulus minerals at the contact. No mineral zonation or grain size (i.e. chilling) was observed at the contact in either the gabbronorite or encompassing coarse-grained leucogabbro. The lensoidal shape of many of the gabbronorite layers and the abrupt change in modal mineralogy at the contact, suggests that gabbronorite intruded the coarse-grained leucogabbro. The absence of a chilled margin suggests that gabbronorite and leucogabbro may have co-existed in a fluid/crystal semi-consolidated state. The gabbronorite layer is locally offset by numerous cross-cutting faults, often making correlation between outcrops and drill intersections difficult.

Within gabbronorite, varying modal proportions of the two cumulus minerals, orthopyroxene and plagioclase, and intercumulus clinopyroxene, which accounts for less than 15 vol.%, are evident. Along strike, gradational variations in the ratio of the relative proportions of orthopyroxene and clinopyroxene produce sections grading from gabbronorite to norite. Within gabbronorite, layers of norite that contain up to 70 vol.% orthopyroxene, grade into gabbro and gabbronorite layers that contain approximately 30 vol.% orthopyroxene. The varying proportions of cumulus and intercumulus minerals occur over very short distances of several centimeters and often results in very distinct colour differences in outcrop. The western margin of gabbronorite appears to be more orthopyroxene-rich than the eastern margin (Figure 3.5). In addition, size-graded layering occurs across the gabbronorite layer, with the coarser grains of orthopyroxene occurring along the western margin of the unit. This is similar to the grain-size distribution observed in the clinopyroxenite, where the coarser

clinopyroxene grains occur along the western margin of the layer. This suggests that stratigraphic tops are to the east, towards the center of the intrusion. A local, moderately developed mineral foliation, defined by the alignment of plagioclase, occurs parallel to the boundary of the gabbro.



Figure 3.5: Photograph of layering within gabbronorite from the northern layered sequence showing the development of modal layering defined by varying proportions of feldspar and clinopyroxene/orthopyroxene grains. Note the gradual darkening of the colour of gabbronorite towards the bottom of the photograph, or west. The long axis of the hammer is oriented approximately north-south, with the head of the hammer towards the north.

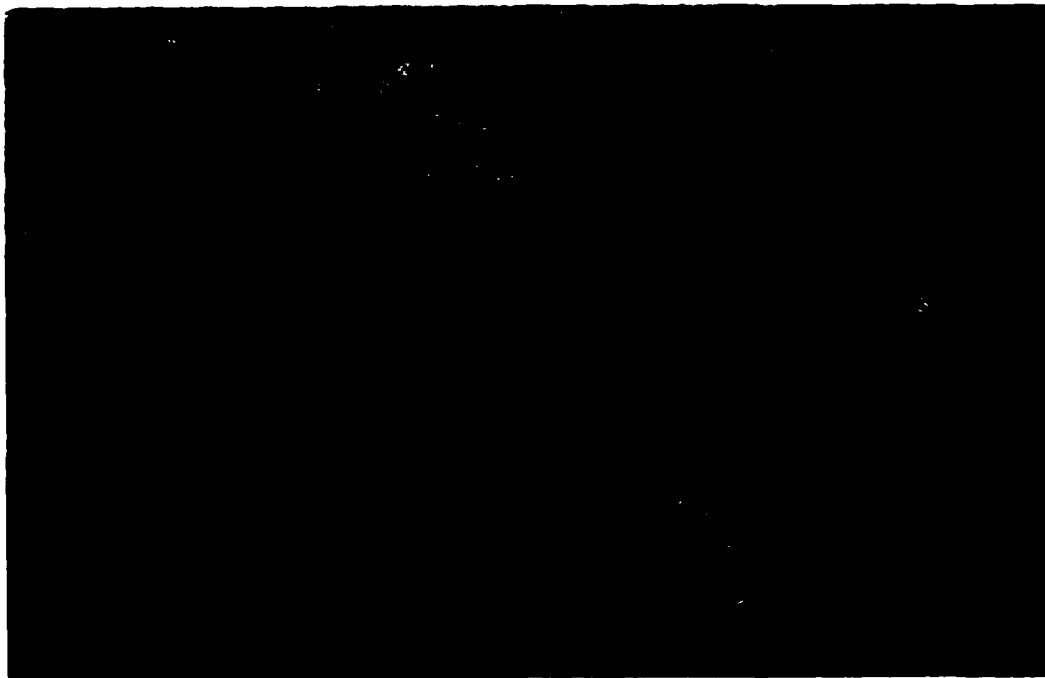


Figure 3.6: Photograph of gabbronorite-leucogabbro contact within the northern layered sequence.

3.1.4 Gabbro

Gabbro in the northern layered sequence is a uniform, medium-grained, isogranular and isomodal cumulate rock and contains a near equal proportion of plagioclase and clinopyroxene grains (Figure 3.7). Gabbroic layers range from 0.5 to 4.0 meters in width and occur mostly at the contact between clinopyroxenite and coarse-grained leucogabbro. The gabbro-coarse-grained leucogabbro contact is very sharp and irregular. Some chilling, or decrease of grain size, was observed in gabbro near the contact with the coarse-grained leucogabbro. This is good evidence that gabbro has intruded the coarse-grained leucogabbro. The eastern contact of the gabbro with clinopyroxenite is very sharp, irregular and often fragmented. Clinopyroxenite forms the matrix for many of the fragmented gabbro blocks.

3.1.5 Coarse-Grained Leucogabbro

Coarse-grained leucogabbro appears is the most abundant rock type in the northern layered sequence. Coarse-grained leucogabbro is a texturally and compositionally uniform relative to many of the other rock types of the Roby Zone. Leucogabbro is isomodal and consists of clinopyroxene and plagioclase feldspar grains ranging from 1.0 to 1.5 centimeters in diameter (Figure 3.8).

Coarse-grained leucogabbro hosts a number of pegmatitic segregations and pods consisting of clinopyroxene and plagioclase grains reaching up to 5.0 centimeters in diameter. The pegmatitic sections, which are often irregularly shaped and range in size up to several

meters, form sharp, well defined contacts with the enclosing leucogabbro. The pegmatitic pods range in composition from leucogabbroic to gabbroic (Figure 3.9). Large, clinopyroxene grains are often concentrated along the boundaries of these pegmatitic sections.



Figure 3.7: Photograph of a cut surface of gabbro from the northern layered sequence showing the exceptional uniformity of the medium-grained cumulate texture.

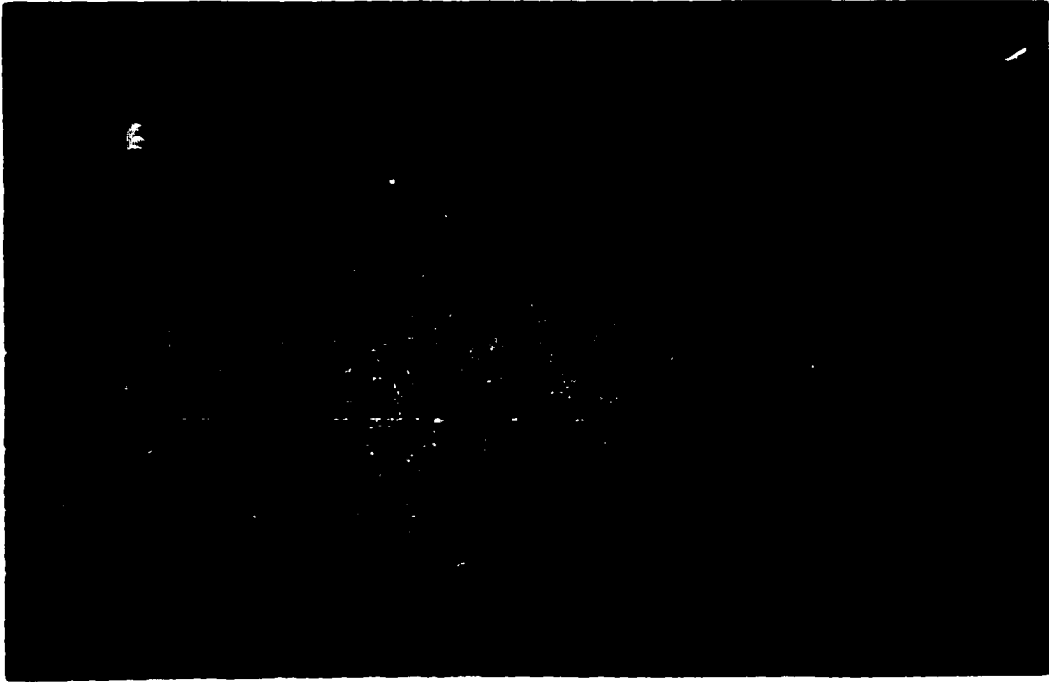


Figure 3.8: Photograph of coarse-grained leucogabbro from the northern layered sequence showing the uniform cumulate texture.



Figure 3.9: Photograph of coarse-grained leucogabbro from the northern layered sequence showing a typical pegmatitic pod that consists of large grains of clinopyroxene and plagioclase feldspar. Notice the sharp, well defined contacts between the pegmatitic gabbroic pod and the enclosing leucogabbro.

3.1.6 Heterolithic Gabbro

The heterolithic gabbro is a texturally and lithologically diverse unit comprising the majority of the rocks in the southern portion of the Roby Zone. Lithologies range in composition from leucogabbroic to pyroxenitic, and grain-size ranges from fine-grained to pegmatitic. Textural and compositional variability can be observed in hand sample and in outcrop. The heterolithic gabbro consists of a predominantly medium- to coarse-grained gabbroic matrix that locally grades into melagabbro. The gabbroic matrix hosts numerous irregularly shaped, angular, rounded and sub-rounded masses (compositionally distinct blebs and angular fragments) ranging in size from several centimeters up to several meters in diameter (Figure 3.10, 3.11 and 3.12). Masses of gabbro and coarse-grained leucogabbro observed in the southern portion of the heterolithic gabbro have considerable lateral extent in plan view; however, drill hole data indicate that these blocks have minor vertical extent. A chloritic rim often occurs along the perimeter of these various masses. The various rock types within the heterolithic gabbro consist of gabbro, coarse-grained leucogabbro, gabbro and clinopyroxenite. Masses or layers of tonalite or granite composition were not observed. The contacts of the various masses and layers within the heterolithic gabbro matrix are very sharp. The original geologic contacts preserved within the masses and between the gabbroic matrix and the contact of the masses are very discordant with each other and with the trend of the geologic contacts observed in the northern layered sequence. These rock types are mineralogically and texturally similar to the intrusive layers that comprise the northern layered sequence of the Roby Zone. The main difference observed between the various masses within the heterolithic gabbro and the layered sequence is the increased amphibole and chlorite alteration identified within the heterolithic gabbro. The degree of variability and the presence of angular fragments are more pronounced in the northern portion of the heterolithic gabbro, located south of the shear zone. The degree of compositional and

textural variability decreases gradually towards the south and the west. The presence of rounded and angular masses of similar mineralogy to the rocks of the northern layered sequence, suggests that the various masses comprising the heterolithic gabbro may have been derived from the northern layered sequence.

Numerous, randomly oriented pegmatitic gabbroic pods up to several meters in diameter occur throughout the heterolithic gabbro. The pegmatitic pods occur as layers, cross-cutting dikes, cusped lenses interleaved with gabbro, and sub-spherical pods often with quartz and tourmaline cores (Figure 3.13). The pegmatitic dikes often propagate from pegmatitic patches or segregations. Laterally, the pegmatitic gabbroic pods become more feldspathic. Many layers and pods of pegmatitic gabbro, which typically strike north-south and dip steeply to the east, contain a pyroxene-rich base with grains up to 10 centimeters in length. The long axes of these mineral grains are oriented orthogonal to the margins of these pods and dikes. The composition across these pods from east to west varies from anorthositic to pyroxenitic. The orientation of these layers, or comb layers (Moore and Lockwood, 1973), and the orientation of the pyroxene grains may be used to determine stratigraphic tops. The convex side of the layers and pods, which are typically to the west and southwest, protrude away from the direction of the accumulating grains and into the direction of the fluid to which the crystals formed. This indicates that the stratigraphic tops are to the east (Moore and Lockwood, 1973; Figure 3.14). Several of the gabbroic masses within the heterolithic gabbro have rinds of either clinopyroxenite or pegmatoidal gabbro, termed orbicular texture, and are found in association with the comb layers.

Numerous, northeast and northwest trending, small-scale faults have offset the dikes, layers and masses up to several meters.

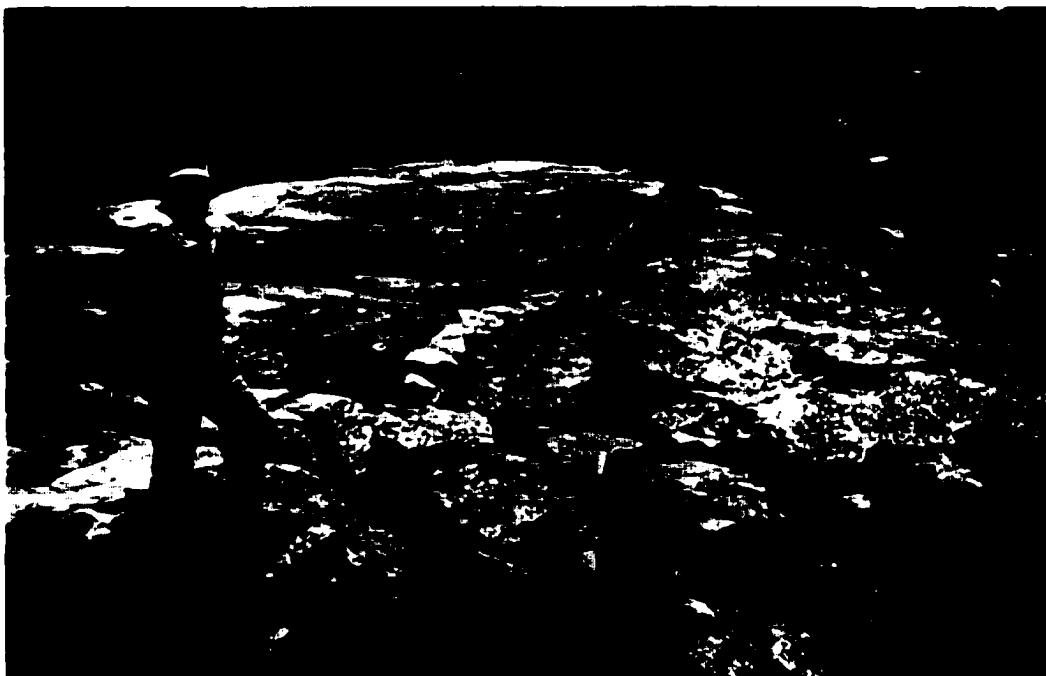


Figure 3.10: Photograph showing the textural and compositional variation within the heterolithic gabbro. Photograph taken at the north end of the heterolithic gabbro near the intersection between the shear zone and the northern layered sequence. The variation in the size and shape, from rounded to angular, and composition can be observed in the photograph. The matrix of the heterolithic gabbro is typically gabbroic, although, as can be observed in the photograph, can be melagabbroic.



Figure 3.11: Photograph showing the textural and compositional variation within the heterolithic gabbro. Photograph taken at the north end of the heterolithic gabbro near the intersection between the shear zone and the northern layered sequence. The variation in the size and shape, from rounded to angular, and composition can be observed in the photograph.



Figure 3.12: Photograph of irregularly shaped gabbronorite section within mafic gabbroic matrix of the heterolithic gabbro.



Figure 3.13: Photograph showing the typical distribution of pegmatoidal gabbroic pods, dikes and layers within the heterolithic gabbro.



Figure 3.14: Photograph showing local layering developed in heterolithic gabbro with the base of the layers defined by large (>5cm.) clinopyroxene grains oriented with their long axes perpendicular to the base of the layer and propogating upwards to the top of the layer.

3.1.7 Shear Zone

The shear zone is the most intensely altered unit of the Roby Zone. The rocks are very fissile and composed almost entirely of secondary silicates, including amphibole and chlorite, that are aligned parallel to the walls of the shear zone (Figure 3.15). The shear zone, having very well defined contacts, occurs within a portion of the clinopyroxenite layer. A more detailed description of the shear zone is presented in Chapter 3, Section 3.

3.1.8 Late-Stage Pegmatitic Gabbro Dikes

Late-stage pegmatitic gabbro dikes, up to 1.5 meters wide, strike east-west and dip vertically (Figure 3.16). The pegmatitic dikes are relatively unaltered and are composed of euhedral clinopyroxene and plagioclase grains up to 5 centimeters in length. The pegmatitic dikes form a sharp boundary with the host rock type and are usually associated with an increased concentration of chlorite and amphibole at the margins. Clinopyroxenes occur predominantly at the contact of the pegmatitic dykes, with the long axes of the mineral grains oriented orthogonally to the contact and extending towards the center of the dike. The pegmatitic dikes are often composed of numerous, parallel pegmatitic dikes that appear to have intruded earlier dikes, suggesting there have been multiple pulses of pegmatitic material. The presence of multiple pulses and clinopyroxenes growing orthogonal to the margins of the dike indicates that the dikes were formed as a result of open-space filling.

The gabbro dikes transect all other rock types comprising the Roby Zone, except for the East Gabbro. The pegmatitic gabbro dikes transect the western contact of the

clinopyroxenite, however are truncated by the shear zone. The pegmatitic dikes cross-cut earlier-formed pegmatitic layers and pods.

3.1.9 Breccia Dikes

Numerous, late-stage breccia dikes cross-cut all of the rock types comprising the Roby Zone. The breccia dikes, which reach widths of up to 1.0 meters, are randomly oriented and anastomose along faults (Figure 3.17). The breccia dikes have very fine-grained chilled margins and contain numerous irregularly sized and angularly shaped fragments of all rock types identified within the Roby Zone, including the tonalitic rocks surrounding the Lac des Iles Complex. The fragments occur in a fine-grained gabbroic matrix.

3.1.10 Biotite Dikes

Several east-west trending and vertically dipping biotite-rich dikes cross-cut the Roby Zone. These dikes, which are typically up to 10 centimeters in width, contain a well-developed biotite mineral foliation. The mineral foliation is parallel to the contacts of the dike and appear to have developed during the emplacement of the dike.

3.1.11 Felsic Dikes

Cross-cutting felsic dikes occur throughout the Roby Zone. The dikes, which are typically up to 1.0 meter wide, are randomly oriented. The felsic dikes range in composition from tonalitic to granitic and often have a core of quartz and tourmaline.

The dikes often contain a well developed mineral foliation parallel to the contacts of the dike.

3.1.12 Diabase Dikes

Numerous diabase dikes cross-cut all rock types of the Roby Zone. The dikes are fine-grained and reach widths up to 0.5 meters. The diabase dikes are randomly oriented, although have been observed most often along northwest and northeast trending faults.



Figure 3.15: Photograph of shear zone outcropping in the Roby Zone open pit showing fissile nature of rocks. Photograph taken facing south.

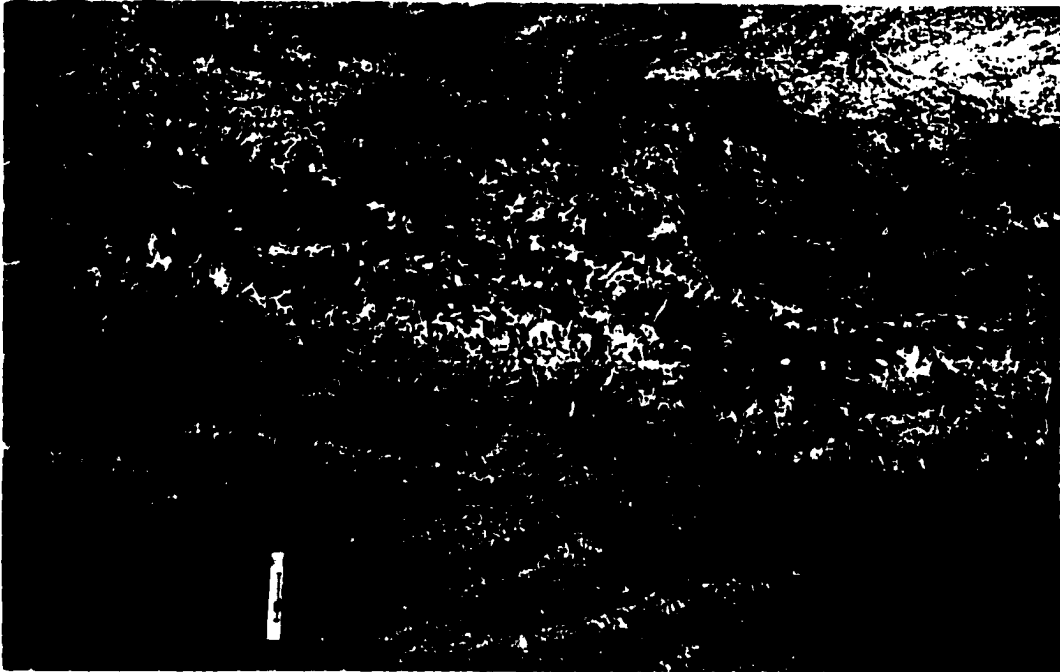


Figure 3.16: Photograph showing late-stage pegmatitic gabbro dike cross-cutting the coarse-grained leucogabbro . Notice the crack and fill texture of the dike, which suggests the presence of multiple pulses of liquid during formation.



Figure 3.17: Photograph of late-stage, randomly oriented, breccia dikes containing angular fragments of the various rock types comprising the Roby Zone and the surrounding tonalitic rocks within a fine-grained gabbroic matrix.

3.1.13 Intrusive Relationships

The contacts between the various igneous layers are very sharp and irregular and often have a dimpled texture. Igneous layering has been defined by the attitude of the layers and the varying proportions of the felspathic and mafic cumulus minerals. Rhythmic layering has been identified in two of the rock types, including gabbro and the medium-grained leucogabbro, or East Gabbro. The mineralogy, petrography and microscopic textures are described in detail in the following chapter.

The orientation and type of geologic contacts were used to determine the intrusive history of the igneous stratigraphy identified in the Roby Zone. Due to the relatively unaltered rocks comprising the northern layered sequence, the layering in this portion of the deposit was used to determine the intrusive history. Well defined contacts, and the lack of zonation at the igneous contacts between the various layers suggest that the layers represent an intrusion of magma into a largely crystallized mush. The presence of dimpled contacts suggest that several of the adjacent layers, particularly the clinopyroxenite-leucogabbro contact, may have co-existed as a semi-solid/crystal mush. Locally, magmatic injections resulted in brittle deformation of the adjacent rocks, evidenced by angular fragments of gabbro and leucogabbro within a clinopyroxenite matrix.

Based on the orientation and type of geologic contacts, the following list in order of oldest to youngest is the sequence of magma intrusion into the Roby Zone: coarse-grained leucogabbro, PGE-rich gabbro, gabbro, East Gabbro and PGE-rich clinopyroxenite. It has been suggested that the clinopyroxenite may be the fractionated equivalent of the northern ultramafic portion of the Lac des Iles Complex (Sutcliffe, 1986).

Grain size-graded layering observed within gabbro and clinopyroxenite suggests that in-situ fractionation has occurred within individual layers. Assuming the grain size-grading is the result of gravitational settling, orthopyroxene grains located along the western boundary of gabbro suggest that stratigraphic tops are to the east. Subsequent deformation has tilted the layers 70 degrees to the east, otherwise, grain size-graded layering would not have been observed in the horizontal plane in the now steeply dipping layers.

3.2 Alteration and Mineralization

Alteration has occurred to varying degrees throughout the Roby Zone and is most prominent in the shear zone and the heterolithic gabbro. Alteration varies with the host lithology and ranges in intensity from weak-to-strong, local-to-pervasive and is commonly intensified along narrow fractures. The orthopyroxenes have been altered to talc, anthophyllite and serpentine; clinopyroxenes have been altered to actinolite, chlorite, tremolite and hornblende; and plagioclase has been altered to zoisite, epidote and sericite. Pervasive alteration results in the complete metamorphism of the primary silicates to amphibole pseudomorphs. The pseudomorphic amphiboles are of use in identifying the primary cumulate mineralogy and for classification of the igneous layers. Narrow zones of mylonitization occur locally, resulting in a significant decrease in grain size of the cumulus and intercumulus minerals.

Platinum group elements occur as discrete minerals commonly associated with sulphide mineralization. Sulphide mineralization, which typically accounts for less than 2 vol.% of the rock, consists of very fine-grained disseminated pyrrhotite, pentlandite, chalcopyrite and pyrite. Within the gabbronorite, sulphide minerals compose up to 1-2 vol.% of the rock, commonly forming a net-texture. Up to 5 vol.% sulphide may occur in the southern portion of the deposit, specifically within the heterolithic gabbro and shear zone. Sulphide minerals occur as irregularly shaped and sized blebs up to several centimeters in diameter, and as fine-grained inclusions within secondary silicates. Platinum group element minerals occur predominantly within the sulphide blebs and along sulphide-silicate boundaries (Sweeny, 1989).

Alteration and mineralization are described in more detail in the following chapter, "4.0 Petrography of the Roby Zone".

3.3 Structural Geology of the Roby Zone

The rocks of the Roby Zone are transected by several sets of small-scale faults. The faults are expressed by topographic lineaments, mylonitization, shearing and fracturing. The faults transect all of the lithologies comprising the Roby Zone. Numerous minor and more discontinuous faults have been identified within the heterolithic gabbro and the northern layered sequence. Three hundred and sixty-three individual fault plane measurements are presented in stereographic projections (Figure 3.18). Several oriented samples were collected for microscopic analysis.

The most prominent structure in the Roby Zone is a 15-meter wide shear zone, which is defined by an alignment of secondary silicates consisting of predominantly actinolite. The shear zone strikes north-northwest and dips steeply to the east. The shear zone, designated as the actinolite-chlorite-talc schist on the Roby Zone geologic map (Figure 3.1), is located along the eastern extent of the observed platinum group element mineralization of the Roby Zone. The shear zone separates the northern layered sequence from the heterolithic gabbro to the south.

The well-developed foliation defines a C/S fabric within the rocks of the shear zone. The C/S fabric consists of a spaced foliation, striking north-northwest and dipping steeply to the east, enclosing a less developed foliation striking northwest and dipping approximately 75 degrees to the southwest (Figure 3.19). The S planes are a penetratively developed strain-sensitive flattening fabric that parallels the XY plane of the finite strain ellipsoid. The C planes are discrete narrow shear bands or shear zones that are parallel to the flow plane of the progressive deformation (Figure 3.20). The principal shortening (Z axis of the strain

ellipsoid) is perpendicular to the S fabric and at a high angle to the C fabric. The spacing between shear bands is up to 5 centimeters. The C/S fabric has been identified in oriented hand samples and thin sections (Figure 3.5). In the area between shear bands, the S foliation is oblique to the C foliation plane and curves into the C foliation as it approaches it. C/S fabric is an excellent indicator of simple shear strain (Lister, 1980). Simple shear strain, or rotational shear strain, is defined as the rotation of the finite strain axes into the plane of maximum strain (Platt, 1983). The formation of the C/S fabric occurs at an early stage of simple shear strain deformation. The S fabric, related to the accumulation of finite strain, develops oblique to the C plane and reflects the change in orientation of the finite strain ellipse into the direction of maximum strain. Periodic variations in the stress produce C planes, which are discretely spaced, slip surfaces parallel to the foliation. Each C plane acts as a small shear zone, where the variable spacing of the C plane is due to the properties of the rock and consistency of the stress on the rock (Hobbs et. al., 1986). The relative sense of movement of the rock is obtained from the curving of the S fabric as it approaches the C fabric (Figure 3.21). The C/S fabric observed in the Roby Zone indicates that dextral shearing has occurred. The line of intersection between the shear bands (C) and the schistose foliation (S) is approximately orthogonal to the direction of movement across the shear zone. The intersection line plunges approximately 75 degrees to the southeast, indicating that the relative sense of movement across the shear zone is sub-horizontal.

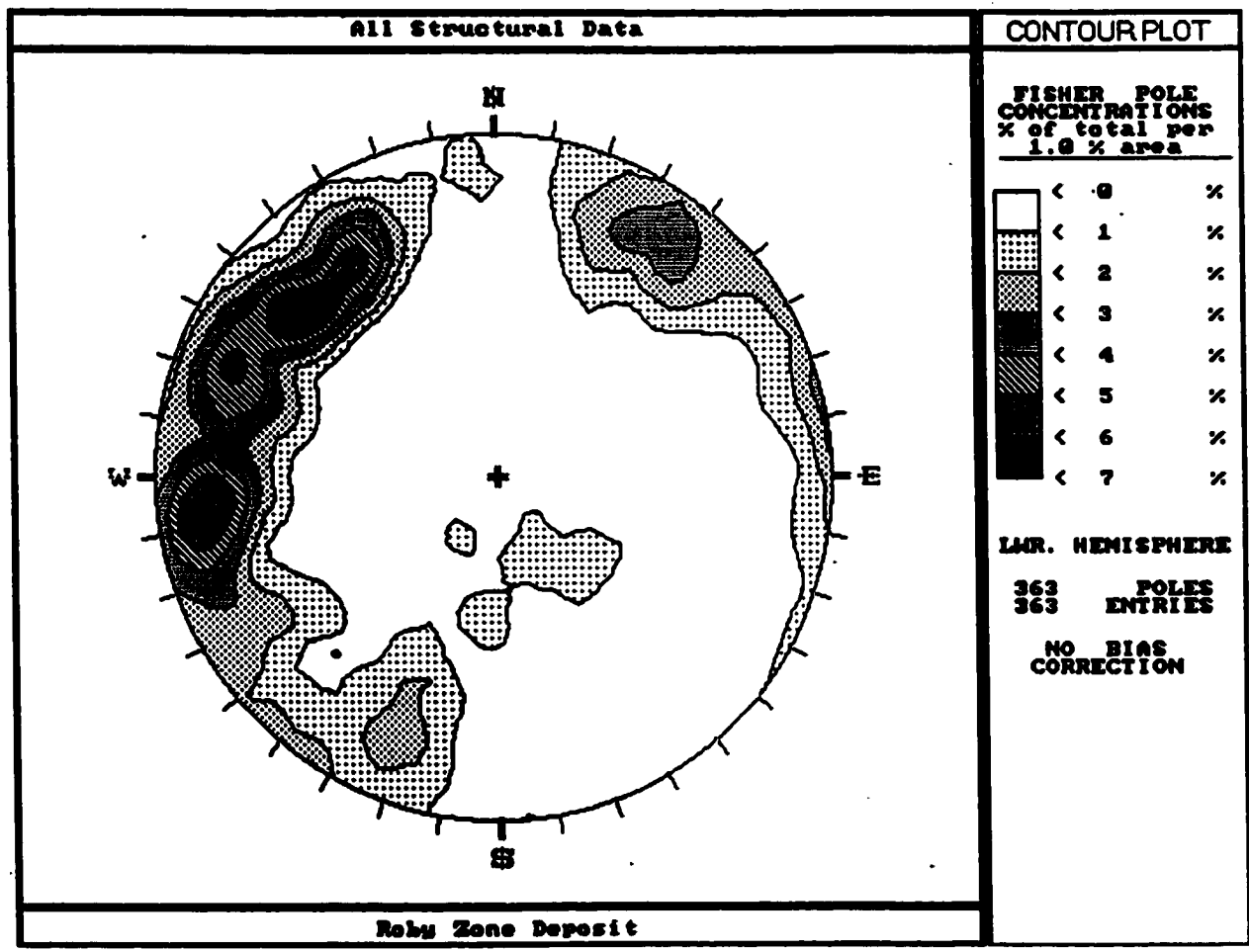


Figure 3.18: Contoured stereonet plot of poles to planar elements collected from the Roby Zone.

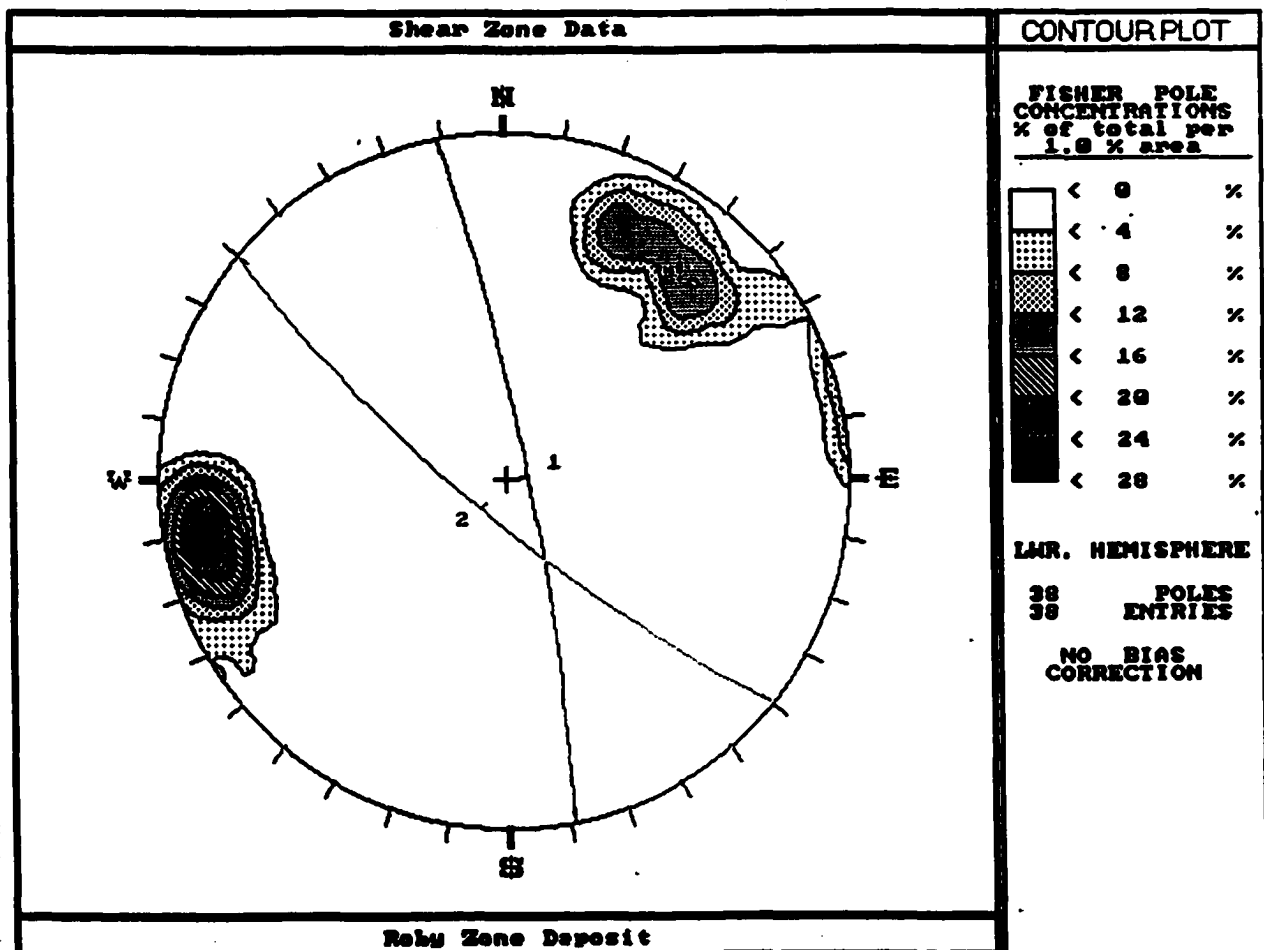


Figure 3.19: Contoured stereonet plot of the poles to planar elements within the shear zone showing the C fabric, labelled 1, and the S fabric, labelled 2. The intersection line between the C and S fabrics plunges approximately 75 degrees to the southeast.



Figure 3.20: Photograph showing typical C and S fabric developed in rocks from the shear zone.

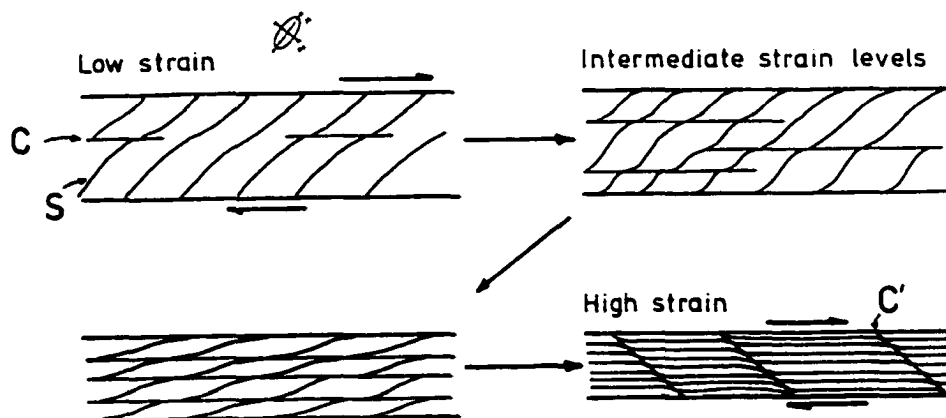


Figure 3.21: Schematic illustration of the development of S and C fabric in ductile shear zones showing the relative sense of movement (after Simpson, 1984).

The relative sense of movement across the shear zone indicated by the C/S fabric is further supported by the identification of asymmetric augen structures, or winged porphyroclasts. Several feldspar grains, orientated with their long axis oblique to the foliation are surrounded by augen structures. The augen structures are composed of fine-grained material similar to the mineral grain they surround and point in the direction of the foliation. Development of the asymmetric augen structure occurs when there is a large contrast of ductility between the mineral grain and the surrounding matrix (Simpson, 1983). Rotation of the larger, rigid feldspar grain towards the foliation is slower than the weaker material of the matrix and produces the greatest amount of strain on the ends of the grain. This results in the fine-grained pieces of the mineral grain breaking off and being deposited behind the mineral in the direction of the foliation (White et al., 1980). Asymmetric augen structures are a result of simple shear strain. The rotation of the mineral grain towards the foliation, or maximum strain, shows the relative sense of movement of the rock (Figure 3.22).

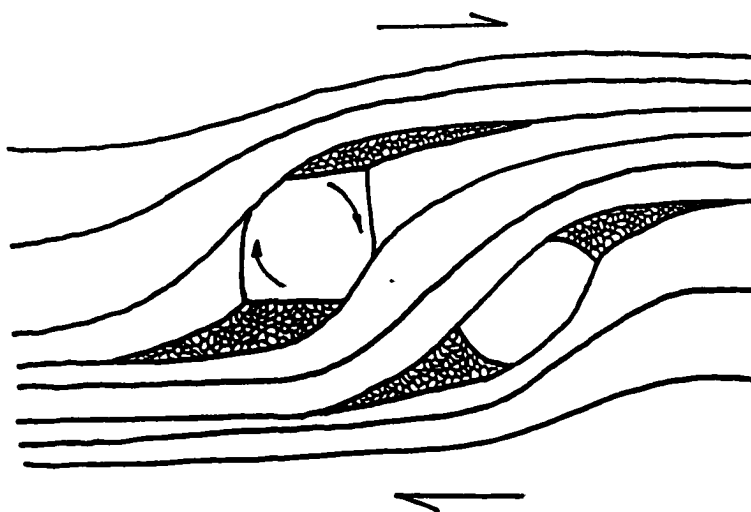


Figure 3.22: Schematic diagram of asymmetric augen structures, or winged porphyroclasts, showing the relative sense of movement in sheared rocks (after Simpson, 1983). The mineral grain has been rotated dextrally.

The shear zone has been produced as a result of simple shear strain causing ductile deformation and local mylonitization. The X-axis of the strain ellipse, the direction of maximum extension or stretching, is oriented east-west. The shear zone displays dextral displacement in a direction plunging approximately 15 degrees to the northwest.

A number of small-scale faults transect the Roby Zone as shown in Figure 3.18. These fault sets include an east-northeast striking and steeply dipping to the southeast set, a north-northwest striking and vertically dipping set, and a northeast striking set of faults dipping approximately 35 degrees to the northwest. These faults, which frequently occur as zones up to several meters in width, are associated with amphibole and chlorite alteration, mylonitization and shearing of the gabbroic wall rock. Displacement across these fault zones ranges from several centimeters up to several meters and appear to post-date the development of the main shear zone.

The most prominent set of these late-stage faults is the east-northeast striking, vertically dipping faults that transect all rock types of the Roby Zone. The sinistral displacement across the fault, which ranges from several centimeters up to several meters, is most pronounced along the clinopyroxenite-East Gabbro (Figure 3.23).



Figure 3.23: Photograph showing the east-northeast striking faults that have sinistrally offset the clinopyroxenite-leucogabbro contact. The original north-northeast trending dimpled intrusive contact is visible. The top of the marker in the photograph is oriented northwards.

4.0 Petrography of the Roby Zone

In general, the rocks of the northern layered sequence are composed of medium-grained to coarse-grained crystal cumulates up to 1.5 centimeters in diameter. These rocks consist of a) plagioclase cumulates, b) plagioclase-orthopyroxene cumulates and c) clinopyroxene cumulates. Olivine was not identified in this study; however, olivine was observed in the vicinity of the "D" Zone in unaltered gabbro (Guamera, 1967). Hornblende occurs in almost equal proportions as a primary igneous mineral in the cumulus and intercumulus phase and as an alteration product often forming pseudomorphs of primary clinopyroxene grains. The intercumulus minerals are predominantly clinopyroxene, plagioclase and hornblende and a variety of secondary minerals including magnetite, ilmenite, apatite and numerous sulphide minerals. The rocks of the Roby Zone are primarily orthocumulates, and less frequently, mesocumulates. Adcumulate textures were observed within clinopyroxenite. Intercumulus clinopyroxene grains occasionally up to 2.0 centimeters in diameter, form poikilitic and/or poikilophitic textures.

4.1 Leucogabbro (East Gabbro)

The rocks of the East Gabbro, or leucogabbro, are medium-grained and isogranular and typically display an orthocumulate texture. Cumulate minerals consist primarily of plagioclase, with a minor amount of hornblende and clinopyroxene. The intercumulus minerals consist of predominantly clinopyroxene, minor plagioclase, hornblende, biotite and a number of oxide minerals including magnetite and ilmenite.

Alteration consists of weak-to-moderate, pervasive uralitization of clinopyroxenes producing actinolite and tremolite pseudomorphs after clinopyroxene. Plagioclase has undergone sausseritization forming patches of zoisite and epidote within the center of the grain and along the grain boundaries. Narrow, randomly oriented fractures transect the leucogabbro and are commonly associated with chlorite, epidote and calcite. Alteration of clinopyroxene and plagioclase grains intensifies near the leucogabbro-clinopyroxenite contact. Epidote alteration is common in this vicinity.

Intercumulus sulphides, which amount to less than 1 vol.%, consist predominantly of pyrite, pyrrhotite and locally chalcopyrite. Intercumulus sulphides near the leucogabbro-clinopyroxenite can locally exceed 3 vol.%.

4.2 Clinopyroxenite

Clinopyroxenite is a compositionally uniform, medium- to coarse-grained unit composed of primarily cumulus and intercumulus clinopyroxenes. The cumulus clinopyroxene grains form a mesocumulate texture and occasionally an adcumulate texture. Cumulus plagioclase and orthopyroxene total approximately 5 vol.%. Although clinopyroxenite displays isomodal layering, very subtle grain size-graded layering has been observed. Coarser grains, up to 1.5 centimeters in diameter, occur along the western margin of the unit, while more medium-grained clinopyroxenes occur along the eastern margin.

Alteration within clinopyroxenite is moderate-to-strong and consists of actinolite, hornblende, chlorite and minor biotite after clinopyroxene (Figure 4.1). Amphibole alteration occurs as pseudomorphs of the clinopyroxene grains and chlorite alteration occurs as patches or mats

interstitial to the cumulus grains (Figure 4.2). Alteration of the clinopyroxene grains is more pronounced in the southern portion of the Roby Zone, where clinopyroxenite occurs as a thin wedge between the shear zone and the East Gabbro and as pods within the heterolithic gabbro. The higher degree of alteration in this area is most likely the result of increased fluid movement along the shear zone that penetrated the adjacent clinopyroxenite.

Sulphide mineralization occurs as fine- to medium-grained disseminations and irregularly shaped blebs up to 0.5 centimeters in diameter. Sulphide mineralization, which accounts for up to 5 vol.%, locally forms a net-texture within the coarser-grained portion of the layer near the western contact. This suggests that the sulphides have formed during primary magmatic conditions. In contrast, sulphides also occur as thin streaks parallel to the long axis of the pseudomorphing secondary silicates, thus suggesting that the sulphides may have been remobilized during alteration (Figure 4.3). Sulphide mineralization consists predominantly of chalcopyrite and pyrite with a lesser amount of pyrrhotite and pentlandite.

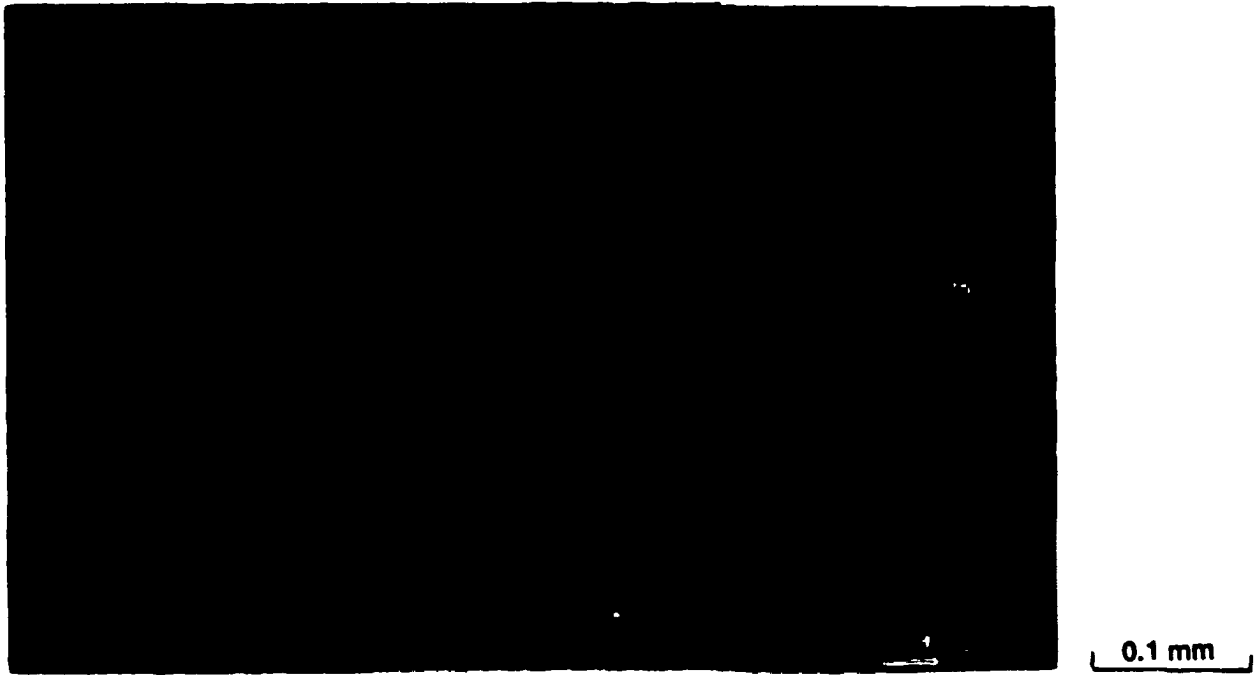


Figure 4.1: Photomicrograph of clinopyroxenite from the northern layered sequence showing pseudomorphic amphibole, predominantly actinolite, on clinopyroxene cumulate grains. [crossed nicols]



Figure 4.2: Photomicrograph of clinopyroxenite from the southern portion of the Roby Zone showing the actinolite alteration of clinopyroxene grains and development of chlorite. [crossed nicols]



Figure 4.3: Photomicrograph of clinopyroxenite showing sulphide blebs (opaques) and streaks within the secondary silicates. This suggests that the sulphide minerals were remobilized during alteration. Platinum group element mineralization is associated with the sulphide minerals occurring within the sulphide blebs and at the sulphide-silicate boundary (Sweeny, 1989). [plane polarized light]

4.3 Gabbronorite

Gabbronorite is predominantly medium-grained with the cumulus phase dominated by stubby, subhedral to euhedral orthopyroxene and plagioclase grains and the intercumulus phase dominated by clinopyroxene, plagioclase and a variety of oxide and sulphide grains in an orthocumulate texture (Figure 4.4). Gabbronorite displays both poikilitic and oikocrystalline textures with intercumulus clinopyroxene grains hosting inclusions of subhedral-to-euhedral grains of plagioclase and orthopyroxene. Although gabbronorite is predominantly medium-grained, several coarser orthopyroxene grains, up to 2.0 centimeters in diameter, have been identified along the western margin of the layer. Many segregations occur between plagioclase-rich sections and orthopyroxene-rich sections. These segregations occur in bands within the gabbronorite that closely parallel the boundaries of the gabbronorite layer.

Gabbronorite has experienced varying degrees of alteration ranging from very weak alteration to strong alteration concentrated along fractures. Within these fractures, which range in width up to several centimeters, cumulus orthopyroxene and plagioclase grains are often granulated or mylonitized resulting in a significant decrease in grain size (Figure 4.5). In these areas, twinning of plagioclase grains is often bent or kinked, suggesting that these rocks have experienced a high degree of physical stress. Physical stress is also evident in orthopyroxene grains that have fractured under the stress. Alteration along these fractures consists of talc and anthophyllite and commonly contain a core of magnetite occurring as fine-grained disseminations or wisps (Figure 4.6). Occasionally, orthopyroxene grains have been completely altered to serpentine, magnetite, talc and anthophyllite. Talc frequently pseudomorphs the original orthopyroxene grains.

Sulphide mineralization in gabbronorite is very sporadic and consists predominantly of fine-grained disseminations that account for less than 1 vol.%. In coarser-grained sections within gabbronorite (i.e. along the western margin), sulphide mineralization locally accounts for up to 5 vol.% commonly forming a net-texture (Figure 4.7). Sulphide mineralization also occurs within fractures cross-cutting orthopyroxene grains and as a matrix to granulated or mylonitized zones. Sulphide minerals consist predominantly of pyrrhotite, pentlandite, chalcopyrite and pyrite. Platinum group element minerals, most commonly vysotskite and braggite, are associated with the sulphide mineralization and occur within the sulphide blebs or at the sulphide-silicate boundaries (Sweeny, 1989). The fine-grained disseminated sulphides and the presence of net-texture within the gabbronorite indicates that the sulphide mineralization is related to primary magmatic mineralization. Late-stage fractures appear to have provided channel ways for deuteric fluids to produce isolated patches of altered orthopyroxene grains and remobilize primary sulphide mineralization and/or introduce sulphide mineralization into these areas.



Figure 4.4: Photomicrograph of gabbro from the northern layered sequence showing the unaltered cumulate texture consisting of subhedral to euhedral orthopyroxene grains and albite twinning of plagioclase feldspar grains. [crossed nicols]



Figure 4.5: Photomicrograph of gabbro from the northern layered sequence showing brecciation of individual orthopyroxene and plagioclase grains. [polished section]



Figure 4.6: Photomicrograph of fractured orthopyroxene grain showing alteration along fractures consisting of talc and serpentine (high birefringence) and magnetite (opaque). [plane polarized light]



Figure 4.7: Photomicrograph of gabbro-norite from the northern layered sequence showing the distribution of net-textured sulphides (opaque). [crossed nicols]

4.4 Gabbro

Gabbro consists of almost equal proportions of cumulus plagioclase and intercumulus clinopyroxene. Alteration consists of local, weak to moderate amphibole alteration of clinopyroxenes and sericite and zoisite alteration of plagioclase. Narrow cross-cutting fractures contain amphibole, chlorite, calcite and epidote. Sulphide mineralization, which typically accounts for less than 1 vol.%, consists of fine-grained disseminated pyrrhotite and pyrite. Trace amounts of magnetite and ilmenite were observed in the interstices between the cumulate grains.

4.5 Coarse-Grained Leucogabbro

The cumulus phase consists predominantly of plagioclase, with a lesser amount of clinopyroxene and orthopyroxene. Cumulus orthopyroxene, which typically accounts for less than 3 vol.%, locally accounts for up to 10 vol.% of the rock in 5.0 to 10.0 centimeter wide layers that have gradational contacts. These layers have limited strike length. Plagioclase grain-size distribution is bimodal, with the majority of the grains in the range from 1.0 to 1.5 centimeters in diameter and a smaller population ranging from 0.25 to 0.75 centimeters in diameter. Orthocumulate to mesocumulate textures predominate within the leucogabbro. Occasionally, poikilophitic textures were observed and consist of large, 2.5 centimeter clinopyroxene grains with inclusions of euhedral plagioclase.

Weak to moderate alteration of coarse-grained leucogabbro consists of amphibole alteration after clinopyroxene and sericite, zoisite and epidote alteration after plagioclase (Figure 4.8).

Chlorite alteration occurs as patches and mats within the interstitial area between cumulus grains. More intense amphibole and chlorite alteration is concentrated along narrow, cross-cutting fractures.

Sulphide mineralization, which is typically less than 1 vol.%, consists of fine-grained disseminated pyrrhotite and pyrite. Locally along the leucogabbro-gabbronorite contact, sulphide mineralization accounts for up to 3 vol.% and consists of irregularly shaped blebs up to 0.5 centimeters in diameter of pentlandite, pyrrhotite, pyrite and chalcopyrite.



Figure 4.8: Photomicrograph of leucogabbro from within heterolithic gabbro showing the strong pervasive amphibole alteration of clinopyroxene and saussurization of plagioclase feldspar. [crossed nicols]

4.6 Heterolithic Gabbro

Alteration within the heterolithic gabbro is more pronounced than in the northern portion of the Roby Zone and varies by rock type. Within the gabbroic matrix and within the majority of the masses, alteration is strong and pervasive and has resulted in the complete alteration of clinopyroxenes to fine-grained amphibole, predominately actinolite, and chlorite.

Orthopyroxene grains have been altered to talc and anthophyllite and plagioclase to sericite, epidote, zoisite and/or chlorite (Figure 4.9). Often the original shape of the clinopyroxene and feldspar grains has been preserved, although completely pseudomorphed by amphibole and sericite, respectively. The alteration mineral assemblage and intensity of alteration varies within each of the rock types comprising the heterolithic gabbro. The mineralogy of the various masses is similar to that of the corresponding layers of the northern layered sequence. The masses are commonly more altered and more fractured than their counterparts from the northern layered sequence. Although the alteration is predominately pervasive within the heterolithic gabbro, very strong amphibole and chlorite alteration occurs in narrow zones up to several centimeters wide.

Sulphide mineralization, which locally comprises up to 5 vol.%, consists of fine- to medium-grained disseminations and irregularly shaped blebs up to several centimeters in diameter. Disseminated sulphide grains and often net-textured sulphides have been observed in the gabbroic matrix of the heterolithic gabbro (Figure 4.10). This indicates that, at least a portion of the sulphide mineralization observed in the heterolithic gabbro may be of a primary magmatic source that was possibly concentrated and redeposited by late-stage hydrothermal and/or hydrothermal fluids. Larger sulphide blebs, up to several centimeters in diameter, occur interstitial to the coarse-grained feldspar and clinopyroxene grains within the

pegmatitic gabbro sections (Figure 4.11). Sulphide mineralization also occurs within randomly oriented narrow faults up to 1.0 centimeters wide (Figure 4.12). In addition, sulphides occur as fine-grained inclusions and thin streaks within actinolite, often paralleling the cleavage of pseudomorphic clinopyroxene. This indicates that the sulphide minerals were remobilized during alteration of the primary cumulus mineralogy (Figures 4.13). The sulphide blebs are composed of chalcopyrite, pentlandite, pyrrhotite and pyrite. Although there appears to be some segregation of the different sulphide minerals, specifically chalcopyrite and pyrrhotite, no systematic trends were observed.

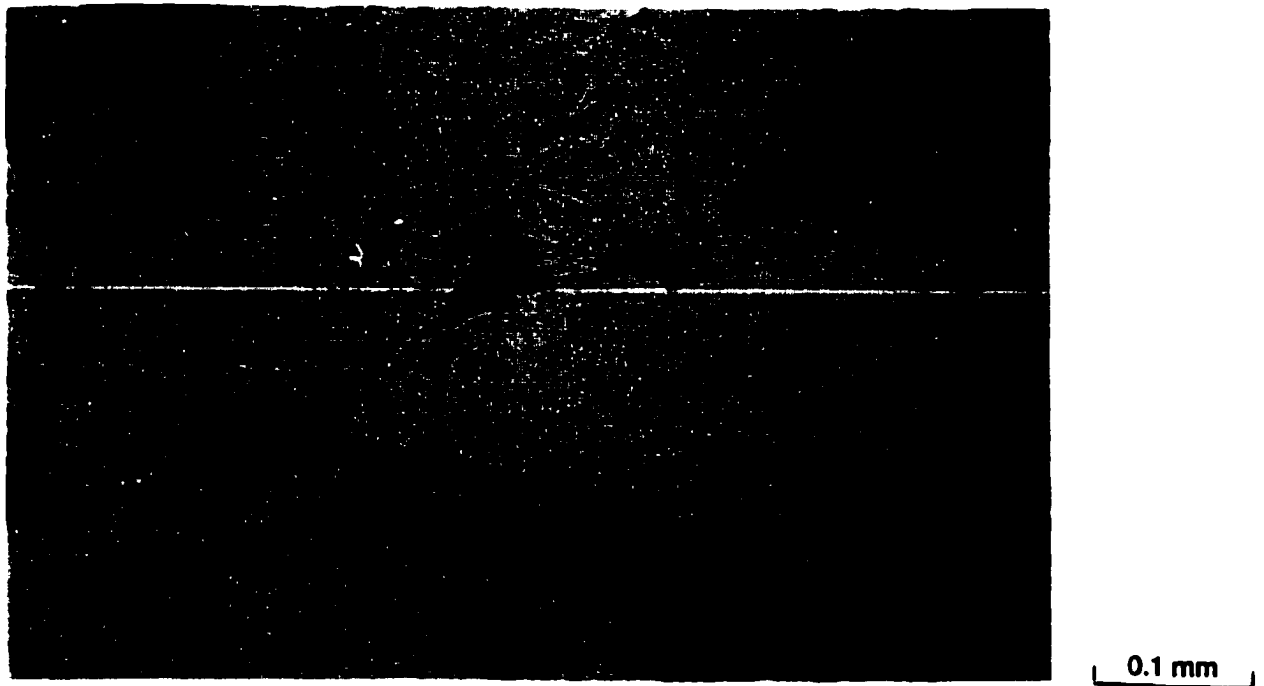


Figure 4.9: Photomicrograph of heterolithic gabbro showing strong pervasive amphibole and chlorite alteration and actinolite pseudomorphing clinopyroxene grains. [crossed nicols]

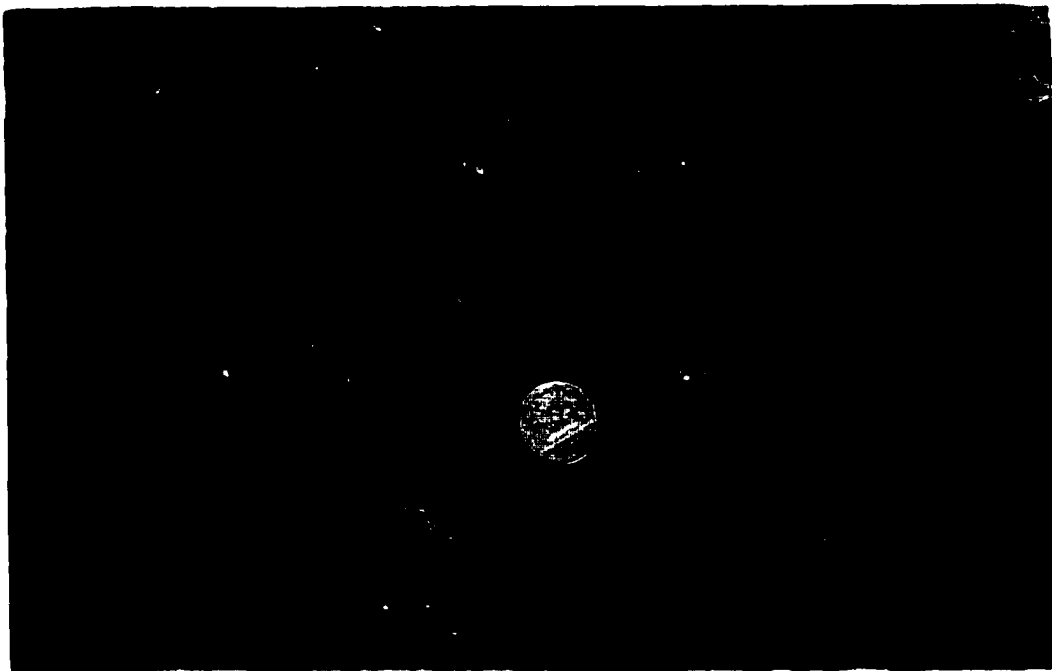


Figure 4.10: Photograph showing pyrrhotite, pentlandite and chalcopyrite mineralization occurring as disseminated grains and blebs up to several centimeters in diameter within the gabbroic matrix of heterolithic gabbro.



Figure 4.11: Photograph of pyrrhotite, pentlandite, chalcopyrite and pyrite mineralization within pegmatitic gabbro section in the heterolithic gabbro.



Figure 4.12: Photomicrograph of sulphide mineralization (opaques) along a narrow fault within the heterolithic gabbro. Notice the increased amphibole and chlorite alteration associated with the sulphide mineralization. [crossed nicols]



Figure 4.13: SEM image of heterolithic gabbro showing the sulphide grains (white areas) as inclusions and streaks within actinolite often paralleling the cleavage of pseudomorphic clinopyroxene.

4.7 Shear Zone:

The mineral foliation dominating the shear zone is composed of aligned mineral grains of predominately actinolite, chlorite, anthophyllite and talc (Figure 4.14). A minor amount of strongly altered, relict, altered clinopyroxene, orthopyroxene and saussuritized feldspar are present within the shear zone. These relict grains of clinopyroxene have been completely pseudomorphed by actinolite and hornblende and are commonly granulated and brecciated as a result of mylonitization. Chlorite occurs as patches within the shear zone. Talc, serpentine, anthophyllite and carbonate comprise the remainder of the shear zone. Recrystallized grains of hornblende, up to 1.5 centimeters in diameter, occur throughout the shear zone.

Sulphide mineralization, which accounts for approximately 1-2 vol.%, occurs as fine-grained disseminations of pyrrhotite, chalcopyrtie and pentlandite. Sulphide mineralization also exists as inclusions or streaks within secondary silicate grains (Figure 4.15).

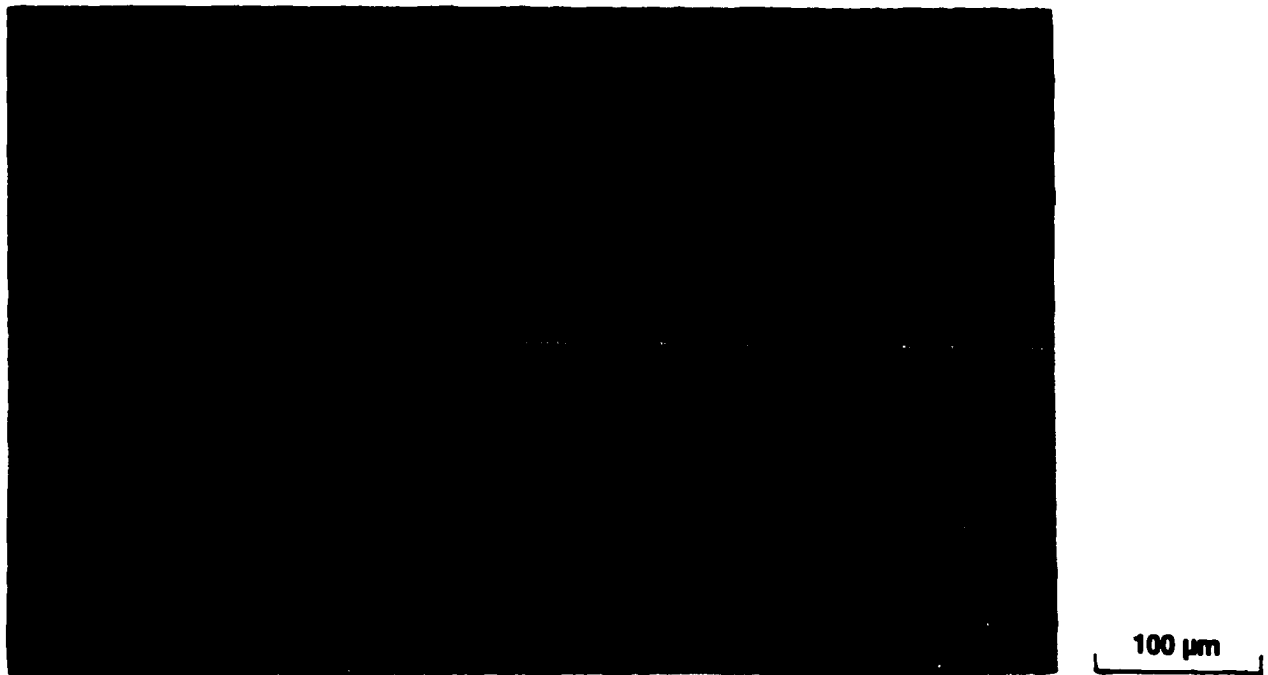


Figure 4.14: Photomicrograph of the shear zone showing the high degree of alteration, alignment of actinolite grains and development of chlorite. [crossed nicols]



Figure 4.15: Photomicrograph of shear zone showing pyrrhotite, pentlandite, chalcopyrite and pyrite mineralization (light coloured) occurring as fine inclusions within secondary silicates and paralleling the long axes of actinolite grains. [polished section]

4.8 Late-Stage Pegmatitic Gabbro Dikes

The pegmatitic gabbro dikes are relatively unaltered and are composed mostly of euhedral clinopyroxene and plagioclase grains up to 5 centimeters in length (Figure 4.16). The mineral grains do not form a typical cumulate texture. Alteration within the pegmatitic gabbro dikes is minimal, consisting of minor amphibole alteration of clinopyroxene and sericite and zoisite and epidote alteration of plagioclase. Sulphide mineralization is sporadic and ranges from trace amounts of fine-grained disseminated pyrrhotite and pyrite to irregularly shaped blebs up to several centimeters in diameter. These sulphide blebs consist of primarily pyrrhotite, pentlandite, chalcopyrite and pyrite. The irregularly shaped sulphide blebs occur interstitial to the clinopyroxene and plagioclase grains (Figure 4.17).

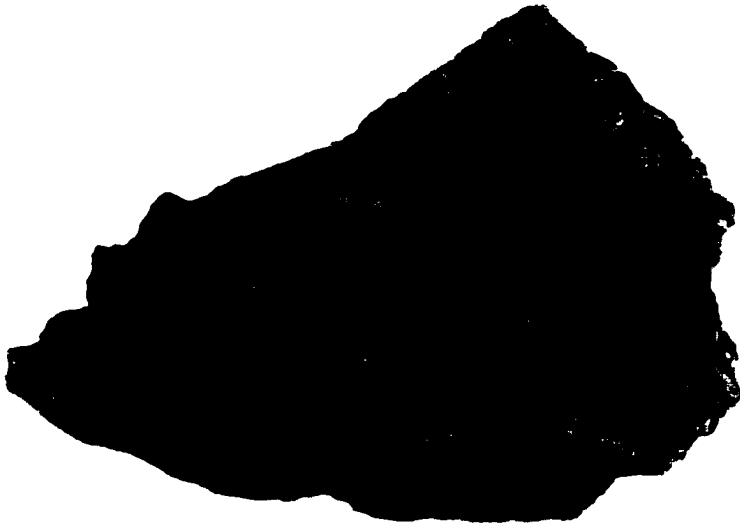


Figure 4.16: Photograph of cut sample surface of pegmatitic gabbro dike showing the randomly oriented large grains, up to 5.0 centimeters in length, of clinopyroxene and plagioclase.

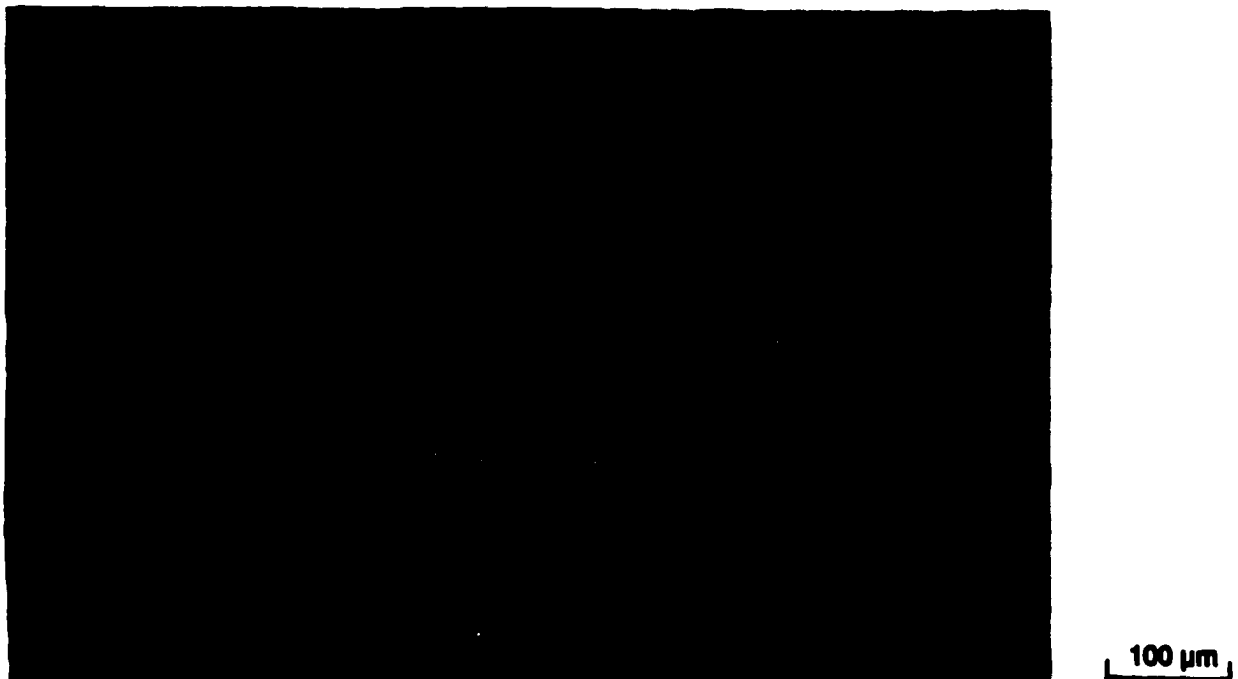


Figure 4.17: Photomicrograph of pegmatitic gabbro dike showing the distribution of feldspar (fel), clinopyroxene (cpn) and sulphide (opaque) minerals. [crossed nicols]

5.0 Whole Rock Geochemistry

5.1 Introduction

During this study 36 rock, hand samples were collected from surface outcrop and drill core and submitted for major, trace and rare earth element analysis. The samples were collected from unaltered and altered rocks representative of each rock type comprising the Roby Zone, including gabbroic and ultramafic rocks of the northern layered sequence, heterolithic gabbro, shear zone, pegmatitic gabbro dikes, felsic and mafic dikes and tonalite gneiss encompassing the Lac des Iles complex. Samples with a weathered rind were not submitted for analysis. The samples submitted for analysis range in weight from 1 to 5 kilograms, which is considered to be of sufficient size to be representative of the textural and compositional variation of the rock types. Previous whole rock data have been given by Sweeny (1989), Guarnera (1967), Pye (1968) and Brugmann and Naldrett (1987). The sample locations are plotted on a map in Appendix A. A description of the sampling and analytical methodologies and a summary of the geochemical data are presented in Appendix B.

5.2 Major elements

Whole rock major element compositional data from unaltered and altered rocks of the Roby Zone form a cluster in the tholeiitic field of the AFM diagram, near the boundary with the calc-alkaline field (Figure 5.1). Within this cluster, a number of distinct subgroups can be identified for each rock type comprising the Roby Zone, including the shear zone, coarse-grained leucogabbro, East Gabbro, clinopyroxenite, gabbro-norite, pegmatitic gabbro dikes and heterolithic gabbro.

The data for the various lithologies show considerable overlap on the AFM plot, which may be due to the varying degrees of alteration within the Roby Zone and varying proportions and types of cumulate and intercumulate minerals.

The lithologic sequence: shear zone, gabbro, coarse-grained leucogabbro and East Gabbro displays progressive alkali enrichment with relatively constant proportion of FeO_T and MgO . The increased alkali content is reflected in the modal mineralogy, which is related to increasing plagioclase feldspar content and decreasing clinopyroxene and orthopyroxene content. Analytical data for the shear zone and clinopyroxenite form two distinct clusters along the FeO_T - MgO tie-line on the AFM diagram. Both of these units contain less than 5 vol.% plagioclase feldspar. Clinopyroxenite is enriched in FeO_T relative to MgO , in comparison to the shear zone and the other gabbroic rocks of the Roby Zone.

Clinopyroxenite, composed of primarily cumulate and intercumulate clinopyroxene, contains up to 5 vol.% interstitial magnetite locally. The shear zone is composed of a wide variety of minerals, including actinolite, tremolite, chlorite, anthophyllite, talc and hornblende, with a minor amount of relict plagioclase feldspar grains. The shear zone rocks are almost entirely devoid of any magnetite or ilmenite. Analytical data for gabbro of the northern layered sequence form a cluster between clinopyroxenite and the other rock types. Gabbro locally contains 2-3 vol.% disseminated, interstitial magnetite. The elevated FeO_T concentrations in gabbro and clinopyroxenite are related to an enrichment of clinopyroxene relative to orthopyroxene and plagioclase feldspar and an enrichment in magnetite and ilmenite concentrations relative to the other rock types.

Outcrop-scale features indicate that the shear zone occurs almost entirely within clinopyroxenite in the southern portion of the Roby Zone. As illustrated on the AFM diagram, the shear zone contains a higher MgO/FeO_T ratio than clinopyroxenite, suggesting that Fe in clinopyroxenite may have been depleted and/or replaced with Mg during shearing and alteration. Analytical data for heterolithic gabbro and pegmatitic gabbro dikes form a cluster central to data for the other rock types. This suggests that the matrix of the heterolithic gabbro and pegmatitic gabbro dikes may have been derived, at least in part, from a combination of rock types from the northern layered sequence.

The major element data for the majority of the rocks of the Roby Zone, excluding gabbro and clinopyroxenite, define a relationship between MgO content and CaO, Al_2O_3 and Na_2O content (Figure 5.2). As MgO content decreases, CaO, Al_2O_3 and Na_2O contents increase at a constant rate, primarily due to the plagioclase-pyroxene modal effect. Higher modal percent plagioclase feldspar in coarse-grained leucogabbro and East Gabbro correspond to elevated concentrations of CaO, Al_2O_3 and Na_2O . Analytical data for heterolithic gabbro and pegmatitic gabbro dikes plot central to and along the same trend defined by the other lithologies. Clinopyroxenite data form a cluster removed from the trend defined by the other rock types and has a lower relative percentage of Al_2O_3 and Na_2O for similar MgO contents.

The majority of rocks of the Roby Zone show that FeO_T and MnO content increases with increasing MgO content, related to the plagioclase-pyroxene modal effect. MnO distribution is similar to FeO_T , as manganese often replaces iron in both silicate and oxide minerals. Clinopyroxenite and gabbro contain elevated concentrations of FeO_T and MnO relative to the other units, related to an increased modal percentage of clinopyroxene and magnetite.

At varying concentrations of MgO, both K₂O and TiO₂ are widely dispersed within the majority of the rock types. Gabbro and clinopyroxenite contain elevated values of TiO₂, related to an increased percentage of magnetite and ilmenite. Detailed analyses of altered and unaltered rocks found that the more intensely altered samples contain elevated concentrations of Fe, K and Na at the expense of SiO₂, Al₂O₃, MgO and CaO (MacDonald et al., 1987). These observations were not confirmed in this study, but suggests that the FeO, MnO and TiO₂ versus MgO indicate more than just a mineral (plagioclase-pyroxene-orthopyroxene) modal effect is responsible for the element distribution. Possibly, a component of alteration has caused Mn, Fe and Ti depletion and/or Mg enrichment. The result is that several of the data points plot away from the major trends defined by the other points, particularly for FeO, MnO and TiO₂ versus MgO. Boron and chlorine were not analysed in this study, but work of previous researchers suggest that these elements were not enriched in altered or unaltered rocks of the Roby Zone (Sweeny, 1989).

The major element analyses does not define any systematic elemental variation across or within the rocks of the northern layered sequence or the heterolithic gabbro, nor would they be expected to. The significance of this observation is discussed later with the results of additional chemical analyses and field features.

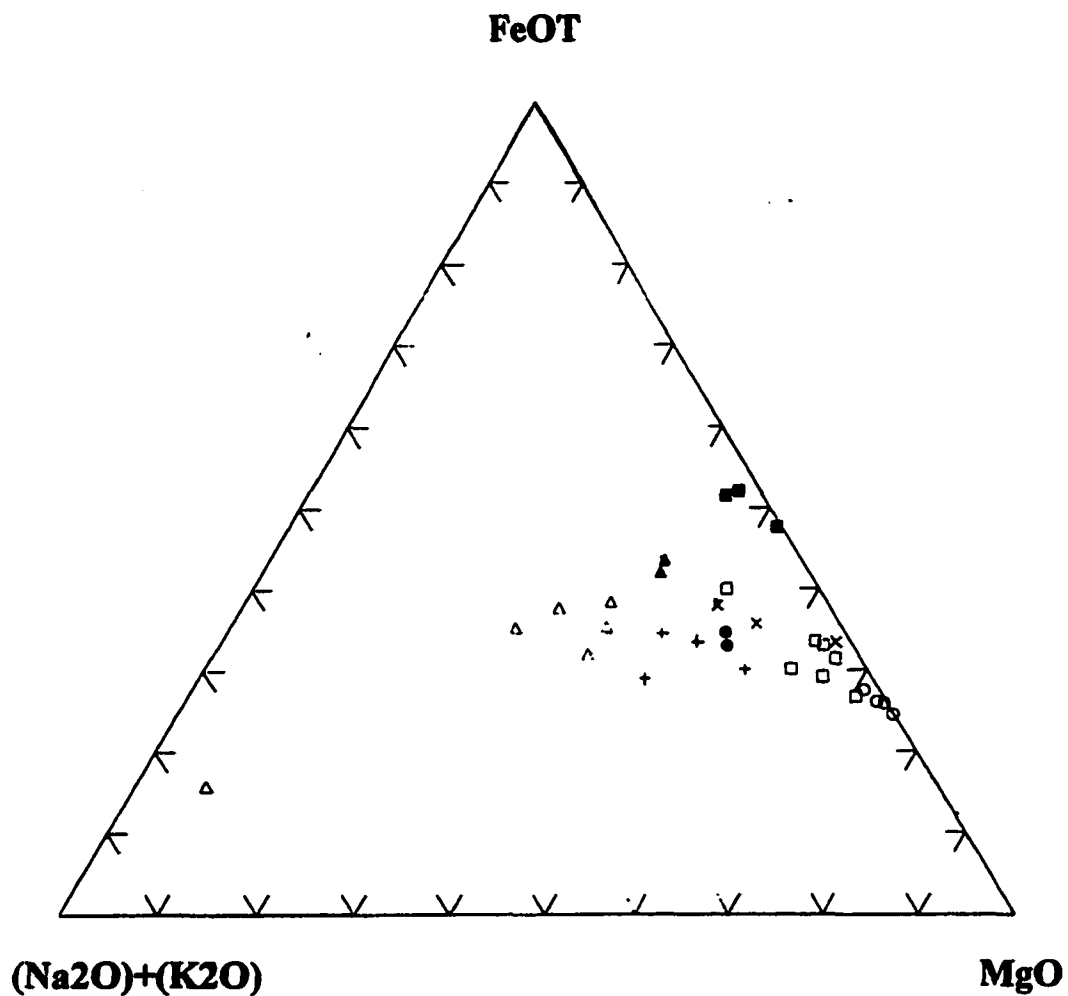


Figure 5.1: Whole rock major elements in weight percent oxides plotted on AFM diagram for shear zone (open circles), gabbronorite (open square), clinopyroxenite (solid square), coarse-grained leucogabbro (+), heterolithic gabbro (x), gabbro (solid triangle), pegmatite gabbro dike (solid circle) and East Gabbro (open triangle).

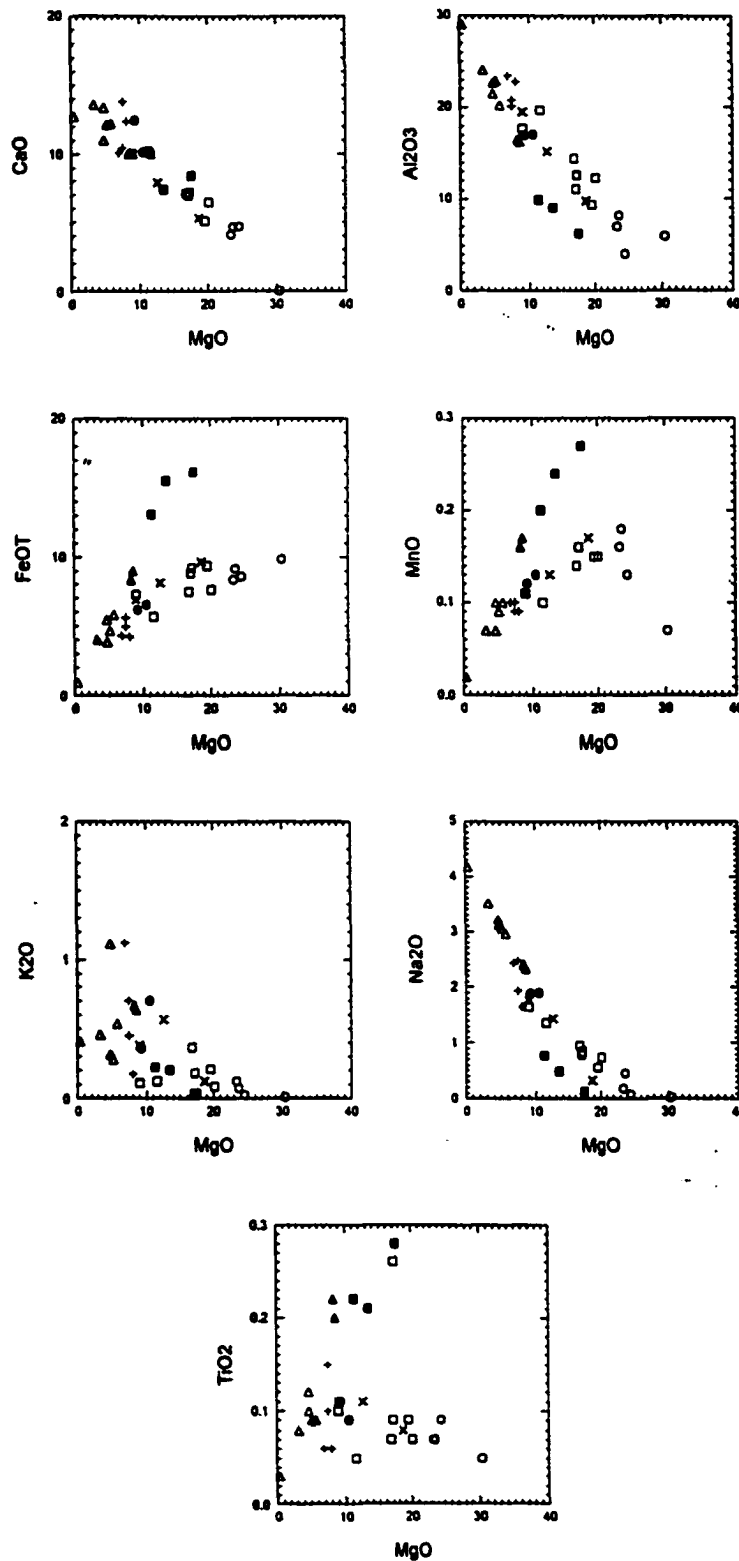


Figure 5.2: Whole rock major elements in weight percent oxides plots of MgO versus MnO, FeOT, Al₂O₃, CaO, TiO₂, Na₂O and K₂O for shear zone (open circles), gabbronorite (open square), clinopyroxenite (solid square), coarse-grained leucogabbro (+), heterolithic gabbro (x), gabbro (solid triangle), pegmatite gabbro dike (solid circle) and East Gabbro (open triangle).

5.3 Trace Elements

The majority of trace elements in the Roby Zone occur in low concentrations and do not vary significantly between rock types. Zirconium concentration is elevated by a factor of approximately two in heterolithic gabbro and late-stage pegmatitic gabbro dikes. Zirconium, which is relatively incompatible in mafic minerals, is often concentrated in the residual melt of a cooling magma (Henderson, 1966). Zirconium is relatively immobile during alteration, making it a useful tool for determining the primary magmatic processes (Henderson, 1966). Heterolithic gabbro, which is composed of various masses texturally and compositionally similar to the northern layered sequence, may have experienced an episode of alteration by deuteric liquids developed within the magma chamber. Pegmatitic gabbro dikes, which are late-stage dikes that crosscut all rock types except the East Gabbro, contain elevated concentrations of zirconium. The concentration of zirconium in a cumulate rock generally reflects the differentiated state of the parent magma and the amount of that magma that is trapped in the cumulate magmas (i.e. amount of post cumulus minerals). The rocks of the shear zone have experienced the strongest degree of alteration of all rock types, however, do not contain elevated values of zirconium. This suggests that the shearing and associated alteration, whether by hydrothermal or deuteric fluids is unrelated to the intrusion of the pegmatite dikes.

Elevated concentrations of bismuth and germanium occur within the heterolithic gabbro and the shear zone, both of which have experienced moderate to strong alteration. Bismuth occurs in discrete platinum group minerals, such as kotulskite, as observed primarily in heterolithic gabbro (Sweeny, 1989). Tellurium and selenium behave in a manner similar to

bismuth, i.e., elevated in the heterolithic gabbro and the shear zone, forming the discrete platinum group minerals kotulskite and merenskyite (Sweeny, 1989). In addition, selenium is enriched in gabbro and clinopyroxenite and correlates well with elevated sulphur concentrations in those samples. A more detailed discussion of the relationship of these elements with platinum group element mineralization is presented in Chapter 7.

Scandium, yttrium, vanadium and cobalt are enriched in clinopyroxenite relative to the other rock types. This enrichment is related to an increased magnetite and ilmenite content in clinopyroxenite, where vanadium and/or cobalt may have replaced iron in magnetite. Molybdenum is randomly dispersed throughout the Roby Zone, related to molybdenite that occurs primarily along fractures crosscutting the Roby Zone.

The highest concentration of chromium occurs in rocks from the shear zone, gabbro and clinopyroxenite, which is in agreement with the observations of Brugmann and Naldrett 1990. Chromium enrichment is related to elevated MgO concentrations. Chromium is compatible in augite and diopside and substitutes for iron in magnetite (Henderson, 1966). Possibly, some of the oxides observed may be Cr-bearing spinel.

Boron, chlorine and fluorine were not analysed in this study, but occur in low concentrations in the gabbroic rocks of the Roby Zone (Sweeny, 1989). Phosphorus is present in minute quantities in the rocks of the Roby Zone. Several apatite grains were identified in this study in the East Gabbro and heterolithic gabbro and, in previous studies associated with magnetite in heterolithic gabbro and gabbro (Sweeny, 1989).

The relatively low concentration of incompatible elements in the rocks of the Roby Zone indicates the minor amount of pore space and interstitial fluid that existed between the cumulate grains. Varying proportions of pore space and intercumulus minerals and the degree of alteration may account for some of the differences between the relative proportions of the various trace elements. Samples collected from gabbro, clinopyroxenite and coarse-grained leucogabbro comprising the northern layered sequence and within the heterolithic gabbro do not have significant differences in major and trace element proportions.

5.4 Rare Earth Elements

Rare earth element (REE) analyses were completed for each of the various rock types comprising the northern layered sequence and for similar sections within the heterolithic gabbro. Analytical results are summarized in Appendix 2 and the REE profiles are plotted in Figures 5.3 to 5.5.

Gabbronorite from the northern layered sequence and within the heterolithic gabbro contain the lowest concentrations of rare earth elements relative to the other rock types, suggesting they are more adcumulate than the others (Figure 5.3a). The REE patterns consistently show a moderate light rare earth element (LREE) enrichment and minor enrichment of the heavy rare earth elements (HREE) with a $La_{(N)}/Yb_{(N)}$ ratio of approximately 3. The REE pattern is concave-upwards, indicating the cumulate is from a parental magma with a fractionated REE pattern (Sutcliffe, 1989) or from a mixture of plagioclase and pyroxene cumulus minerals. Gabbronorite has a relatively high positive Eu anomaly reflecting the presence of cumulate plagioclase feldspar. Previous studies (Brugmann, 1989) found gabbronorite depleted in LREE, an observation not confirmed in this study.

Gabbro from the northern layered sequence contains elevated values for all of the rare earth elements, with LREE enrichment relative to the HREE (Figure 5.3b). Gabbro has a highly variable $La_{(N)}/Yb_{(N)}$ ratio reflected in two samples with $La_{(N)}/Yb_{(N)}$ of 9/1 and 5/3. $La_{(N)}/Yb_{(N)}$. The high, but variable ratios suggest that these rocks have experienced a high degree of fractionation and may contain a higher proportion of intercumulus minerals. The REE patterns have different slopes for each of the two samples. Gabbro has a moderate positive Eu anomaly, related again to the presence of cumulate plagioclase feldspar.

REE profiles for clinopyroxenite from the northern layered sequence and within heterolithic gabbro have a flat curve with only slight HREE enrichment. This profile is typical of pyroxenes since HREE are slightly less incompatible in pyroxenes than LREE (Figure 5.3c). The profiles do not contain an Eu anomaly related to the lack of appreciable amounts of plagioclase feldspar.

REE patterns for East Gabbro show a strong positive Eu anomaly with LREE enrichment and $La_{(N)}/Yb_{(N)}$ ratios of approximately 3 (Figure 5.4a). The strong positive Eu anomaly is related to the presence of abundant plagioclase feldspar. Coarse-grained leucogabbro has a moderate positive Eu anomaly and a strong LREE enrichment with a $La_{(N)}/Yb_{(N)}$ ratio of approximately 9 (Figure 5.4b). This strong LREE enrichment is also related to the presence of abundant plagioclase feldspar.

Heterolithic gabbro and pegmatitic gabbro dikes define a concave-upward curve, with moderate LREE and HREE enrichment (Figure 5.4c). The REE patterns are consistent for the various samples, which is surprising considering the lithological variation within the heterolithic gabbro. Although field evidence indicates the pegmatitic gabbro dikes may represent the latest stage of fluid movement in the magma chamber, REE analyses suggest that they were not derived from highly fractionated liquids and often contain lower total REE concentrations than several of the other rock types, including gabbro and coarse-grained leucogabbro. This suggests that the pegmatitic gabbro dikes may have been derived from elsewhere in the magma chamber and not necessarily from the residual melt.

Total REE abundances increase in the sequence: gabbro, clinopyroxenite, heterolithic gabbro, East Gabbro, gabbro and coarse-grained leucogabbro. The REE profiles for the aforementioned rock types suggest that they may contain varying proportions of intercumulus minerals and/or have experienced varying degrees of alteration. The overall REE concentrations for the rocks of the Roby Zone have values higher than the chondritic values, suggesting that they were derived from differentiated magmas. The REE patterns show that as LREE content increases, the Eu anomaly decreases. The decreased Eu value is related to the higher proportion of intercumulus liquid relative to cumulus plagioclase feldspar. The intercumulus liquid is Eu depleted, whereas the plagioclase cumulates are Eu enriched. The crystallization sequence of orthopyroxene-clinopyroxene shown in the rocks of the Roby Zone is typical of tholeiitic intrusions in continental crust (Campbell, 1985). Zr, MgO and SiO₂ do not have a direct correlation with the REE patterns, related to the varying proportions of intercumulus phases. No significant differences were observed in REE patterns between compositionally similar samples from the northern layered sequence and within heterolithic gabbro.

The rocks of the shear zone have the most variable REE patterns of all rock types, ranging from almost flat with slight HREE enrichment to steeply sloping profiles with a high degree of LREE enrichment (Figure 5.5a). The La_(N) values range up to 60. The Eu content varies from moderately negative to moderately positive. The majority of samples have a negative Eu anomaly, related to the lack of cumulate plagioclase feldspar in the rocks of the shear zone. The highly variable REE patterns suggests that the shear zone is composed of material derived from various sources that may have been introduced into the shear zone during multiple alteration episodes, when shearing and fluid movement may have been reactivated.

The REE data for samples collected from the felsic dikes cross-cutting the rocks of the Roby Zone and for samples collected from the tonalite gneiss surrounding the Lac des Iles Complex are plotted on Figure 5.5b. The late-stage felsic dikes are LREE enriched with a $\text{La/Yb}_{(N)}$ ratio of approximately 30. The REE patterns have a strong positive Eu anomaly, related to the abundance of cumulate plagioclase feldspar. The tonalite gneiss has lower overall REE concentrations than the felsic dikes, however, contains a very strong positive Eu anomaly, related to the high modal proportion of plagioclase feldspar in these rocks.

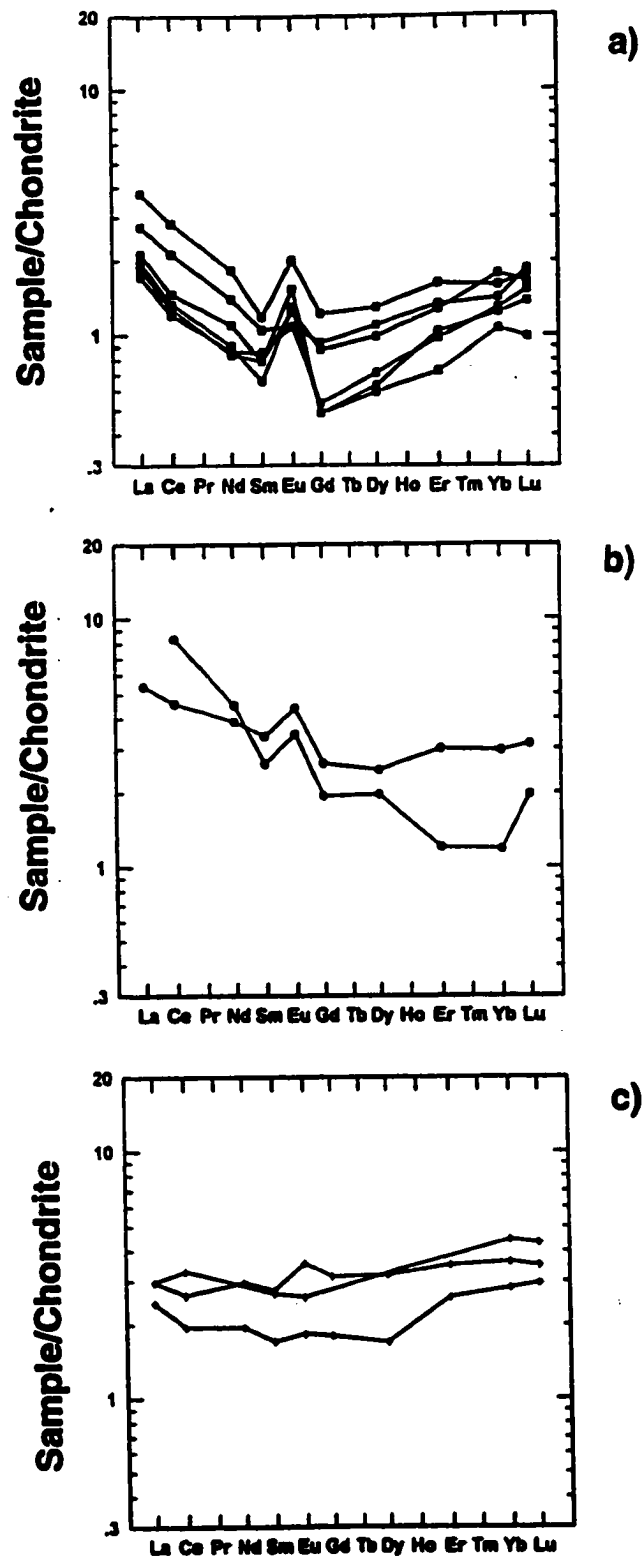


Figure 5.3: Chondrite normalized rare earth element profiles for rocks of the Roby Zone; (a) gabbronorite, (b) gabbro, and (c) clinopyroxenite. Chondrite normalizing values from Nakamura (1977).

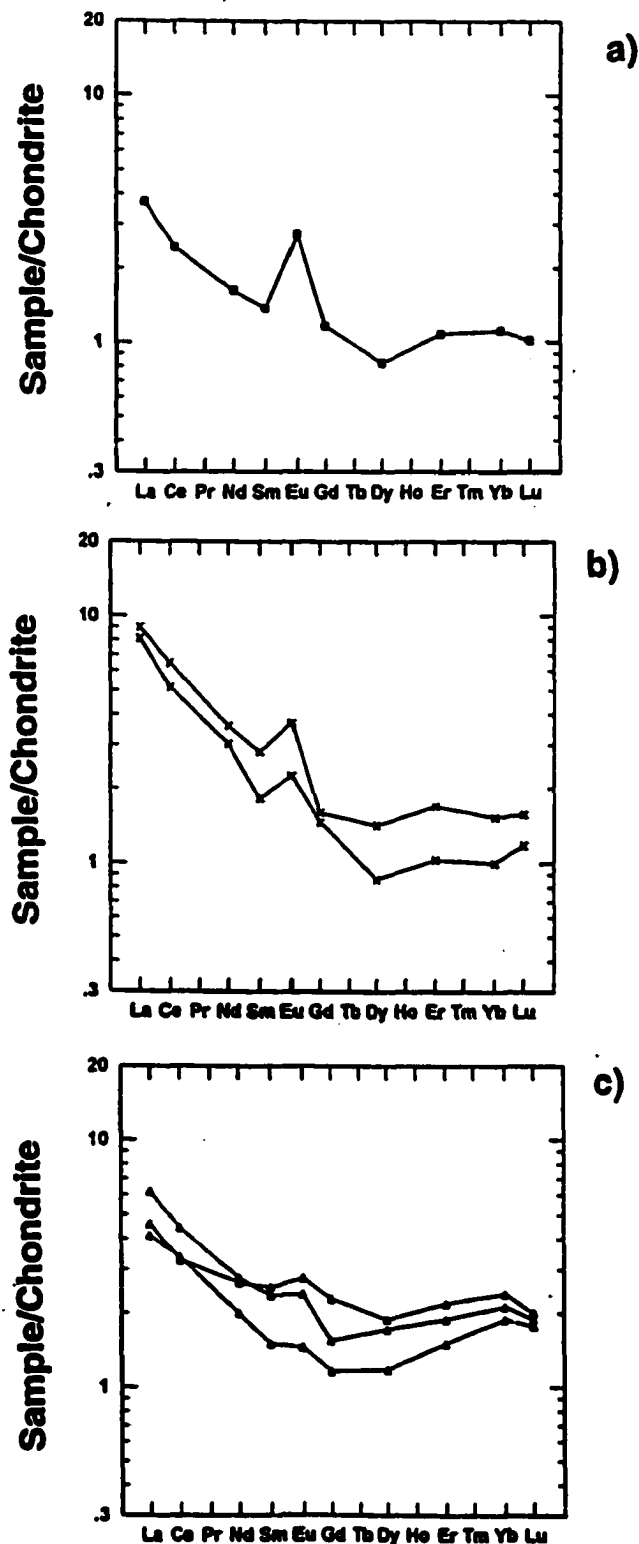


Figure 5.4: Chondrite normalized rare earth element profiles for rocks of the Roby Zone; (a) East Gabbro, (b) coarse-grained leucogabbro, and (c) heterolithic gabbro (open triangle) and pegmatite gabbro dike (solid triangle). Chondrite normalizing values from Nakamura (1977).

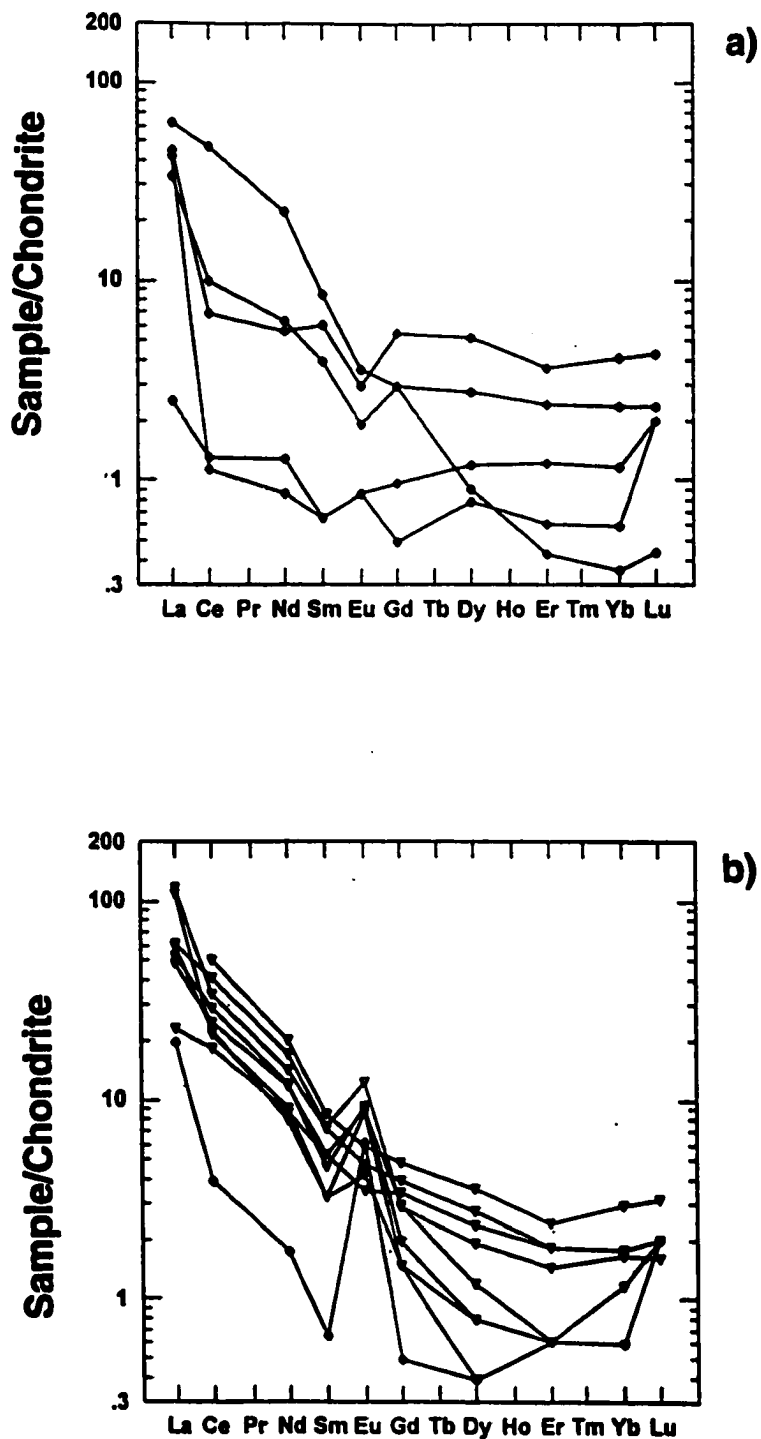


Figure 5.5: Chondrite normalized rare earth element profiles for rocks of the Roby Zone; (a) shear zone, and (b) felsic dikes (open inverted triangles) and tonalite gneiss (solid diamonds). Chondrite normalizing values from Nakamura (1977).

6.0 Silicate Mineral Composition

During this study, the compositions of orthopyroxene, clinopyroxene, feldspar and amphibole were determined using a scanning electron microscope to a) characterize the various lithologies; b) identify any systematic elemental trends within lithologies and across the northern layered sequence; c) compare similar lithological sections within heterolithic gabbro and the northern layered sequence; d) identify secondary alteration minerals; and e) identify the presence of chemical zoning within mineral grains. Mineral analyses were completed on altered and unaltered samples from layers comprising the northern layered sequence, heterolithic gabbro, pegmatitic gabbro dikes, shear zone and from tonalite encompassing the Lac des Iles Complex. A detailed description of the analytical methods and a listing of the results are presented in Appendix 3.

6.1 Orthopyroxene

A total of thirty orthopyroxene grains were analysed from six different samples representing gabbro, clinopyroxenite and coarse-grained leucogabbro layers within the northern layered sequence and within masses in the heterolithic gabbro. The majority of orthopyroxene grains analysed are cumulus grains, with a lesser number of intercumulus grains. Chemical analyses were completed primarily on the core areas of the mineral grain, although a lesser number of analyses were completed on the margins of the grain.

Orthopyroxenes have a compositional range of $En_{74}Wo_4Fs_{22}$ to $En_{80}Wo_1Fs_{19}$ for gabbro, $En_{66}Wo_7Fs_{27}$ to $En_{78}Wo_2Fs_{20}$ for coarse-grained leucogabbro, and $En_{61}Wo_4Fs_{35}$ to $En_{75}Wo_2Fs_{23}$ for clinopyroxenite (Table 6.1, Appendix 3). The compositional range for these lithologies show considerable overlap. The overall compositions of

orthopyroxenes plot primarily in the enstatite field of the pyroxene quadrilateral diagram (Figure 6.1). Orthopyroxenes from gabbro have the most restricted compositional range of all lithologies, which is often typical of adcumulate and mesocumulate textured rocks of a common parental magma (Sutcliffe et al., 1989). Orthopyroxenes from clinopyroxenite and coarse-grained leucogabbro have a much less restricted compositional range. Overall, the Fe:Mg ratio in orthopyroxene varies considerably for the rocks of the Roby Zone, whereas the Ca content has a limited range. Orthopyroxenes from gabbro have a significantly lower Fe:Mg ratio than orthopyroxenes from coarse-grained leucogabbro and clinopyroxenite, indicating that gabbro is the most primitive lithology having experienced less fractionation than the other two rock types.

Significant elemental variation in orthopyroxene composition correlates with modal igneous layering observed across the northern layered sequence. Elemental variation in orthopyroxene composition, in particular the Fe:Mg ratio, across the northern layered does not define a systematic elemental trend related to stratigraphic position. The lack of an observed trend may be due, at least in part, to the paucity of orthopyroxene grains and to the limited sampling across the various layers. Cyclic layering, or repetition of Fe- and/or Mg-rich layers, was not observed within the layered sequence, confirming observations from a previous study (Dunning, 1979).

Similarities in orthopyroxene composition from lithologically similar sections within heterolithic gabbro and the northern layered sequence are consistent with field and geochemical data suggesting the various lithologic sections within the heterolithic gabbro may have been derived from the northern layered sequence. Minor differences were observed in orthopyroxene composition between the core and margin areas of the grains for Al_2O_3 , TiO_2 , MnO and CaO . Typically, MnO , TiO_2 and CaO are enriched along the margins

of the grain. The En content varied by several percent between the core and margin areas of the grain, although no systematic variations were identified within the same sample or between samples.

Table 6.1: Representative Compositions of Orthopyroxenes from the Roby Zone.

Sample #	Lac-63	Lac-40	D1	D5	Lac-33
Rock type	Gabbronorite	Pyroxenite	Gabbronorite	Pyroxenite	Leucogabbro
Grain area	core	core	core	core	rim
SiO ₂	54.82	52.99	55.13	53.38	56.60
TiO ₂	0	0	0	0	0.16
Al ₂ O ₃	2.12	1.01	1.52	1.36	1.02
FeO	12.25	22.01	13.06	21.08	16.05
MnO	0.29	0.46	0	0.27	0.62
MgO	29.39	21.57	29.63	23.79	22.10
CaO	0.91	2.10	0.54	1.17	3.28
Na ₂ O	0	0.47	0	0.68	0.51
Total	99.78	100.61	99.880	101.730	100.34

Number of ions based on 6 oxygen atoms

Si	1.950	1.970	1.962	1.948	2.044
Al ^{IV}	0.050	0.030	0.038	0.052	0
Al ^{VI}	0.039	0.014	0.025	0.007	0.043
Ti	0	0	0	0	0.004
Fe	0.364	0.684	0.389	0.643	0.485
Mn	0.009	0.014	0	0.008	0.019
Mg	1.559	1.195	1.572	1.294	1.190
Ca	0.035	0.084	0.021	0.046	0.127
Na	0	0.034	0	0.048	0.036
Fs	18.6	34.8	19.6	32.4	26.9
Wo	1.8	4.3	1.1	2.3	7.0
En	79.6	60.9	79.3	65.3	66.0

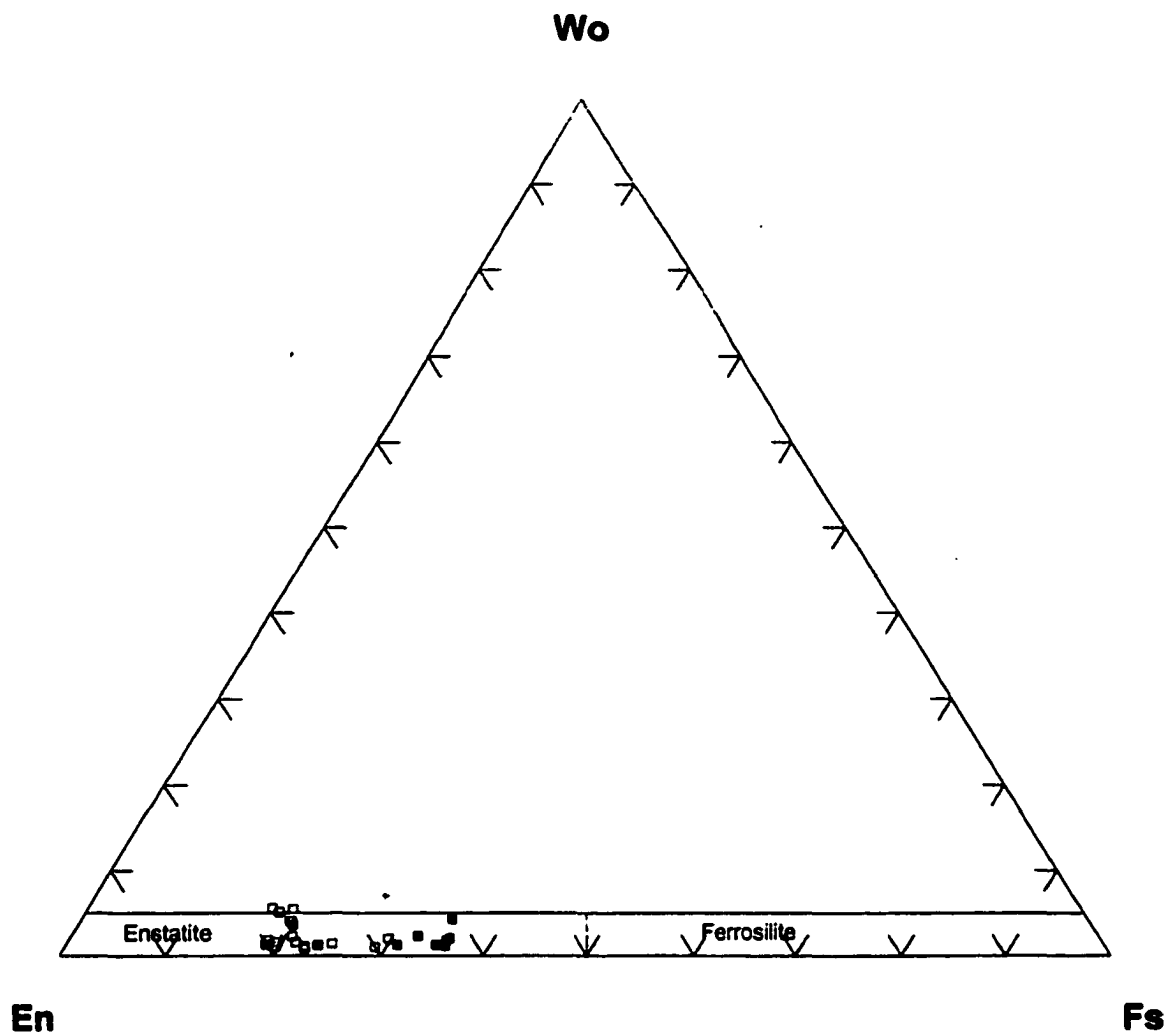


Figure 6.1: Pyroxene triangular plot showing the compositional range of orthopyroxenes from several of the rock types comprising the Roby Zone. The data points represent SEM analyses of grain cores and margins. Gabbronorite (open square), gabbro (solid triangle), coarse-grained leucogabbro (plus sign), clinopyroxenite (solid square) and pegmatitic gabbro dyke (solid circle) are shown. Nomenclature from Morimoto et al. (1988)

Fs = FeSiO_3

Wo = CaSiO_3

En = MgSiO_3

6.2 Clinopyroxene

A total of twenty-four clinopyroxene grains were analysed from eight samples representing the majority of rock types comprising the Roby Zone (Table 6.2, Appendix 3). The relatively low number of analyses of clinopyroxene grains is indicative of the difficulty experienced in locating unaltered samples. Both the core and margin areas of mineral grains were analysed from cumulus and intercumulus grains. Clinopyroxene compositions plot as a large cluster predominantly in the diopside and augite fields of the pyroxene quadrilateral diagram (Figure 6.2). Clinopyroxene compositions from the two samples of gabbronorite show little variation and lie in the range $En_{46-47}Wo_{45-47}Fs_{6-8}$, whereas clinopyroxene from two samples of clinopyroxenite lie in the range $En_{39-45}Wo_{36-48}Fs_{13-19}$. Clinopyroxene compositions from clinopyroxenite show considerable variation in Ca content relative to the other lithologies, which may be due to the greater percentage of intercumulus clinopyroxene. Clinopyroxene compositions from other rock types of the Roby Zone plot near the centre of the clinopyroxene field and have a much less restricted compositional range for Ca, Fe and Mg than for gabbronorite. The compositions of clinopyroxene for these other rock types have considerable mutual overlap.

Clinopyroxenes from clinopyroxenite layers and pegmatitic gabbro dikes have elevated Fe:Mg ratios relative to the other rock types. This suggests that clinopyroxenite and pegmatitic gabbro dikes have experienced the highest degree of fractionation, whereas gabbronorite has experienced the lowest degree of fractionation from the original magma. The high degree of fractionation indicated by clinopyroxene composition within pegmatitic gabbro dikes suggest pegmatitic gabbro dikes were emplaced during the latest stages of magma differentiation. The relatively high Fe:Mg ratio observed in clinopyroxenes from clinopyroxenite correlates well with the results of previous research, suggesting that

clinopyroxenite may be the fractionated equivalent of the northern ultramafic portion of the Lac des Iles Complex (Brugmann et al., 1990). The varying Fe:Mg ratio in clinopyroxenes across the various rock types of the northern layered sequence and the abrupt changes in modal proportion of cumulus minerals across geologic contacts suggests the various layers may have been derived from the same magma source and have experienced varying degrees of fractionation prior to emplacement.

Only minor differences were observed in clinopyroxene composition from similar masses within heterolithic gabbro and the northern layered sequence, suggesting that these sections may have been derived from the northern layered sequence. Minor differences were observed in clinopyroxene composition between intercumulus and cumulus grains, although the observed variation is not systematic within the same sample or between samples. Minor compositional differences were observed in CaO, MnO and TiO₂ content between the core and margin areas of clinopyroxene mineral grains. The CaO content is typically enriched in the core areas of clinopyroxene; however, elevated values of CaO were often observed along the margins of the grain. This indicates the presence of chemical zoning within clinopyroxenes and agrees with observations reported by previous researchers (Dunning, 1979). Exsolution was not evident in orthopyroxene grains.

Table 6.2: Representative Compositions of Clinopyroxenes from the Roby Zone.

Sample #	D5	Lac-33	Lac-40	Lac-36	D13
Rock type	Pyroxenite	Leucogabbro	Clino-pxn	Peg dike	Gabbronorite
Grain area	rim	Core	core	core	core
SiO ₂	53.02	51.51	49.46	52.58	52.97
TiO ₂	0.47	0.55	0.52	0.41	0.29
Al ₂ O ₃	3.02	2.18	3.97	2.11	3.19
FeO	9.48	7.24	9.80	9.66	5.07
MnO		0.22	0.34	0.25	
MgO	14.34	14.41	13.23	14.03	16.49
CaO	22.09	23.06	20.02	21.38	22.84
Na ₂ O	0.44	0.49	0.99	0.63	0.44
Total	102.86	99.66	98.33	101.05	101.29

Number of ions based on 6 oxygen atoms

Si	1.922	1.924	1.886	1.945	1.918
Al ^{IV}	0.078	0.076	0.114	0.055	0.082
Al ^{VI}	0.051	0.020	0.065	0.037	0.054
Ti	0.013	0.015	0.015	0.011	0.008
Fe	0.287	0.226	0.313	0.299	0.153
Mn	0	0.007	0.011	0.008	0
Mg	0.775	0.803	0.752	0.774	0.890
Ca	0.858	0.923	0.818	0.847	0.886
Na	0.031	0.035	0.073	0.045	0.031
Fs	14.9	11.6	16.6	15.6	7.9
Wo	44.7	47.3	43.4	44.1	45.9
En	40.4	41.1	39.9	40.3	46.1

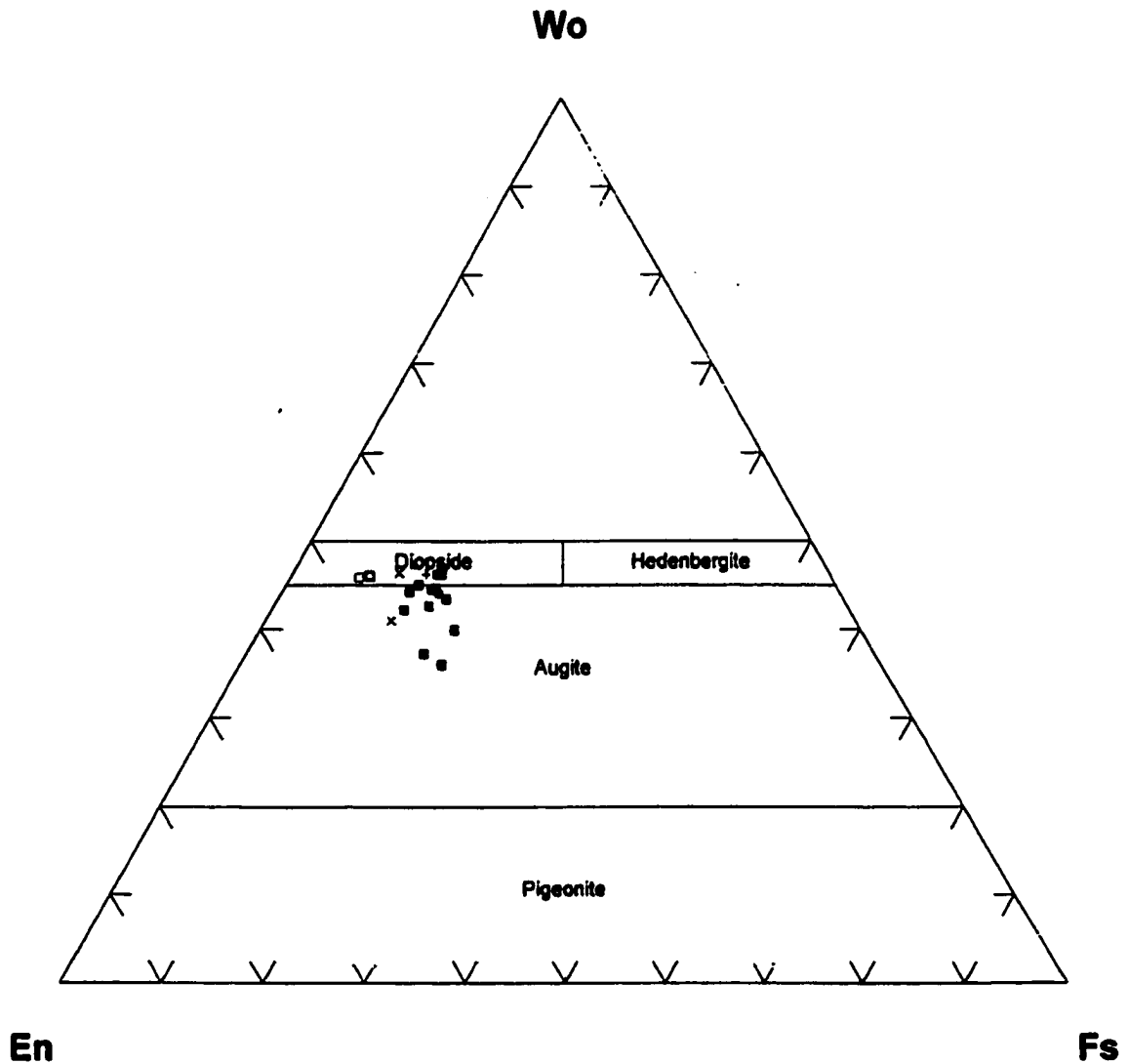


Figure 6.2: Pyroxene triangular plot showing the compositional range of clinopyroxenes from several of the rock types comprising the Roby Zone. The data points represent SEM analyses of grain cores and margins. Gabbronorite (open square), coarse-grained leucogabbro (+), East Gabbro (open triangle), clinopyroxenite (solid square), pegmatite gabbro dike (solid circle) and tonalite (X) are shown. Nomenclature from Morimoto et al. (1966)

Fs = FeSiO_3

Wo = CaSiO_3

En = MgSiO_3

6.3 Plagioclase

A total of sixty-three plagioclase grains were analysed from twelve samples representing the majority of rock types comprising the Roby Zone (Table 6.3, Appendix 3). The majority of mineral grains analysed were cumulus grains, although several intercumulus plagioclase grains were analysed. Plagioclase compositions range from predominantly bytownite to labradorite. The compositional range for plagioclase in gabbronorite, leucogabbro, clinopyroxenite (with the exception of one anomalous sample) and East Gabbro is very restricted, in the range An_{75-81} , An_{75-81} , An_{54-75} and An_{61-68} , respectively (Figure 6.3).

Plagioclase from gabbro, the shear zone and pegmatitic gabbro dikes have a much less restricted chemical composition ranging from An_{40-66} , An_{35-44} and An_{30-68} , respectively.

Plagioclases from gabbronorite and leucogabbro have the highest An-composition, suggesting that these two lithologies have experienced the lowest degree of fractionation. Plagioclase from East Gabbro and clinopyroxenite have the lowest An composition of the other rock types of the Roby Zone and may reflect that the plagioclase is, at least in part, post-cumulus. In addition to a relatively low An-content, clinopyroxene from clinopyroxenite, the shear zone and pegmatitic gabbro dikes have a corresponding elevated concentration of K_2O in the range $Or_{0.8-1.1}$ in clinopyroxenite to $Or_{6.4-8.1}$ in the shear zone. Due to the elevated Or-content and corresponding relatively low An-content for plagioclase, clinopyroxenite appears to have formed by fractionation of a tholeiitic magma. Plagioclases from the shear zone have not only elevated Or-concentrations, but are extremely wide ranging compositionally relative to the other rock types. Observations of outcrop-scale features suggest the shear zone is the altered equivalent of clinopyroxenite layering identified in the northern layered sequence. Since plagioclases within clinopyroxenite do not have the wide ranging An-content of that observed in the shear zone, it suggests that the shear zone may have experienced multiple episodes of alteration by deuteric and/or hydrothermal fluids.

Potassium is a very mobile element during hydrothermal alteration, thus the elevated Or-content in plagioclase may reflect a high fluid content during shearing and recrystallization. The relatively high and inconsistent An content of plagioclase within pegmatitic gabbro dikes confirm earlier interpretations based on outcrop-scale features that suggest the dikes are late-stage, fractionated deuteritic fluids derived from different locations within the magma chamber.

Although the overall plagioclase composition varies significantly in the Roby Zone, no systematic elemental variations were identified within individual rock types or across the igneous stratigraphy, although the number and details of the sampling may have been too limited to detect any trends. This agrees with the observations for clinopyroxene compositions, suggesting in-situ fractionation has not played a significant role in the formation of the northern layered sequence.

Significant compositional zoning up to An₁₀ has been observed between the core and margin areas of plagioclase grains. Occasionally, Na-enrichment in the core areas of several grains has been observed, indicating the presence of normal and reverse chemical zoning in plagioclase. No significant differences in plagioclase composition were observed for lithologically similar sections within heterolithic gabbro and the northern layered sequence.

This observation is in agreement with observations of orthopyroxene and clinopyroxene compositions. The similarity in mineral composition suggests the lithologically similar sections within heterolithic gabbro may be derived from the northern layered sequence.

Table 6.3: Representative Compositions of Feldspars from the Roby Zone.

Sample #	Lac-5	Lac-63	D16	Lac-65	Lac-33	Lac-98	Lac-36
Rock type	East	Gabbronorite	Clinopyrox	East	Leuco-	Het Gab	Peg dike
Grain area	Gabbro	Rim	Rim	Gabbro	gabbro	core	core
	core			core	core		core
SiO ₂	52.53	49.13	54.15	51.48	47.07	49.24	53.35
Al ₂ O ₃	31.96	34.10	27.67	28.77	33.36	33.6	30.37
FeO	0	0.26	2.68	0	0.42	0	0.28
CaO	13.05	16.12	6.0	13.18	16.79	14.5	11.76
Na ₂ O	4.18	2.71	5.29	0	2.03	2.91	4.68
K ₂ O	0	0	1.14	4.52	0.09	0	0.13
Total	101.72	102.32	98.87	97.95	99.76	100.25	100.57

Number of ions based on 8 oxygen atoms

Si	2.340	2.200	2.481	2.411	2.171	2.235	2.400
Al	1.678	1.800	1.494	1.588	1.813	1.798	1.610
Fe	0	0.010	0.103	0	0.016	0	0
Ca	0.623	0.773	0.294	0.661	0.830	0.705	0.567
Na	0.361	0.235	0.470	0	0.182	0.256	0.408
K	0	0	0.067	0.270	0.005	0	0.007
Or	0	0	8.1	0	.5	0	.7
An	63.3	76.7	35.4	71.0	81.6	73.4	57.7
Ab	36.7	23.3	56.6	29.0	17.9	26.6	41.5

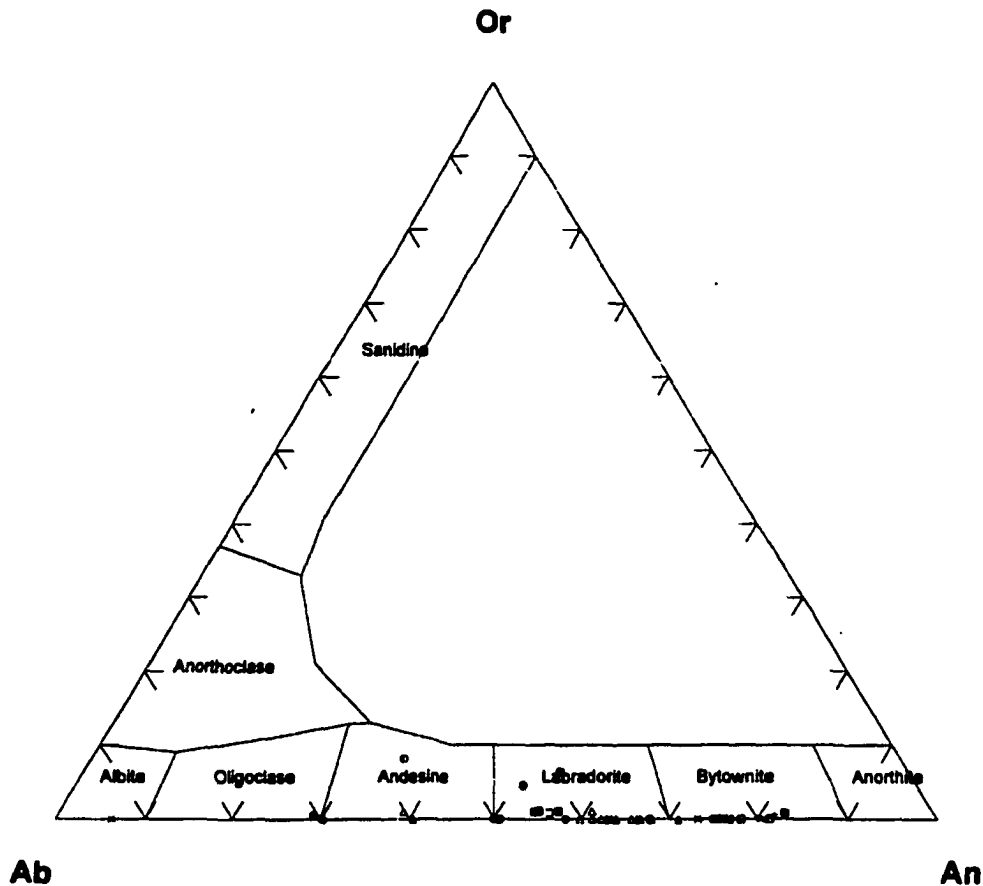


Figure 6.3: Feldspar triangular plot showing the compositional range of feldspars from the majority of rock types comprising the Roby Zone. The data points represent SEM analyses of grain cores and margins. Gabbronorite (open square), gabbro (solid triangle), coarse-grained leucogabbro (+), East Gabbro (open triangle), clinopyroxenite (solid square), shear zone (half-filled circle) pegmatite gabbro dike (solid circle) and tonalite (X) are shown.



6.4 Amphibole

A total of eighty-four amphibole minerals were analysed from thirteen samples representing the majority of rock types comprising the Roby Zone (Table 6.4, Appendix 3). The amphibole minerals occur primarily as pseudomorphs of cumulus and intercumulus silicates and occasionally, and as primary cumulate grains of hornblende. Amphiboles have a very broad chemical composition, ranging from actinolite to tremolite as pseudomorphs of clinopyroxene, anthophyllite as pseudomorphs of orthopyroxene (Figure 6.4). Amphibole classification was completed according to Leake (1978).

6.5 Other Minerals

During this study, several apatite grains were identified in the East Gabbro and gabbronorite, although the chemical composition of these apatite grains were not determined. Previous studies have found the presence of minor fluorine (0.0-1.06%) and chlorine (0.0-2.23%) in apatite from two samples from the Roby Zone, although typical concentrations are very close to detection limits (Sweeny, 1989).

Table 6.4: Representative Compositions of Amphiboles from the Roby Zone.

Sample # Rock type	D5 Pyroxenite	Lac-60 Het Gab	Lac-33 Leuco gabbro	D1 Gabbronorite	D15 Clinopyrx	Lac-42 Peg dike	Lac-5 East Gabbro	Lac-31 Gabbro
Grain area	rim	core	core	core	rim	core	rim	rim
SiO ₂	54.85	54.44	56.82	53.47	58.47	56.6	54.5	52.6
TiO ₂	0	0	0.17	0	0.4	0.23	0.19	0
Al ₂ O ₃	2.36	2.45	1.96	4.35	4.22	3.4	3.81	4.22
FeO	12.44	10.99	9.37	6.71	11.34	7.86	12.6	12.28
MnO	0.44	0.34	0	0	0.25	0	0	0
MgO	17.95	17.14	19.14	20.67	12.27	18.78	16.04	16.24
CaO	11.05	12.45	12.98	11.78	8.75	11.97	12.44	12.82
Na ₂ O	0.48	0.4	0.34	0.74	0.61	0.5	0.58	0.59
K ₂ O	0	0	0	0.24	0	0	0	0
Total	99.57	98.21	100.78	97.96	96.31	99.34	100.16	98.75

Number of ions based on 24 (O, F, Cl)

Si	7.706	7.731	7.780	7.474	8.253	7.775	7.627	7.493
Al ^{IV}	0.294	0.269	0.220	0.526	0	0.225	0.373	0.507
Al ^{VI}	0.097	0.141	0.097	0.190	0.702	0.325	0.255	0.202
Ti	0	0	0.018	0	0.042	0.024	0.020	0
Mg	3.759	3.628	3.907	4.307	2.582	3.846	3.346	3.449
Fe	1.462	1.305	1.073	0.784	1.339	0.903	1.475	1.463
Mn	0.052	0.041	0	0	0.030	0	0	0
Ca	1.663	1.894	1.904	1.764	1.323	1.762	1.865	1.957
Na	0.131	0.110	0.089	0.201	0.167	.133	0.157	0.163
K	0	0	0	0.043	0	0	0	0
O	24	24	24	24	24	24	24	24
Grunerite	21.2	19.1	15.6	11.4	25.5	13.9	21.0	21.3
Anthophyllite	24.2	27.7	27.7	25.7	25.2	27.1	19.4	28.5
Tschermak's molecule	54.6	53.1	56.8	62.8	49.2	59.1	59.7	50.2

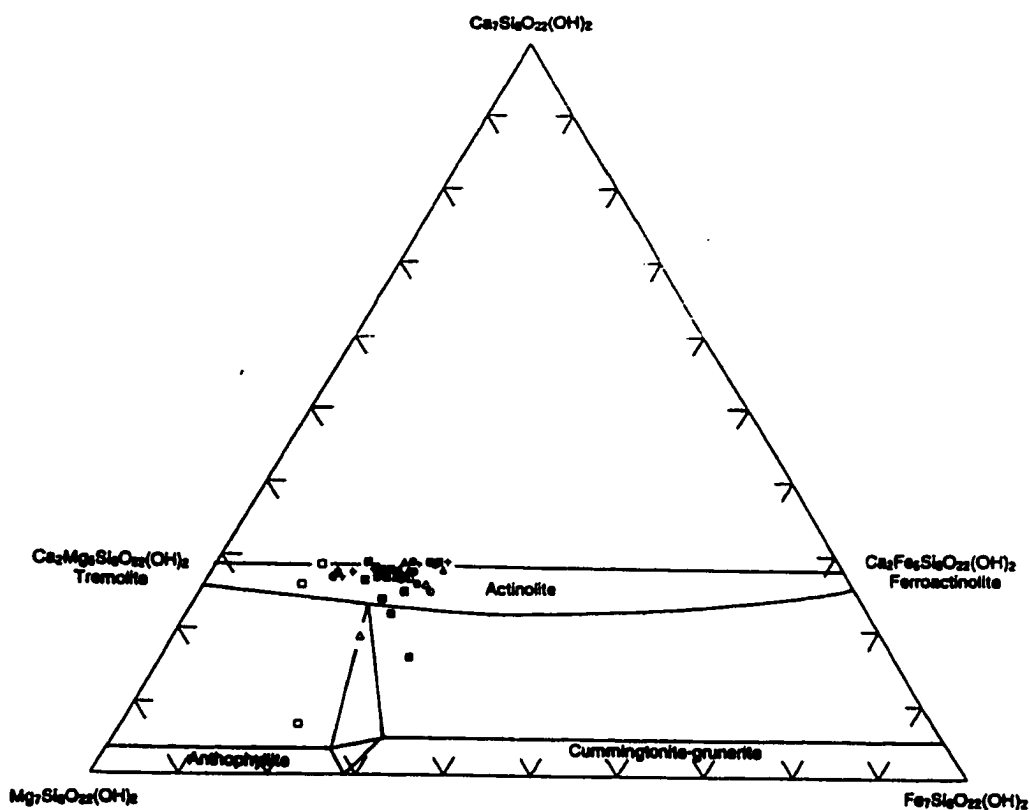


Figure 6.4: Amphibole triangular plot showing the compositional range of amphiboles from various rock types comprising the Roby Zone. The data points represent SEM analyses of grain cores and margins. Gabbronorite (open square), gabbro (solid triangle), coarse-grained leucogabbro (plus sign), East Gabbro (open triangle), clinopyroxenite (solid square), pegmatitic gabbro dyke (solid circle) and tonalite (X) are shown. Nomenclature after Klein and Hurlbutt (1993).

$\text{Ca}_7\text{Si}_6\text{O}_{22}(\text{OH})_2$ – Tschermak's molecule

$\text{Mg}_7\text{Si}_6\text{O}_{22}(\text{OH})_2$ - Anthophyllite

$\text{Fe}_7\text{Si}_6\text{O}_{22}(\text{OH})_2$ - Grunerite

7.0 Platinum Group Element Mineralization

7.1 Introduction

Platinum group elements (PGE) occur in variable amounts in almost every rock type comprising the Roby Zone, including the northern layered sequence, heterolithic gabbro, pegmatitic gabbro dikes and the shear zone. Previous studies have identified the habit and composition of individual platinum group minerals (Sweeny, 1989; Dunning, 1979). As part of this study, a broader-based quantitative approach was undertaken to determine the relative concentration and relationship between PGEs, chalcophile elements and sulphur within the various rock types comprising the Roby Zone. In an attempt to identify the different conditions that were present during PGE mineralization, the relationship between these elements was compared to rock type, alteration pattern and varying sulphide content. The relative concentration of PGEs, chalcophile elements and sulphur were used as a basis for comparison with other PGE deposits in order to identify the processes involved in PGE mineralization within the Roby Zone that are common to other types of PGE deposits.

During this study, a total of 33 altered and unaltered rock samples of diverse sulphide content were collected from each of the rock types comprising the Roby Zone and submitted for platinum group element analyses. The analyses were completed by neutron activation at Activation Laboratories Ltd., Ancaster, Ontario. A brief description of the methodology, detection limits and a listing of the results are presented in Appendix 4.

7.2 Sulphide Mineralization

Sulphide mineralization within the Roby Zone varies considerably in habit and concentration throughout the deposit. Sulphide mineralization, which rarely exceeds 5 vol.%, is most pronounced in the heterolithic gabbro and pegmatitic gabbro dikes, consisting of fine-grained disseminations and irregularly shaped blebs up to 1.0 centimeter in diameter. Net-textured sulphides are common in gabbronorite and clinopyroxenite. Pyrrhotite and pyrite blebs, which are often intergrown with pentlandite and chalcopyrite, form the bulk of the sulphide mineralization; however, the relative proportion of sulphide minerals varies among rock type. Fine-grained pyrite and chalcopyrite are often found within secondary silicates surrounding a sulphide bleb (Sweeny, 1989). Additional sulphide minerals previously identified in the Roby Zone that typically occur in trace amounts consist of millerite, violarite, sphalerite and galena (Dunning, 1979). Molybdenite has been observed along narrow fractures in this study.

7.3 Platinum Group Element-Gold-Copper-Nickel Mineralization

Twelve platinum group minerals have been previously identified in the Roby Zone, including braggite, kotulskite, isometrieite, merenskyite, moncheite, palladoarsenide, sperrylite, stibiopalladinite, stilwaterite, vysotskite, unnamed $\text{Ag}_4\text{Pd}_3\text{Te}_4$ and unnamed Pd_5As_2 (Watkinson, 1975; Dunning, 1979; Cabri and Lafamme, 1979; Sweeny, 1989). The relative order of abundance of the platinum group minerals varies considerably across the deposit. Braggite and vysotskite predominate within the northern layered sequence, whereas kotulskite and merenskyite predominate in many areas within the southern portion of the Roby Zone, specifically in the shear zone and heterolithic gabbro (Sweeny, 1989). The majority of platinum group minerals occur wholly within sulphides or associated with

sulphides at sulphide-silicate boundaries (Sweeny, 1989). Platinum group minerals also occur as discrete minerals within secondary silicates of altered rocks, such as the shear zone and heterolithic gabbro. In addition to forming discrete platinum group minerals, palladium also occurs in solid solution in melonite, gold, and pentlandite (Dunning, 1979).

The concentration of PGEs and chalcophile elements varies considerably between and within rock types of the Roby Zone (Figure 7.1). PGE mineralization is abundant in gabbro, clinopyroxenite, the shear zone and heterolithic gabbro. Sampling and assaying completed as part of this study identified numerous zones of anomalous palladium concentration up to 29.0 ppm Pd from a sample of gabbro. PGE mineralization within gabbro and clinopyroxenite is associated with fine-grained disseminated and net-textured sulphides, including primarily pyrrhotite, pentlandite, chalcopyrite and pyrite. PGE minerals consist of primarily braggite and vysotskite (Sweeny, 1989). PGE content varies across and along strike of the layers comprising the northern layered sequence; however, no obvious trends were observed. Within the shear zone and heterolithic gabbro, the highest Pd and Pt concentrations were observed in the central portion of the Roby Zone near the contact between the shear zone and the northern layered sequence. Palladium and platinum mineralization within the shear zone consists of predominantly fine-grained PGE sulphide and telluride minerals, merenskyite and kotulskite, which are present interstitially to cumulate grains and as inclusions within secondary silicates. PGE mineralization within the shear zone ends abruptly at the eastern contact. Within the thin wedge of clinopyroxenite between the shear

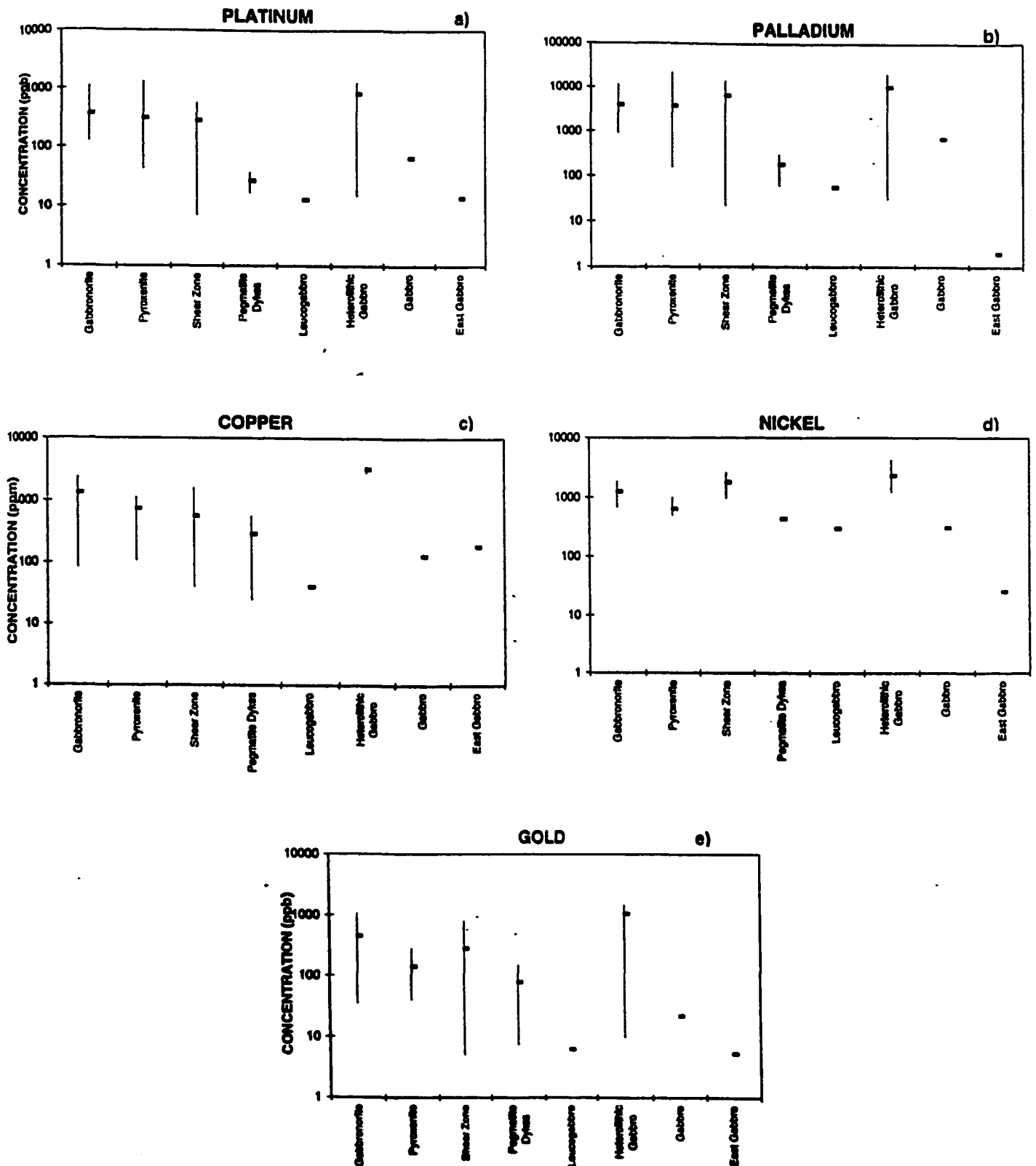


Figure 7.1: Plot showing the range of values (thin black line) and average concentration (thick dash) for a) Pt, b) Pd, c) Cu, d) Ni, and e) Au for each of the rock types comprising the Roby Zone.

zone and the East Gabbro, PGE mineralization is similar in habit and concentration to that of the clinopyroxenite layers in the northern layered sequence. Within the heterolithic gabbro, PGE mineralization extends almost 100 metres east to west at its widest point and gradually decreases to the west and south. The PGMs within the heterolithic gabbro, which consist of predominantly kotulskite, merenskyite, braggite and vysotskite, are associated with fine-grained disseminations and irregularly shaped sulphide blebs of pyrrhotite, pyrite, pentlandite and chalcopyrite. The PGE mineralization is directly related to the degree of alteration and compositional and textural variability of the heterolithic gabbro, and occurs within the gabbroic matrix and gabbronoritic and clinopyroxenitic masses. Sulphide minerals and associated PGMs also occur as fine-grained inclusions within secondary silicates and as microscopic-scale wispy veinlets along fractures. PGE minerals that occur as fine-grained inclusions within secondary silicates in the shear zone and heterolithic gabbro suggest that the precious metals have been remobilized during alteration (Sweeny, 1989). Remobilization and concentration have played an important role in the observed distribution of the PGEs and is most likely responsible for some of the large variations in PGE content observed in the southern portion of the Roby Zone.

The majority of rocks of the Roby Zone are enriched in Pd and Pt relative to Os, Ir, Ru, Rh and Re, which occur in low abundance, often below detection limits. The ratio $Pt+Pd/Os+Ir+Ru$ is often directly related to the composition of the host rock (Cabri, 1981). Tholeiitic-hosted magmatic sulphide deposits in gabbroic rocks are characterized by $Pt+Pd/Os+Ir+Ru$ ratios typically greater than 13 (Naldrett and Duke, 1980). Ratios for rocks of the Roby Zone are highly variable, ranging from 3 to 37,000 with an average of approximately 7,700. The highest $Pt+Pd/Os+Ir+Ru$ ratios were observed in gabbronorite, whereas the lowest ratios were observed in clinopyroxenite. High $Pt+Pd/Os+Ir+Ru$ ratios are

often associated with hydrothermal deposits, such as Rathbun Lake, and may reflect the relative solubilities of the PGEs (Rowell and Edgar, 1986). Lower ratios are often associated with magmatic PGE deposits (Naldrett, 1981). These trends common to other PGE deposits, were not observed in the Roby Zone. Some of the highest Pt+Pd/Os+Ir+Ru ratios were observed in unaltered gabbronorite, whereas highly altered rocks from the shear zone and heterolithic gabbro have some of the lowest Pt+Pd/Os+Ir+Ru ratios. The presence of PGMs in secondary hydrosilicates is good direct evidence for PGE redistribution during hydrothermal or deuteric alteration. The high Pt+Pd/Os+Ir+Ru may also be related to the fact that Pt and Pd are more compatible with the sulphide melt than Os, Ir and Ru. In addition, Pd and Pt have somewhat higher sulphide/silicate melt partition coefficients than Os, Ir and Ru in a low sulphur magma (Brugmann and Naldrett, 1990). Therefore, variable Pt+Pd/Os+Ir+Ru ratios within the Roby Zone may reflect the different degrees of partial melting of a sulphide-bearing mantle source or to fractional crystallization from the sulphide melt prior to the emplacement of the melt into the Roby Zone. The large variability of the Pd+Pt/Os+Ir+Ru ratio across the Roby Zone indicates that the PGE mineralization within the Roby Zone is not typical to that of other deposits. In fact, several different processes, including magmatic processes and modification by deuteric and hydrothermal fluids, may have combined to form the observed PGE mineralization of a portion of the Roby Zone deposit.

Although Pt and Pd are enriched relative to other PGEs, Pd is enriched by an order of magnitude relative to Pt. The Pd:Pt ratio varies considerably across the deposit ranging from approximately 1:1 to 25:1, with an average of approximately 10:1 (Figure 7.2). Gabbronorite and the shear zone typically contain the highest Pd:Pt ratios of the deposit, averaging 17:1 and 15:1, respectively. Clinopyroxenite has some of the lowest Pd:Pt ratios of the Roby

a line with a positive slope, indicating that Pd is enriched with respect to Pt as the overall PGE concentration increases (Figure 7.3). The correlation between Pd and Pt is related to rock type. The shear zone and clinopyroxenite have a high correlation coefficient, 0.872 and 0.998, respectively, relative to gabbro and heterolithic gabbro. The correlation coefficients for Pd, Pt, Au, chalcophile elements and sulphur are presented in Table 7.1. The varying Pd:Pt ratio for the various rock types indicates that several different processes may be responsible for the PGE mineralization within the Roby Zone.

Diagrams where Pt- or Pd- or Au/Ir ratios are plotted against Pt or Pd or Au (Figure 7.4) show a positive correlation. Ratios of Pd/Ir range up to 40,000 and ratios of Pt/Ir and Au/Ir range up to 2,000. Since PGEs have similar silicate-sulphide partition coefficients in mantle-derived magmas with high sulphur concentrations (Brugmann and Naldrett, 1990), the data plotted in Figure 7.4 should define a line with a slope of zero. The positive slope indicates that other processes, besides PGE concentration in a sulphide liquid, may be responsible for the enrichment of Pt, Pd and Au with respect to Ir. It is possible that Pd, Pt and Au may have behaved more incompatibly than Ir during fractional crystallization of the sulphide/silicate melt. Higher Pd/Ir ratios have been observed in hydrothermal deposits such as Rathbun Lake, whereas lower Pd/Ir ratios are more characteristic of magmatic deposits (Rowell and Edgar, 1986). Although the Pd-, Pt- and Au/Ir ratios vary considerably between rock type, no elemental trends related to rock type were observed. The large variation observed in the Pd-, Pt- and Au/Ir ratios, which is not typical of many other PGE deposits, may be due, at least in part, to the degree of alteration, particularly in the heterolithic gabbro and the shear zone, which may have remobilized the precious metals. The observed ratios may also be due to the PGE distribution in the original magma source.

Table 7.1: Correlation coefficients for Pt, Pd, Au, chalcophile elements and sulphur for the Roby Zone. Correlation coefficients (r) are indicated for 95% confidence for the sample size (N) in each grouping below.

Roby Zone – All Samples (N=25, r=0.396)

	Pt	Pd	Au	Cu	Ni	S
Pt	1					
Pd	0.89548218	1				
Au	0.869154805	0.786154	1			
Cu	0.628343265	0.524561	0.77904	1		
Ni	0.579492126	0.466235	0.562217	0.576672	1	
S	0.163957743	0.095918	0.279512	0.500457	0.137141	1

Gabbronorite (N=9, r=0.666)

	Pt	Pd	Au	Cu	Ni	S
Pt	1					
Pd	0.872363347	1				
Au	0.696538458	0.444172	1			
Cu	0.556964012	0.171027	0.923155	1		
Ni	0.394673274	0.201237	0.272424	0.424436	1	
S	-0.05535609	-0.32815	0.60237	0.654711	-0.30639	1

Clinopyroxenite (N=6, r=0.811)

	Pt	Pd	Au	Cu	Ni	S
Pt	1					
Pd	0.998055566	1				
Au	0.255954719	0.207767	1			
Cu	-0.926061702	-0.93316	0.078562	1		
Ni	0.973866929	0.984253	0.031764	-0.96945	1	
S	-0.644258423	-0.6216	-0.83142	0.308881	-0.48254	1

Shear Zone (N=4, r=0.950)

	Pt	Pd	Au	Cu	Ni	S
Pt	1					
Pd	0.9906253	1				
Au	0.888659132	0.942972	1			
Cu	0.861679279	0.922923	0.998441	1		
Ni	0.51381742	0.626196	0.850014	0.87809	1	
S	0.877093666	0.934486	0.999697	0.999513	0.862732	1

Heterolithic Gabbro (N=6, r=0.811)

	Pt	Pd	Au	Cu	Ni	S
Pt	1					
Pd	0.909333458	1				
Au	0.997422159	0.936845	1			
Cu	0.07318016	0.481498	0.144556	1		
Ni	0.158650912	-0.26653	0.087394	-0.97308	1	
S	0.791268392	0.97394	0.833106	0.667735	-0.47819	1

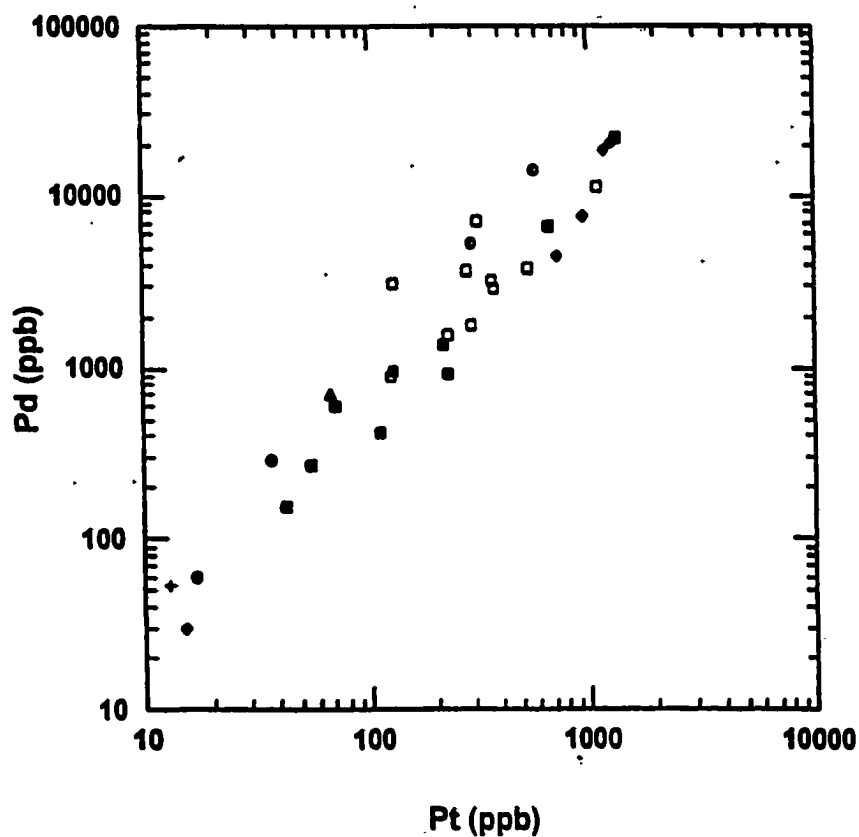


Figure 7.2: Log-log plot of Pd versus Pt for each of the rock types comprising the Roby Zone. Notice the well developed correlation between Pd and Pt. Gabbronorite (open square), gabbro (solid triangle), coarse-grained leucogabbro (+), East Gabbro (open triangle), clinopyroxenite (solid square), shear zone (half-filled circle) pegmatite gabbro dike (solid circle), heterolithic gabbro (solid diamond) and tonalite (X) are shown.

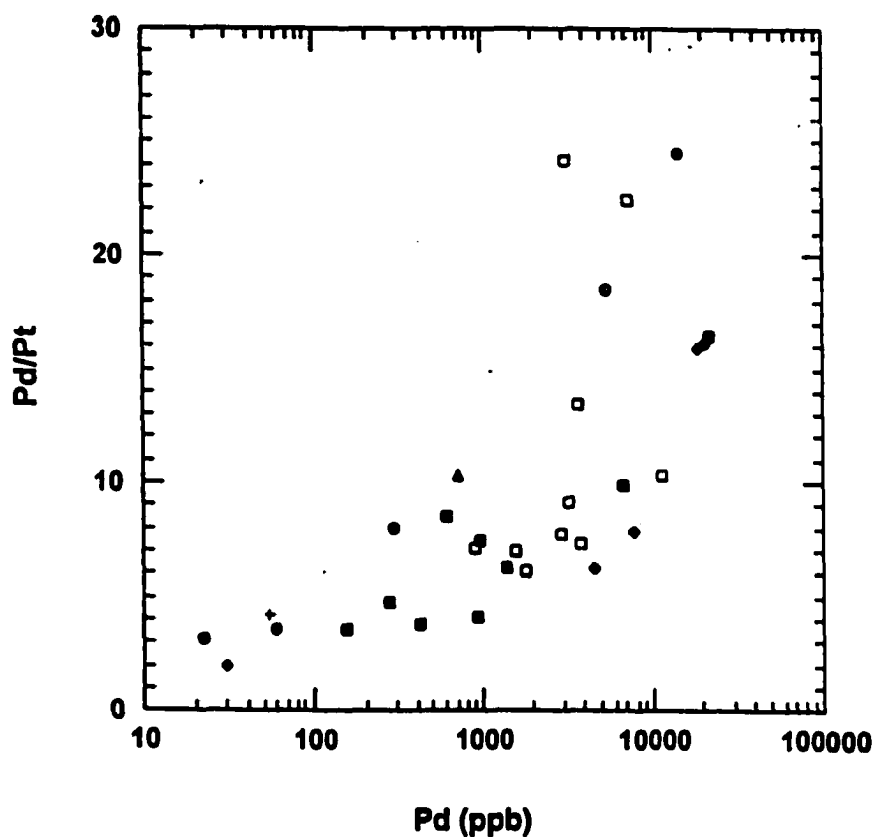


Figure 7.3: Normal-log plot of Pd/Pt versus Pd for each of the rock types comprising the Roby Zone. Notice the positive slope defined by the data that illustrates the enrichment of Pd with respect to Pt with increasing PGE content. Gabbronorite (open square), gabbro (solid triangle), coarse-grained leucogabbro (+), East Gabbro (open triangle), clinopyroxenite (solid square), shear zone (half-filled circle) pegmatite gabbro dike (solid circle), heterolithic gabbro (solid diamond) and tonalite (X) are shown.

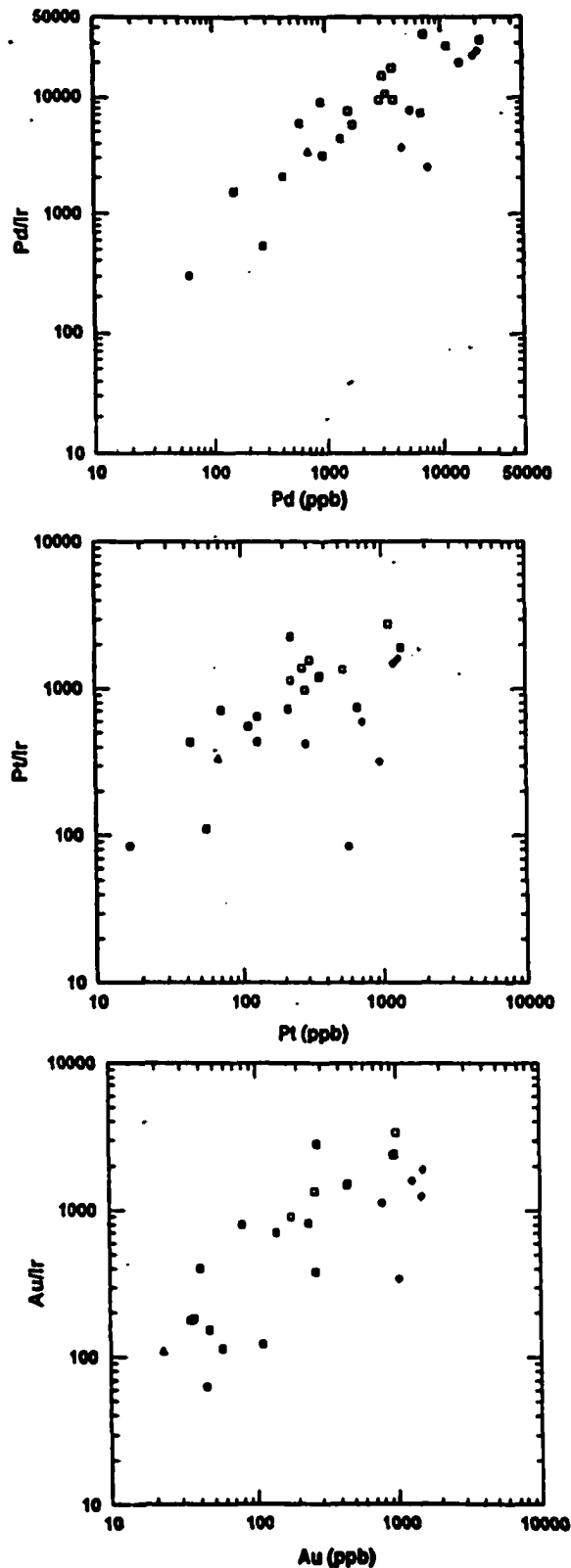


Figure 7.4: Log-log plots of a) Pd/Ir versus Pd, b) Pt/Ir versus Pt, and c) Au/Ir versus Au for gabbro (solid triangle), coarse-grained leucogabbro (+), East Gabbro (open triangle), clinopyroxenite (solid square), shear zone (half-filled circle) pegmatite gabbro dike (solid circle), heterolithic gabbro (solid diamond).

Sulphur has been shown to play an important role in the distribution and relative concentration of PGE mineralization within magmatic deposits (Naldrett, 1989). Although no direct correlation was identified between platinum, palladium, gold, copper, nickel and sulphur for the Roby Zone by Sweeny (1989), Watkinson and Dunning (1979) and Talkington and Watkinson (1984), good correlations often do exist (Naldrett, 1989). The lack of a good correlation provides an indication of the variability in the relative proportions of PGEs, chalcophile elements and sulphide mineralization between the various rock types comprising the Roby Zone.

A relatively high correlation exists between sulphur, PGEs, specifically Pd, and chalcophile elements for heterolithic gabbro and the shear zone, whereas a relatively weak correlation exists for gabbronorite and clinopyroxenite (Table 7.1). The weak correlation between sulphur and Pt or Pd within the northern layered sequence indicates that the sulphide minerals may not be entirely responsible for controlling the distribution of PGEs. Evidence supporting this includes the presence of Te- and Bi-rich platinum and palladium minerals along narrow faults, including kotulskite and merenskyite (Sweeny, 1989). In addition, Pd may also substitute into orthopyroxene and to a lesser degree, clinopyroxene. Several negative correlations exist between Cu and Pt and Pd in clinopyroxenite and between Cu and Ni in the heterolithic gabbro. This negative correlation may be related to the more incompatible behaviour of Pt and Pd compared to Cu in mafic melts (Henderson, 1966). Nickel typically has a low correlation with sulphur throughout the Roby Zone, suggesting that nickel is present within primary silicates (Sweeny, 1989).

Platinum, palladium and chalcophile elements show varying degrees of correlation amongst the various rock types (Table 7.1). In many magmatic PGE deposits, increasing PGE content is often related to increasing Cu or Ni content. Remobilization of the precious metals during alteration typically produces elevated PGE concentrations for relatively constant Cu and Ni concentrations (Naldrett, 1986). These trends were not always observed in the Roby Zone, specifically the shear zone and heterolithic gabbro that have a strong correlation between PGEs and Cu and/or Ni, yet have experienced the highest degree of alteration. Log-log plots for the above elements are presented in Figure 7.5.

A plot of $Pt/(Pt+Pd)$ versus $Cu/(Cu+Ni)$ for the various rock types comprising the Roby Zone defines a cluster of points at relatively constant $Pt/(Pt+Pd)$ ratios, ranging from 0.05 to 0.2, versus variable $Cu/(Cu+Ni)$ ratios, ranging from 0.05 to 0.8 (Figure 7.6). A negative linear relationship between $Pt/(Pt+Pd)$ and $Cu/(Cu+Ni)$ has been defined for PGE sulphide-rich ores associated with tholeiitic magmas (Naldrett and Cabri, 1976; Naldrett, 1981). The samples representing the various rock types of the Roby Zone plot predominantly outside the field of PGE ores associated with tholeiitic magmas, although there is some scatter of points representing the sulphide-rich samples of the deposit (greater than 0.3 vol% sulphur) towards one end of the tholeiitic field. The deviation of the data points from the field of typical tholeiitic-hosted deposits suggests that the observed PGE mineralization of the Roby Zone was not produced under conditions typical of a fractionating tholeiitic magma. Any deviation between the typical tholeiitic-hosted PGE deposits and the Roby Zone, which has a low concentration of sulphur compared to many other magmatic PGE deposits, may be due, at least in part, to differences in sulphide content. In addition, differences could be related to the varying sulphide/silicate partition coefficients that has concentrated Pd and Pt relative to Cu and Ni during partial melting and/or fractionation of a mantle source. The scatter of data

points for the Roby Zone does not appear to be related to rock type or to the overall PGE content.

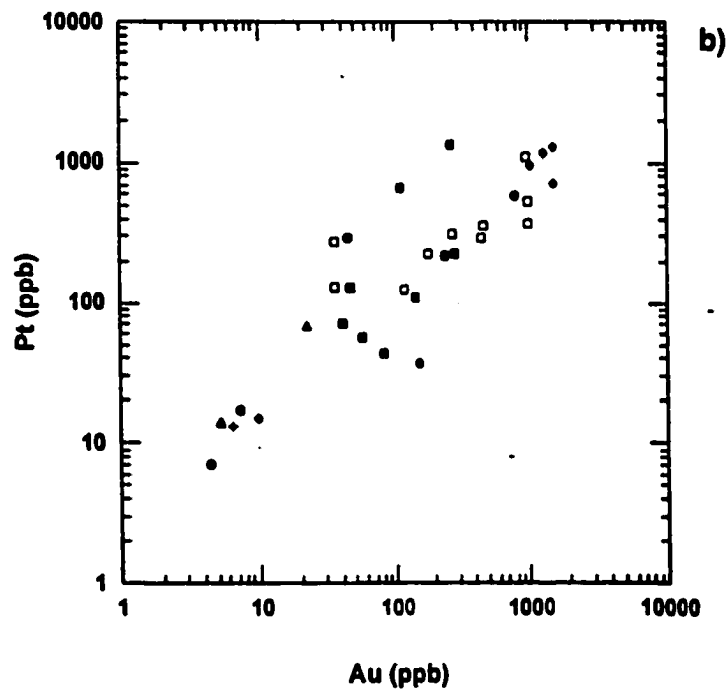
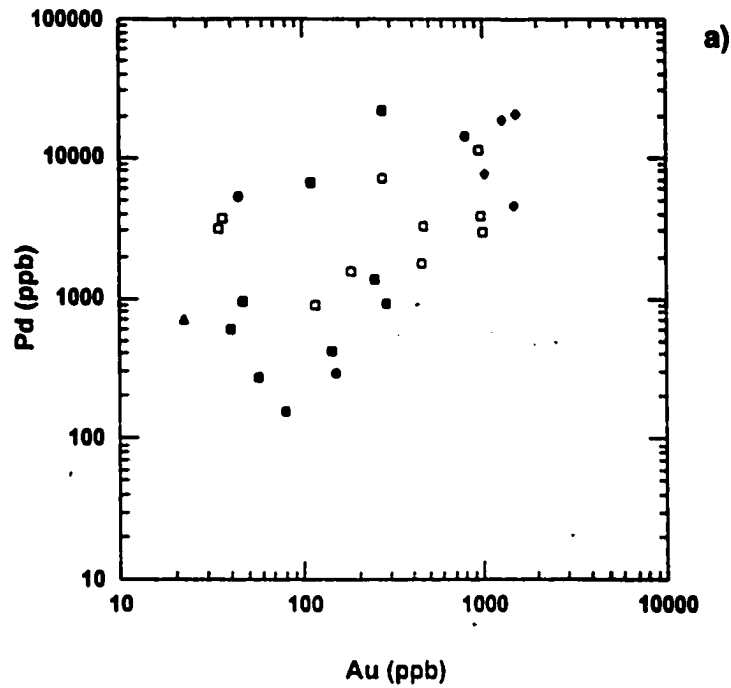


Figure 7.5: Log-log plots a) and b) showing correlation between Pt, Pd and chalcophile elements for each of the rock types comprising the Roby Zone. Gabbronorite (open square), gabbro (solid triangle), coarse-grained leucogabbro (+), East Gabbro (open triangle), clinopyroxenite (solid square), shear zone (half-filled circle) pegmatite gabbro dike (solid circle), heterolithic gabbro (solid diamond) and tonalite (X) are shown.

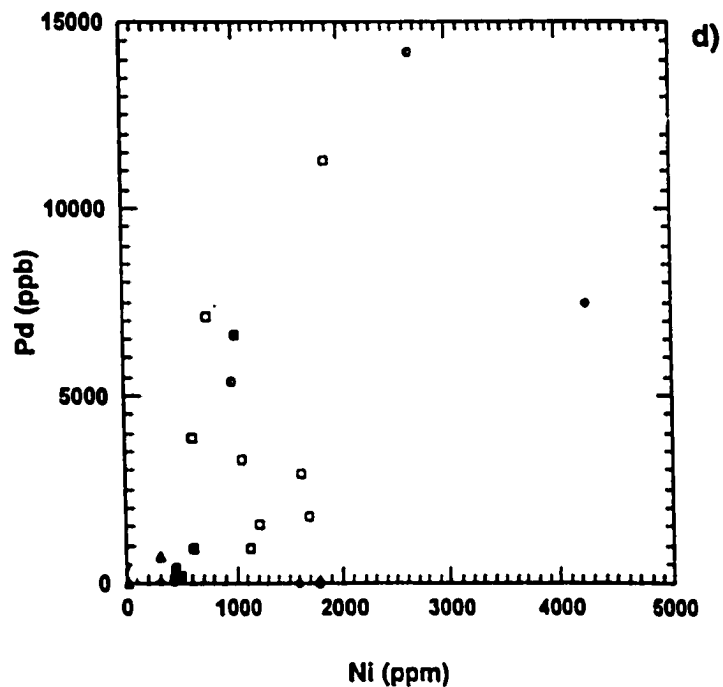
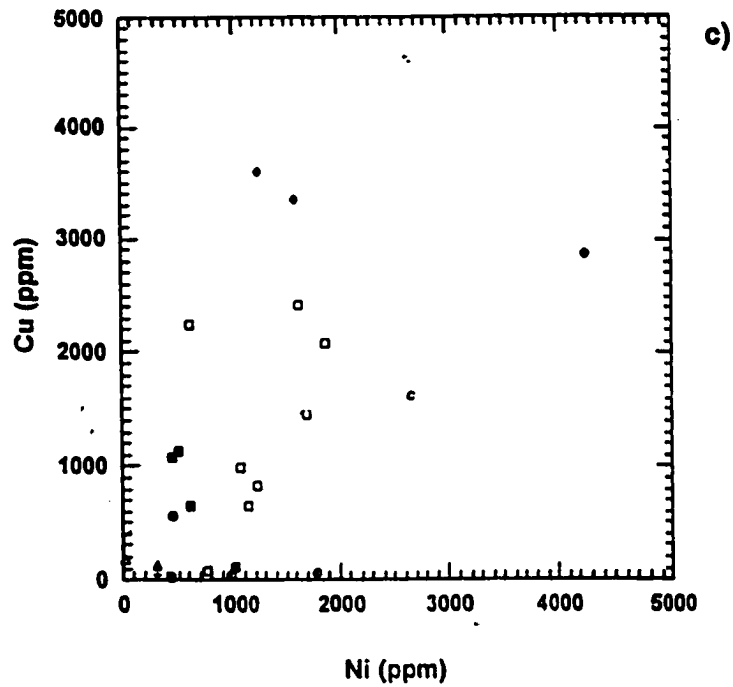


Figure 7.5: Log-log plots c) and d) showing correlation between Pt, Pd and chalcophile elements for each of the rock types comprising the Roby Zone. Gabbro (solid triangle), coarse-grained leucogabbro (+), East Gabbro (open triangle), clinopyroxenite (solid square), shear zone (half-filled circle) pegmatite gabbro dike (solid circle), heterolithic gabbro (solid diamond) and tonalite (X) are shown.

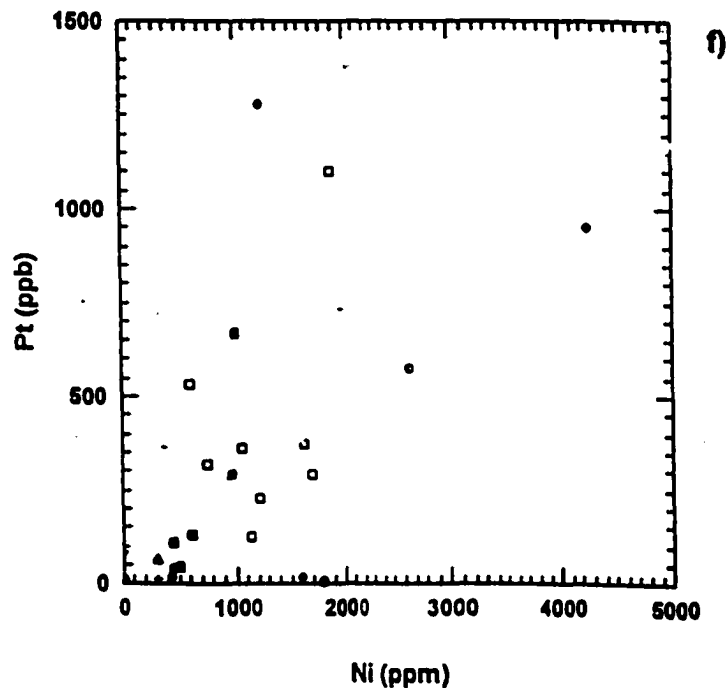
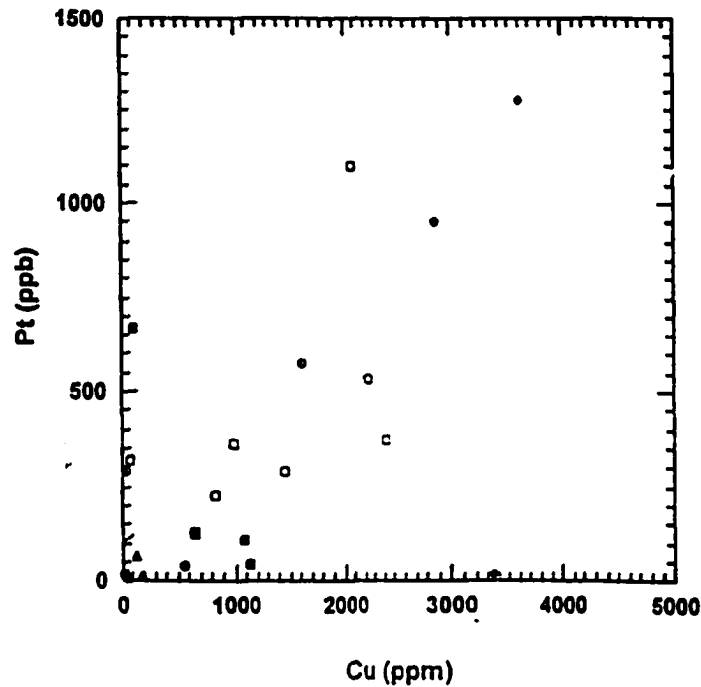


Figure 7.5: Log-log plots e) and f) showing correlation between Pt, Pd and chalcophile elements for each of the rock types comprising the Roby Zone. Gabbro (open square), gabbro (solid triangle), coarse-grained leucogabbro (+), East Gabbro (open triangle), clinopyroxenite (solid square), shear zone (half-filled circle) pegmatite gabbro dike (solid circle), heterolithic gabbro (solid diamond) and tonalite (X) are shown.

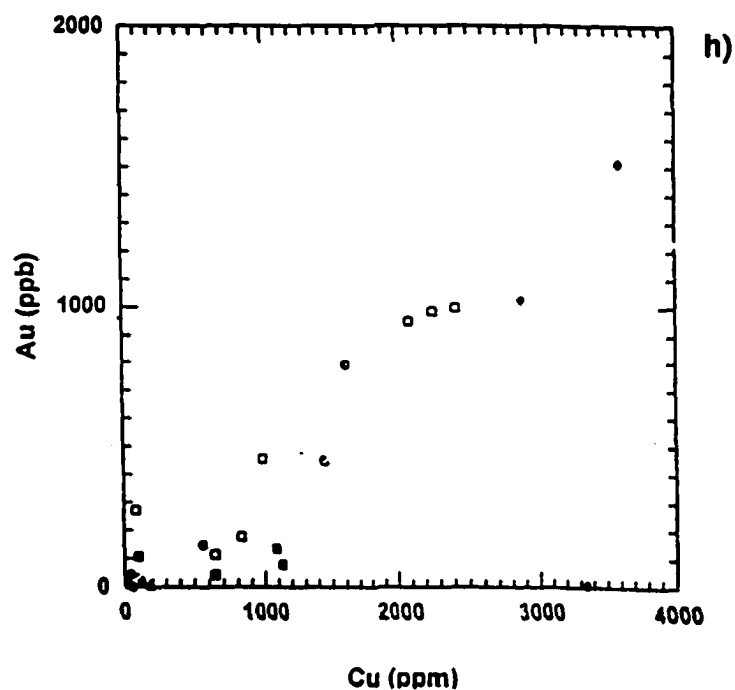
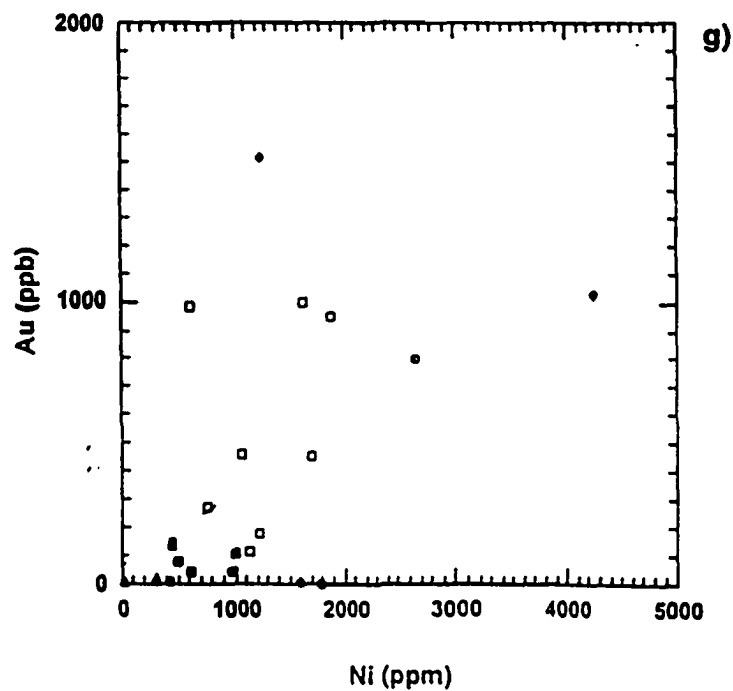


Figure 7.5: Log-log plots g) and h) showing correlation between Pt, Pd and chalcophile elements for each of the rock types comprising the Roby Zone. Gabbro (solid triangle), coarse-grained leucogabbro (+), East Gabbro (open triangle), clinopyroxenite (solid square), shear zone (half-filled circle) pegmatite gabbro dike (solid circle), heterolithic gabbro (solid diamond) and tonalite (X) are shown.

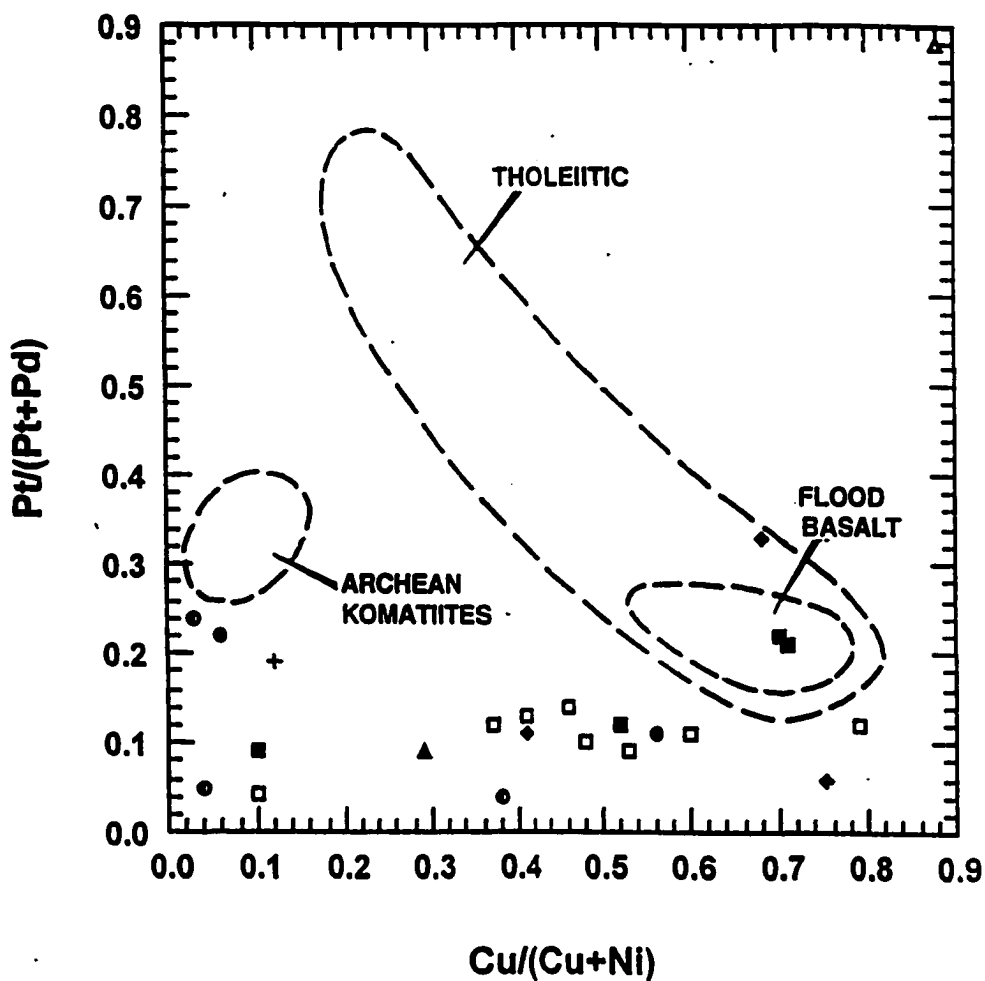


Figure 7.6: Plot of $\text{Cu}/(\text{Cu}+\text{Ni})$ versus $\text{Pt}/(\text{Pt}+\text{Pd})$ for rocks of the Roby Zone. Gabbronrite (open square), gabbro (solid triangle), coarse-grained leucogabbro (+), East Gabbro (open triangle), clinopyroxenite (solid square), shear zone (half-filled circle) pegmatite gabbro dike (solid circle), heterolithic gabbro (solid diamond) and tonalite (X) are shown. Fields for tholeiitic-hosted PGE deposits and Archean komatites from Naldrett and Cabri (1976).

The rocks of the Roby Zone show considerable enrichment in Pt, Pd and Au compared to Ir, Os and Ru when plotted on the basis of 100% sulphide content and chondrite-normalized (Figure 7.7). The normalized values were calculated using a methodology outlined by Naldrett (1981). The majority of assays for Os, Ru and Rh were below assay detection limits, and therefore, the detection limit was used in the calculation. The detection limits for each of the PGEs are listed in Appendix 4. The average values for each rock type plotted in Figure 7.7 defines a number of very similar profiles for variable sulphide content. The steep slope of these profiles is typical of PGE deposits in gabbroic rocks (Cabri, 1981). Only the East Gabbro does not show an enrichment of Pt, Pd or Au relative to the other PGEs and, in fact, shows depletion in these metal concentrations. This indicates that the PGE mineralization of the East Gabbro has not experienced the same processes responsible for the PGE mineralization observed in the other rocks of the Roby Zone. In addition, the majority of samples analysed from the East Gabbro have PGE concentrations near detection limits.

In Figure 7.8, the average PGE and Au content for the Roby Zone are plotted along with data from other PGE deposits on the basis of 100% sulphide content and chondrite-normalized. In many magmatic PGE deposits, the concentration of PGEs is related to the amount of sulphides in the rock, such as in the Stillwater and Bushveld Complexes (von Gruenewaldt, 1979). A good correlation exists between sulphur and Pd, Pt and Au in the shear zone and heterolithic gabbro. The lack of good correlation between PGE and sulphide content in the remaining rock types comprising the Roby Zone may be due to the presence of discrete PGM hosted in silicates, as well as PGE-tellurides. PGE-tellurides are known to occur in significant amounts throughout the deposit (Sweeny, 1989; Dunning, 1979). These factors may account for some of the observed differences in the profiles defined in Figure 7.8 between the Roby Zone and some other deposits based on the recalculation to 100%

sulphide content. The profile defined for the Roby Zone is very similar to that of the Stillwater Complex, albeit approximately one order of magnitude lower. Chondrite-normalized values for Pd, Pt and Au for the Roby Zone are very similar to those of Rathbun Lake, although the values for Os, Ir and Rh are higher by several orders of magnitude. The similarity of the profile for the Roby Zone with the Stillwater Complex and Rathbun Lake deposit, which contains PGE minerals produced by hydrothermal processes, suggests that both magmatic and hydrothermal processes may have been responsible for the observed PGE mineralization in the Roby Zone.

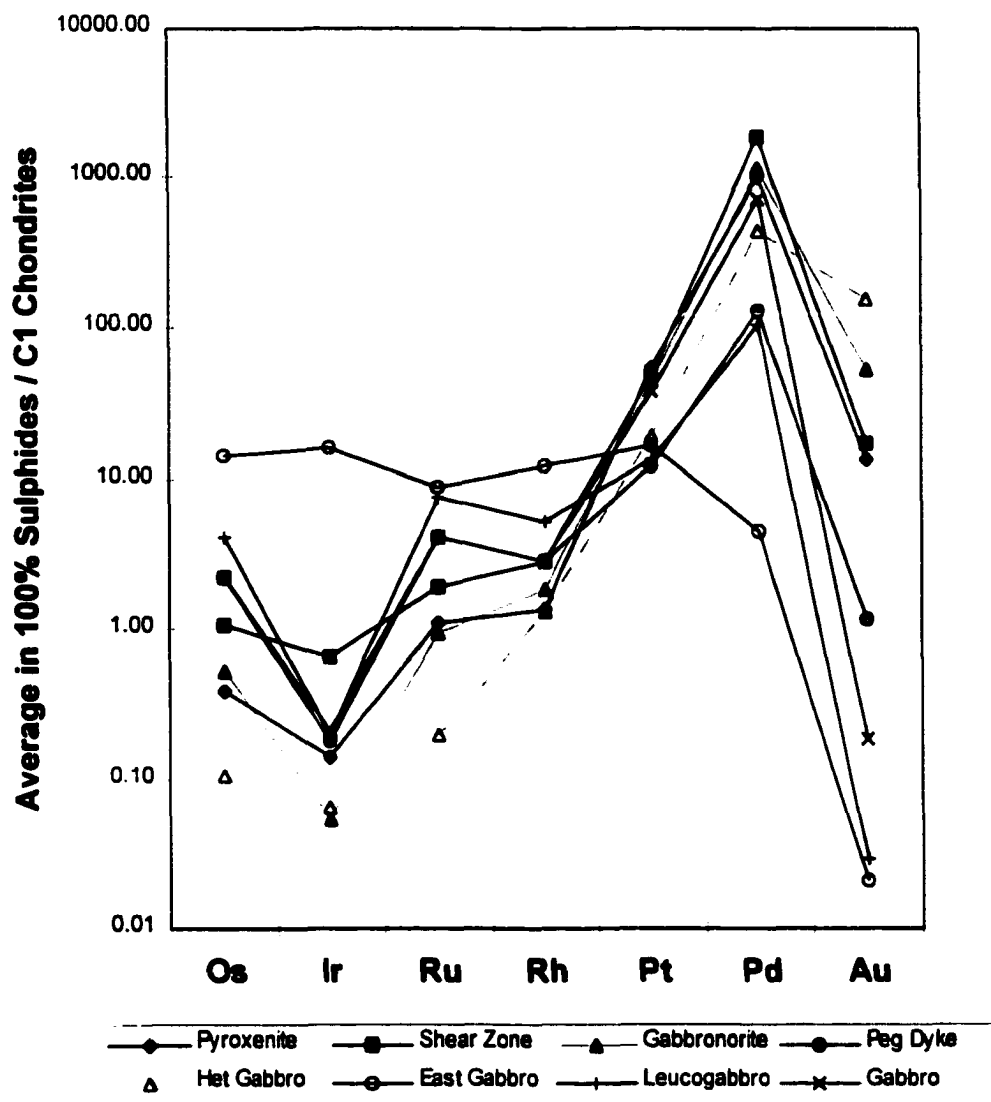


Figure 7.7: Comparison of average PGE and Au values for each of the rock types comprising the Roby Zone. The data has been recalculated to 100% sulphide, then chondrite-normalized based on methodology of Naldrett (1981).

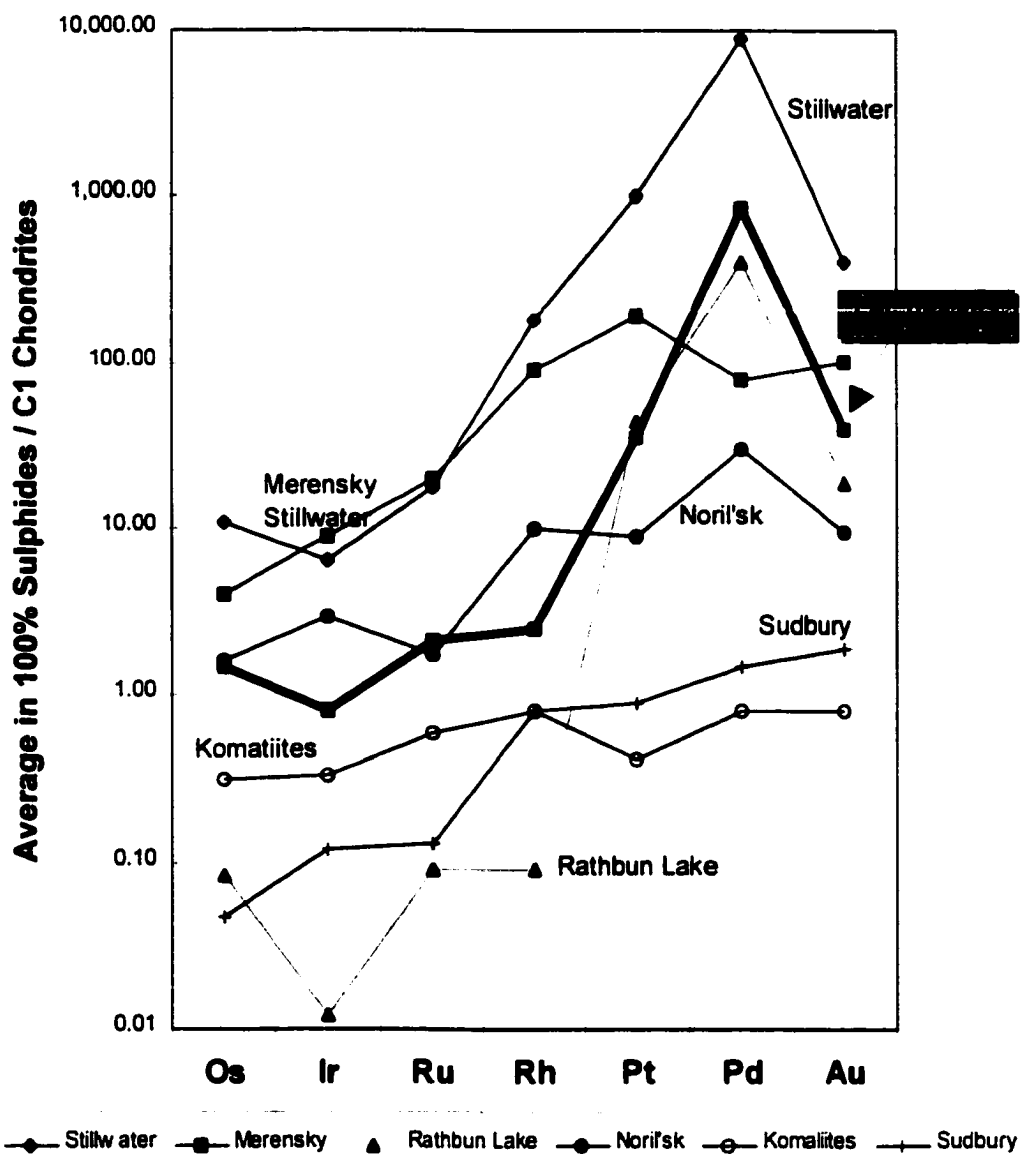


Figure 7.8: Comparison of average PGE and Au values for the Roby Zone and other PGE deposits. The data has been recalculated to 100% sulphide, then chondrite-normalized based on methodology of Naldrett (1981). Komatiite, Sudbury, Noril'sk, Merensky and Stillwater profiles after Naldrett (1981). Rathbun Lake profile after Rowell and Edgar (1986).

8.0 Discussion

8.1 Introduction

The formation of the Roby Zone deposit and its attendant PGE-Au-Cu-Ni mineralization is related to a complex sequence of magmatic events that have experienced varying degrees of modification by late- and post-magmatic processes. This discussion attempts to explain the origin and relationship of the magma, the formation of the heterolithic gabbro, PGE-Au-Cu-Ni mineralization and the importance of deuteritic and hydrothermal fluids using field observations and geochemistry. The discussion considers the various magmatic and post-magmatic processes that have produced the observed textures and geochemical trends, including magma mixing, liquid immiscibility, magma contamination, brecciation, assimilation, and the effect of hydrothermal and deuteritic fluids and late-stage regional alteration. In addition, field features and geochemical trends observed for the Roby Zone deposit will be compared with those of other deposits in order to identify and explain any similarities or differences that may exist. These observations were used to develop a model for the formation of the Roby Zone deposit and the associated PGE-Cu-Au-Ni mineralization.

Work completed by previous researchers has produced a number of models to explain the PGE mineralization of the Roby Zone deposit. Most notably of these models consist of magma mixing, specifically between the tonalitic complex and the gabbroic magma of the Lac des Iles Complex (Sutcliffe, 1986), and between the West Gabbro and the East Gabbro gabbroic magmas (Dunning, 1979). More recent models include a complex sequence of magma mixing, subsequently modified by deuteritic and hydrothermal fluids (Sweeny, 1989; Brugmann and Naldrett, 1986).

8.2 Origin and Relationship of Magma

In order to construct a model for the development of the Roby Zone and to determine the effects of late- or post-magmatic modification of the magmatic textures and compositions, it is important to determine the origin of the magma within the Roby Zone and the source of the PGEs. In addition, the intrusive history and relationship of the magma that formed the observed geochemical trends must be determined.

Data collected during this study and by Sutcliffe et al. (1989), suggest that the gabbroic portion of the Lac des Iles Complex was derived from a tholeiitic basalt parental magma of high-alumina affinity. This magma is thought to be derived from primitive magmas that have experienced contamination with rocks from the crust, possibly as a result of underplating (Sutcliffe et al., 1989; Naldrett et al., 1986). The PGE-rich nature of the Lac des Iles Complex suggests that the magma source may have been enriched in PGE (Watkinson and Dunning, 1979). Additional evidence suggesting that the original magma was derived from a mantle source that was subsequently contaminated by crustal material includes the paucity of olivine observed within the Roby Zone as part of this study and during previous studies. The REE data are inconclusive in that the elevated REEs are enriched by either partial melting of the mantle or contamination of the mantle source by crustal material. Only complete melting of the mantle would produce chondritic values.

Partial melting of the crust resulting in the contamination of the mantle-driven magma is further supported by the presence of high Pt+Pd/Os+Ir+Ru ratios for the Roby Zone deposit relative to other known PGE deposits. The enrichment of Pd and Pt relative to the other PGEs may be related to the preference Pd and Pt have with the sulphide phase of the magma. In contrast, Os, Ir and Ru prefer the silicate phase of the magma. During partial melting of the crust, the tholeiitic basalt magma will incorporate most of the sulphides

but little of the olivine (Naldrett et al., 1979). The collaborative evidence mentioned above suggest that the combination of partial melting of the crust and magma from a mantle source may have formed the initial composition of the magma forming the Roby Zone and the PGE metal ratios and concentrations. Although not completed as part of this study, sulphur isotope data is required to prove whether the mantle-derived magma was contaminated by partial melting of the crust.

The orientation and type of geologic contacts were used to determine the intrusive history of the igneous stratigraphy identified in the Roby Zone. Well defined contacts and the lack of zonation at the igneous contacts between the various layers suggest that the layers represent an intrusion of magma into a largely crystallized mush. The presence of dimpled contacts suggest that several of the adjacent layers, particularly the clinopyroxenite-leucogabbro contact, may have co-existed as a semi-solid/crystal mush. Locally, magmatic injections resulted in brittle deformation of the adjacent rocks, evidenced by angular fragments of gabbro and leucogabbro within a clinopyroxenite matrix.

Based on the orientation and type of geologic contacts, the following list in order of oldest to youngest is the sequence of magma intrusion into the Roby Zone: coarse-grained leucogabbro, PGE-rich gabbro, gabbro, East Gabbro and PGE-rich clinopyroxenite. It has been suggested that the clinopyroxenite may be the fractionated equivalent of the northern ultramafic portion of the Lac des Iles Complex (Sutcliffe, 1986).

Grain size-graded layering observed within gabbronorite and clinopyroxenite suggests that in-situ fractionation has occurred within individual layers. Assuming the grain size-graded layering is the result of gravitational settling, orthopyroxene grains located along the western boundary of gabbronorite suggest that stratigraphic tops are to the east. Subsequent deformation has tilted the layers 70 degrees to the east, otherwise, grain size-graded layering would not have been observed in the horizontal plane in the now steeply dipping layers. The 70-degree dip is therefore, is not the primary angle of the intrusive margin.

Upon solidification of the Roby Zone, late-stage pegmatitic gabbro dikes crosscut all of the igneous layers except the East Gabbro. The dikes crosscut the western contact of the clinopyroxenite but not the eastern contact. This is due to the fact that clinopyroxenite, which readily alters to talc and amphibole, behaved in a ductile manner and did not allow brittle faults to propagate. The pegmatitic gabbro dikes are related to fault zones.

Shearing in the Roby Zone occurred within a portion of the clinopyroxenite in the southern portion of the deposit. Due to the ultramafic composition of the clinopyroxenite, ductile deformation occurred. The shearing may be contemporaneous with the tilting of the layers. Numerous, parallel, east-northeast striking sinistral faults have locally offset the intrusive contacts up to several meters. This faulting has produced the eastward trending concave shape of the deposit.

8.3 Formation of the Heterolithic Gabbro

Any model proposed for the formation of the heterolithic gabbro must address the textural and compositional variation of the unit, the mineralogical and compositional similarity

between the various sections within the heterolithic gabbro and the northern layered sequence, the presence of pegmatitic gabbro dikes and pods and the geometry of the heterolithic gabbro and its relationship to the northern layered sequence, the shear zone and the proximity of the encompassing tonalitic complex. The following discussion describes the various magmatic and post-magmatic processes and sequences that may have produced the observed field features and geochemistry. This discussion considers a number of processes typical of other PGE deposits.

Magma mixing has been considered previously as one of the main magmatic processes responsible for the formation of the heterolithic gabbro. These models suggest that magma mixing occurred between the surrounding tonalitic magma and gabbroic magma from the Roby Zone (Sutcliffe, 1986) or between the West Gabbro and the East Gabbro (Dunning, 1979). Typically, mixing of two chemically distinct magmas often produces a hybrid magma (Naldrett, 1981). The resultant composition of the hybrid magma is intermediate between the composition of the two end-members. The composition of the matrix of the heterolithic gabbro varies considerably and does not define a trend between the composition of the tonalite and the gabbroic package of rocks or between the composition of the West Gabbro (coarse-grained leucogabbro) and the East Gabbro (Figure 3.1, Chapter 3). Preliminary U/Pb zircon data indicate that the gabbroic rocks of the Lac des Iles Complex are 2.69 Ga. The surrounding gneissic tonalites and hornblende tonalites are 2.77 Ga and 2.73 Ga (D.W. Davis, Royal Ontario Museum, unpublished data). Based on field relationships, Sutcliffe (1989) considered that hornblende tonalite and the mafic-ultramafic intrusions of the Lac des Iles Complex were contemporaneous. The geochronology does not support these conclusions and the mixing textures identified previously are most likely related to an older phase of magmatism than that which generated the major mafic-ultramafic plutons (Sutcliffe, 1990). The lack of compositional zoning of mineral grains and the lack of non-equilibrium

phenocryst assemblages also suggests that mixing has not occurred on a scale that would produce the heterolithic gabbro. The contact between the Lac des Iles Complex and the encompassing tonalitic rocks is very sharp, and there is no unequivocal evidence of magma mixing.

The heterolithic gabbro is composed of numerous angular and rounded masses of varying compositions and textures. The angular masses, or fragments, are comprised predominantly of gabbro, gabbro and clinopyroxene and are similar in composition to their corresponding layers in the northern layered sequence. The similar composition of the masses with the composition of the various rocks of the northern layered sequence and the angular shape of the fragments provides good evidence that the fragments within the heterolithic gabbro were derived from the northern layered sequence during an episode of brittle deformation. The rounded masses are comprised predominantly of leucogabbro, with a minor amount of clinopyroxene, gabbro and gabbro. Masses that are tonalitic in composition were not observed. The various rounded masses have convoluted boundaries with numerous tongues or lobes that protrude into the adjacent rock. This indicates that the rounded blebs and the adjacent magma co-existed in a liquid or crystal mush state. The angular and rounded sections are hosted within a gabbroic matrix. One possible explanation of this texture is that explosive, volatile-rich gabbro may have intruded the solidified, or partially solidified layers of the Roby Zone resulting in the fragmentation of the layered sequence. This injection of magma may have been preceded by or contemporaneous with an episode of tectonic brecciation of the igneous layers within the Roby Zone. The gabbroic magma injected into the Roby Zone and became the matrix to the fragments. Some of the layers may have been in a crystal mush state prior to brecciation and injection of the gabbroic magma, in particular, the coarse grained leucogabbro magmas that form the majority of the rounded blebs within the heterolithic gabbro. The hot liquids may have

promoted partial melting of some of the fragments to varying degrees depending on the composition of the fragment. Partial melting of the fragments occur on the perimeter of the fragment initially, often modifying the original angular shape of the fragment to spherical. Tectonic abrasion can also possibly cause rounding of fragments during brecciation, but is unlikely due to the absence of any smaller fragments proximal to and similar in composition to the larger fragments.

Partial melting often produces two types of scenarios, fractional fusion, where melted liquid is removed from the solid phase, creating a wider compositional range, and equilibrium fusion, where the liquid remains in contact with the solid. This latter scenario appears to be feasible for the formation of the heterolithic gabbro. Partial melting is controlled by a number of factors, including host rock composition, temperature, extent of melting, volatile content, and whether fractional or equilibrium fusion has occurred. It appears that within the heterolithic gabbro, the degree of partial melting varied considerably shown by the high degree of variability in fragment shape and composition.

Partial melting in tholeiitic magmas may produce iron-rich globules within silica rich-liquids (Philpotts, 1979). Liquid immiscibility forms within slow cooling magmas and is thought by Philpotts to be an important process in the differentiation of tholeiitic magmas. Although various textures showing evidence of liquid immiscibility were not identified, such as iron-rich globules in plagioclase grains or the formation of pyroxene grains within a sphere, the presence of numerous rounded blebs of varying composition, leucogabbroic to clinopyroxenitic, within the heterolithic gabbro suggest that liquid immiscibility may have developed. It is doubtful that simple mixing between two contrasting viscosity magmas could have produced this texture consisting of more than two compositions of masses. The significant variation in composition between many of the fragments may have promoted

immiscibility between the more iron-rich sections of gabbro, clinopyroxenite and gabbro with the more feldspathic, coarse-grained leucogabbro.

Numerous pegmatitic gabbro dikes and pods occur within the heterolithic gabbro and often displaying comb layering (MacDonald, 1986). The direction of growth of the crystals at the base of the layer has been used to determine that the stratigraphic tops of the Roby Zone deposit face to the east. The top direction agrees with the stratigraphic top direction determined from the direction of grain size-graded layering observed within the northern layered sequence. Field relationships indicate that these liquids are some of the most differentiated to have intruded the Roby Zone. The lack of any pegmatitic dikes or pods higher in the stratigraphic sequence than clinopyroxenite (i.e. east of clinopyroxenite) suggests that the clinopyroxenite may have served as a cap for magma and volatiles that percolated upwards through the fragmented rocks of the Roby Zone.

The presence of numerous isolated patches of alteration suggest that deuteric fluids have modified the original magmatic textures and compositions. The deuteric (or hydrothermal) fluids are responsible for the intense amphibole, talc and sericite alteration observed within the heterolithic gabbro. The alteration varies with rock type. Many of the original magmatic textures and compositions remain in pristine condition within the cores of several of the larger fragments within the heterolithic gabbro.

Regional metamorphism does not appear to have had a significant effect on the Roby Zone deposit, and typically consists of hornblende metamorphism locally throughout the Lac des Iles Complex (Sutcliffe, 1986).

8.4 PGE-Au-Cu-Ni Mineralization in the Roby Zone Deposit

The PGE-Au-Cu-Ni mineralization of the Roby Zone varies significantly between the northern layered sequence, the heterolithic gabbro and the shear zone. The main differences that have been identified include the habit of the PGE minerals, composition, relationship to silicate and sulphide minerals, PGE metal ratios and the relationship with siderophile and chalcophile elements. These factors suggest that several different processes may have been involved in the PGE mineralization of the Roby Zone deposit.

Northern Portion

The presence of net-textured sulphides and intercumulus sulphides suggest that the sulphide mineralization in the northern layered sequence is the result of magmatic processes (Naldrett, 1979). The net-textured sulphides occur primarily within unaltered gabbronorite and clinopyroxenite, although net-textured sulphide mineralization has been identified within unaltered fragments of gabbronorite and clinopyroxenite within the heterolithic gabbro. The presence of vysotskite and braggite suggest that the PGE mineralization has formed by magmatic processes (Sweeny, 1989). These minerals are considered to be high-temperature minerals that form early in the formation of many magmatic deposits (Cabri and Lafamme, 1976). Additional evidence of a magmatic process includes the presence of the mineral assemblage pyrrhotite-pentlandite-pyrite-chalcopyrite. This assemblage represents the exsolution from a primary magmatic sulphide solution (Dunning, 1979). The temperatures of formation for orthopyroxene and clinopyroxene in the Roby Zone (Sutcliffe et. al., 1989) are sufficiently high to allow for the existence of monosulphide sulphide solution (Craig and Vaughan, 1981). The PGE mineralization within the northern layered sequence is confined to two layers, gabbronorite and clinopyroxenite. Because the PGE mineralization is confined to specific rock types, the effect of late-stage deuteric or hydrothermal fluids remobilizing PGEs

is minimal. Most likely, the immiscible sulphide melt collected within gabbronoritic and clinopyroxenitic magma prior to emplacement into the Roby Zone. Local alteration in gabbronorite, associated with late-stage faults, appears to have reconcentrated some PGE mineralization. Within these faults, the PGE minerals occur as fine-grained inclusions within secondary silicates of talc, serpentine and anthophyllite. The East Gabbro contains very minute quantities of PGEs and sulphide mineralization. This suggests that the East Gabbro was not saturated in sulphide during its crystallization.

The ratio of Pd:Pt varies considerably between gabbronorite and clinopyroxenite. The ratio of Pd:Pt for gabbronorite is 18:1, whereas clinopyroxenite is 7:1. Factors influencing the Pd:Pt ratio include the amount and composition of an immiscible sulphide liquid, the composition of the magma and the source of the PGEs. The Cu:Ni ratio for gabbronorite is approximately 1:1, whereas clinopyroxenite has a ratio of approximately 3:1.

Southern Portion

The PGE mineralization in the southern portion of the Roby Zone occurs within the heterolithic gabbro and the shear zone. The PGE mineralization occurs in three forms, as primary magmatic PGE mineralization within unaltered fragments derived from the northern layered sequence, as coarse-grained blebs within pegmatitic gabbro pods and as fine-grained inclusions and streaks within secondary silicates. PGE mineralization within the heterolithic gabbro consists of primarily PGE sulphides and tellurides, including braggite, vysotskite, merenskyite and kotulskite (Sweeny, 1989). The average Pd:Pt ratio for the rocks of the heterolithic gabbro and the shear zone is approximately 10:1. The difference observed in the Pd:Pt ratio between the heterolithic gabbro and gabbronorite and clinopyroxenite is likely due to the mixture of fragments incorporated into the heterolithic gabbro having varying

PGE ratios. In addition, late-stage deuteritic fluids percolated through the heterolithic gabbro may have preferentially remobilized and deposited the Pd and Pt metals within the heterolithic gabbro.

The presence of bismuthotellurides is attributed to deuteritic fluids (Sweeny, 1989) that have percolated through the brecciated gabbroic pile and concentrated and deposited the PGEs within secondary silicates. The bismuthotellurides have not crystallized from a mafic silicate melt (Edgar and Sweeny, 1989). There appears to be a good correlation between the PGE concentration and the degree of alteration. The more intense the alteration, the higher PGE concentration. During deuteritic alteration, PGEs, Au, Cu and Ni are redistributed, often overprinting the original magmatic textural and geochemical trends (Talkington and Watkinson, 1984). Evidence of remobilization of PGEs by deuteritic fluids within the heterolithic gabbro consists of the presence isolated patches of secondary silicates containing fine-grained inclusions and streaks of sulphide mineralization along cleavage planes of pseudomorphic pyroxene. Similar observations have been documented in the Merensky Reef, where the PGE and mineralization is related to deuteritic fluids (Crocket et al., 1976). These bismuthotellurides are very common in lower temperature deposits such as the Rathbun Lake deposit (Rowell and Edgar, 1986) and the New Rambler deposit (Loucks and McCallum, 1980).

The abundant sulphide mineralization (5 vol.%) within the heterolithic gabbro is considerably enriched relative to gabbronorite and clinopyroxenite (1-2 vol.%) of the northern layered sequence. These observations suggest that a different process may have been responsible for the formation of the PGE mineralization in the southern portion of the Roby Zone. Partial melting of the coarse-grained leucogabbro, gabbronorite and clinopyroxenite may have formed an immiscible liquid within the more mafic gabbro matrix. The addition of felsic

magma into a mafic magma often promotes sulphide precipitation (Naldrett, 1980). In addition, the intrusion of the gabbroic magma may also have introduced more sulphur into the heterolithic gabbro.

The pegmatitic pods and dikes within the heterolithic gabbro commonly contain abundant PGE and sulphide mineralization. These pegmatitic pods may have formed as a result of late-stage liquids that have percolated through the brecciated pile scavenging and concentrating PGEs.

PGE mineralization within the shear zone consists of primarily kotulskite and merenskyite (Sweeny, 1989). These minerals occur almost entirely as fine-grained inclusions and as streaks within secondary silicates, indicating that remobilization and deposition of PGEs was accomplished by deuteric and/or hydrothermal fluids. The remobilization of PGEs within the shear zone may have occurred on several occasions, most likely contemporaneously with the shearing episodes.

The distribution of PGE-Au-Cu-Ni in the northern layered sequence, shear zone and heterolithic gabbro can be used to identify the source of the magma and the PGE mineralization, in addition to identifying any late- or post-magmatic processes. The rocks of the Roby Zone have a high Pd+Pt/Ir+Os+Ru ratio relative to other magmatic PGE deposits, including the Stillwater and Bushveld deposits (Naldrett, 1981). The average Pd+Pt/Ir+Os+Ru ratio for the Roby Zone is approximately 7,000. The highest ratios were observed within gabbro-norite, whereas the lowest ratios can be found within clinopyroxenite. It has been suggested, based on REE analyses and whole rock geochemistry (Sutcliffe, 1986) that the Roby Zone was derived from a mantle source contaminated by crustal rocks.

This may have produced the enrichment of Pd and Pt relative to the other PGEs. During melting, Os, Ir and Ru may be preferentially concentrated in olivine, whereas Pd and Pt often remain in the sulphide phase within the magma due to their incompatibility (Naldrett, 1979). Formation of a tholeiitic magma by melting of crustal rocks will incorporate more of the sulphide phase in the melt than in the olivine (Naldrett et.al., 1979). In addition, Pd and Pt will behave incompatibly in the magma relative to Os, Ir and Ru and therefore will be concentrated in the sulphide melt. The result is a magma that has Pd and Pt enrichment relative to the other PGEs (Naldrett and Duke, 1980).

The similar chondrite-normalized PGE values for the various rock types comprising the Roby Zone suggest that the magma was derived from the same parent magma, although representing varying degrees of fractionation. The chondrite-normalized PGE values for the Roby compare reasonably well with the profiles of data for the Stillwater and Rathbun Lake deposits. The similarity between two deposits, one formed by magmatic processes and the latter formed by hydrothermal fluids, suggest that the Roby Zone PGE mineralization is consistent with other evidence suggesting a combination of these two processes. The primary evidence of hydrothermal factors in the PGE mineralization are the textural association with secondary silicates and the higher PGE concentrations associated with altered areas.

8.5 Model for the Development of the Roby Zone deposit

The following is a brief discussion of the various processes and sequences involved in a proposed model for the development of the Roby Zone deposit and the associated PGE-Au-Cu-Ni mineralization. A schematic model for development is presented in Figure 8.1.

Stage 1:

During fractionation of a tholeiitic magma, an immiscible sulphide liquid that concentrated the Pd and Pt developed within gabbro-noritic and clinopyroxenitic magma. The fractionated magma intruded the Archean tonalite. The order of intrusion from oldest to youngest was coarse-grained leucogabbro, gabbro-norite, gabbro, East Gabbro and clinopyroxenite. These layers represent fractionated equivalents of the magma in the lower chamber. The layers have sharp, irregular and often dimpled contacts, and probably co-existed in a crystal mush state. Minor in-situ fractionation may have occurred within individual layers. The PGE mineralization, consisting of high-temperature, magmatic, sulphide minerals, predominantly vysotskite and braggite, formed near the base of clinopyroxenite and gabbro-norite.

Stage 2:

Upon cooling of the Lac des Iles complex, the semi-crystalline layers continued to solidify to varying degrees throughout the Roby Zone. A volatile-rich gabbroic magma forcefully injected the layered sequence resulting in brecciation of the partially and completely solidified areas, thus producing the observed textures and compositions in the heterolithic gabbro. The forceful injection of gabbro magma may have been preceded by or contemporaneous with a tectonic brecciation. The hot gabbroic magma and continued influx of deuteric fluids caused partial melting of some of the fragments within the heterolithic gabbro. The mixing of these compositionally distinct magmas with each other and with the gabbroic matrix may have triggered liquid immiscibility between the various magmas. The incorporation of felsic magma into the mafic tholeiitic melt promoted sulphide precipitation

and the formation of blebs and disseminations of PGE-Au-Cu-Ni sulphides within the gabbroic matrix. The immiscible liquids often formed pegmatitic pods and dikes that contained significant PGE sulphide mineralization.

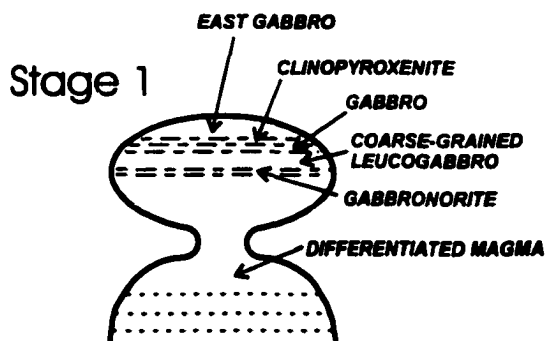
Deuteric fluids continued to percolate through the fragmented pile concentrating and depositing PGE-Au-Cu-Ni. Within the heterolithic gabbro, deuteric alteration overprinted the original magmatic textures and compositions. PGE mineralization within the heterolithic gabbro, other than the original magmatic PGE mineralization that remained intact within the core of many fragments, is directly related to the intensity of deuteric alteration. The PGE mineralization within heterolithic gabbro is associated with lower temperature minerals of merenskyite and kotulskite, which occur primarily as fine-grained inclusions within secondary silicates. The deuteric fluids were restricted to height in gabbroic rocks stratigraphically below the clinopyroxenite layer. Clinopyroxenite served as a cap for the upward migrating deuteric fluids. The original magmatic textures and compositions of the northern portion of the Roby Zone were not affected by these deuteric fluids.

Stage 3:

Once again, cooling allowed the Roby Zone to solidify. Once solidified, late-stage pegmatitic gabbro dikes intruded the Roby Zone along eastward-striking fault zones. Intrusion of the dikes occurred on several occasions, evident from the crack-and-fill textures observed. The pegmatitic gabbro dikes crosscut all of the rock types comprising the Roby Zone, stratigraphically below clinopyroxenite that because of its ductile behaviour under tectonic stress that did not allow the propagation of faults across the clinopyroxenite layer. Pegmatitic gabbro dikes have not been observed in the East Gabbro.

Stage 4:

Subsequent deformation of the Roby Zone resulted in tilting of the Roby Zone approximately 70 degrees to the east, as determined by the geometry and orientation of the igneous layers and the direction of gravitational size-graded layering observed in the northern layered sequence. Shearing occurred within a portion of the clinopyroxenite. Contemporaneous with the shearing, hydrothermal fluids further modified the magmatic textures and compositions and concentrated and deposited PGEs. The shearing episode may have occurred several times, possibly contemporaneously with the tilting of the Roby Zone. A number of late-stage east-northeast striking sinistral faults locally offset the intrusive contacts up to several meters and produced the eastward trending concave shape of the deposit.



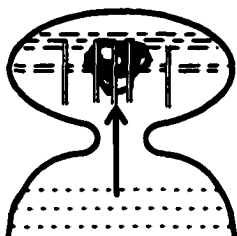
- ◆ Fractionation of Magma in lower chamber
- ◆ Formation of immiscible sulphide liquid in gabbroitic and clinopyroxenitic magma
- ◆ Intrusion of fractionated Gabbronorite, East Gabbro and Clinopyroxenite into Roby Zone
- ◆ In-situ fractionation within individual layers
- ◆ Magmatic PGE and sulphide mineralization forms near

Stage 2



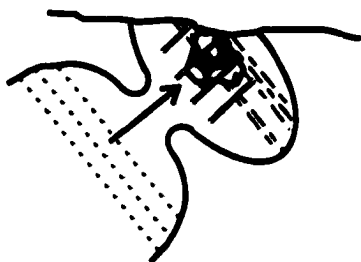
- ◆ Partial solidification of layers
- ◆ Explosive injection of volatile-rich gabbroic magma causing brecciation of layered sequence (possibly contemporaneous with tectonic brecciation)
- ◆ Partial melting of fragments by volatiles and gabbroic magma triggered liquid immiscibility
- ◆ Deuteric fluids percolate through brecciated rock concentrating and redepositing PGEs. Deuteric fluids produce isolated alteration

Stage 3



- ◆ Intrusion of late-stage pegmatitic gabbro dikes
- ◆ Fractures and dikes cross-cut Roby Zone stratigraphically beneath the clinopyroxenite cap

Stage 4



- ◆ Tilting of layers approximately 70 degrees to the east
- ◆ Erosion of portion of the Roby Zone
- ◆ Shearing occurs within portion of clinopyroxenite allowing hydrothermal alteration and additional remobilization of

Figure 8.1: Schematic cross-section showing the different stages of development of the formation of the Roby Zone PGE mineralization.

8.6 Summary and Conclusions

Previous classification of PGE deposits has placed the Roby Zone deposit in the magma-mixing subclass of orthomagmatic deposits (MacDonald, 1987). Evidence suggests that primary magmatic mineralization exists within the northern portion of the deposit, whereas later deuteric or hydrothermal fluids have modified the magmatic textures and compositions and remobilized PGE-Au-Cu-Ni within the southern portion of the deposit. The Roby Zone PGE mineralization has similarities with magmatic PGE deposits, such as the Stillwater deposit, and hydrothermal deposits, such as the Rathbun Lake deposit. The formation of the Roby Zone appears to be a combination of both of these processes.

9.0 References

- Atifi, A.M. and Essene, E.J., 1989. MINFILE computer software program, Shareware, Department of Geological Sciences, University of Michigan.
- Bates, R.L. and Jackson, J.D. eds. 1987. Glossary of Geology, third edition. American Geological Institute, Alexandria, Virginia, 788 p.
- Boudreau, A.E., Mathez, E.A. and McCallum, I.S. 1986. Halogen geochemistry of the Stillwater and Bushveld Complexes: evidence for transport of the platinum-group elements by Cl-rich fluids. *Journal of Petrology*, v. 27, p.967-986.
- Brugmann, G.E. and Naldrett, A.J. 1987. Platinum-group element abundances in mafic and ultramafic rocks: preliminary geochemical studies at the Lac des Iles Complex, District of Thunder Bay, Ontario. In Geoscience Research Grant Program, Summary of Research 1986 - 1987, Ontario Geological Survey Miscellaneous Paper 136, p.99-114
- Brugmann, G.E., Naldrett, A.J. and Macdonald, J., 1989. Magma mixing and compositional zone refining in the Lac des Iles Complex, Ontario: Genesis of the platinum-group element mineralization. *Economic Geology*, v. 84, p.1557-1573.
- Brugmann, G.E. and Naldrett, A.J. 1990. Vapour-induced partial melting in the gabbroic part of the Lac des Iles Complex, Ontario and the genesis of platinum group element mineralization; in Current Research, Part C, Geological Survey of Canada, Paper 90-1C, p. 281-291.
- Brugmann, G.E. and Naldrett, A.J. 1990. Origin of copper-nickel-platinum group element mineralization in the ultramafic part of the Lac des Iles Complex, Ontario; p. 293-303 in Current Research, Part C, Geological Survey of Canada, Paper 90-1C.
- Cabri, L.J. 1981. Analyses of minerals containing platinum-group elements; p.151-174 in: *Platinum Group Elements: Mineralogy, Geology and Recovery*. Edited by L.J. Cabri. Canadian Institute of Mining and Metallurgy, Special Volume 23.
- Cabri, L.J. and Laflamme, J.H.G. 1979. Mineralogy of samples from the Lac des Iles area, Ontario. Canadian Institute of Mining and Metallurgy. Energy, Mines and Resources, Canada, Report 79-27, 20 p.
- Cabri, L.J., Laflamme, J.H.G., Steward, J.M., Turner, K. and Skinner, B.J. 1978. On cooperite, braggite and vysotskite. *The American Mineralogist*, v.63, p.832-849.
- Campbell, I.H. 1985. The difference between oceanic and continental tholeiites: a fluid dynamic explanation. *contributions to Mineralogy and Petrology*, v.91, p.37-43.
- Craig, J.R. and Vaughan, D.J. 1981. Ore microscopy and ore petrography. New York, John Wiley and Sons, 406 p.
- Crocket, J.H., Teruta, Y. and Garth, J. 1967. The relative importance of sulfides, spinels and platinoid minerals as carriers of Pt, Pd, Ir and Au in the Merensky Reef at Western Platinum Limited, near Marikana, South Africa. *Economic Geology*, v. 71, p.1308-1323.

- Deer, W.A., Howie, R.A. and Zussman, J. 1966. An introduction to rock forming minerals. Longman Group Limited, Essex, England. 528 p.
- Dunning, G.R. 1979. The geology and platinum-group mineralization of the Roby Zone, Lac des Iles complex, northwestern Ontario. Unpublished M.Sc. Thesis, Carleton University, Ottawa, Ontario, 129 p.
- Dunning, G.R. Watkinson, D.H. and Mainwaring, P.R. 1981. Correlation of platinum-group elements with lithology in the Lac des Iles Complex, Canada; p.83-102 in Proceedings of the International Symposium on Metallogeny of Layered Mafic-Ultramafic Intrusions, Athens, Greece. International Geological Correlation Program, Project 169.
- Dunning, G.R., Laflamme, J.H.G. and Criddle, A.J. 1984. Sopscheite: a second Canadian occurrence, from the Lac des Iles Complex, Ontario. Canadian Mineralogist, v.22, p.233-237.
- Edgar, A.D. and Sweeny, J.M., 1991. The geochemistry, origin and economic potential of the PGE bearing rocks of the Lac des Iles Complex, Northwestern Ontario, Ontario Geoscience Research Grant Program, Grant No. 286; Ontario Geological Survey, Open File Report 5746, 87p.
- Fortescue, J.A.C. and Webb, J.R. 1986. An orientation geochemical study at the Lac des Iles Complex, District of Thunder Bay; In Summary of Field Work and Other Activities 1986, by the Ontario Geological Survey, Ontario Geological Survey Miscellaneous Paper 132, 435 p.
- Guarnera, B.J. 1967. Geology of the McKernan Lake phase of the Lac des Iles Intrusive, Thunder Bay District, Ontario. Unpublished M.Sc. thesis, Michigan Technical University, Houghton, Michigan.
- Gupta, V.K., Wadge, D.R., Nakashima, A. and Mark, P. 1986. Gravity studies of mafic and ultramafic intrusions in the Lac des Iles area, District of Thunder Bay; In Summary of Field Work and Other Activities 1986, by the Ontario Geological Survey Miscellaneous Paper 132, 435 p.
- Henderson, P. 1966. Inorganic Geochemistry. Pergamon Press, New York, New York. 353 p.
- Hanson, G.N. 1978. The application of trace elements to the petrogenesis of igneous rocks of granitic composition. Earth and Planetary Science Letters, v. 38, p. 26-43.
- Hobbs, B.E., Means, W.D. and Williams, P.F. 1976. An outline of structural geology. Wiley, New York.
- Irvine, T.N. 1981. Terminology for layered intrusions. Journal of Petrology, v.23 p. 127-162.
- Irvine, T.N. and Baragar, W.R.A. 1971. A guide to the chemical classification of the common volcanic rocks. Canadian Journal of Earth Sciences, v.8, p 523-546.
- IUGS Subcommittee on the Systematics of Igneous Rocks, 1973. Classification and nomenclature of plutonic rocks, recommendations - Geol. Newsletter, 1973, 2: p. 110-127.

Jolliffe, F. 1933. Block Creek map-area, Thunder Bay District, Ontario: Geological Survey of Canada, Summary Report 1933, pt. D. p.7-15, Ottawa. (Published 1934)

Lambert, D.D. and Simmons, E.C. 1988. Magma evolution in the Stillwater Complex, Montana II: rare earth element evidence for the formation of the J-M Reef. *Economic Geology*, v. 83, p1109-1126.

Leake, B.E. 1978. Nomenclature of amphiboles. *Canadian Mineralogist*, v. 16, p 501-520.

Linhardt, E. and Sutcliffe, R.H. 1986. Petrological and economic geological studies on the northern Lac des Iles Complex, District of Thunder Bay; p.80-81 In *Summary of Field Work and Other Activities 1986*, by the Ontario Geological Survey, Ontario Geological Survey Miscellaneous Paper 132, 435 p.

Linhardt, E. and Bues, C.C. 1987. Geology of the northern Lac des Iles Complex, District of Thunder Bay; p.281-285 In *Summary of Field Work and Other Activities 1987* by the Ontario Geological Survey, Ontario Geological Survey Miscellaneous Paper 137, 429 p.

Lister, G.S. and Williams, P.F. 1979. Fabric development in shear zones: Theoretical controls and observed phenomena. *Journal of Structural Geology*, Vol. 1, p. 283-297.

Loucks, R.R. and McCallum, M.E. 1980. Platinum-group minerals in the New Rambler cooper-nickel deposit, Wyoming. *Proceedings of the 11th International Mineralogical Association Meeting, Novosibirsk*, v. 1, p.200-218.

Klein, C. and Hurlbutt, C.S., Jr. 1993. *Manual of Mineralogy*, twenty-first edition, John Wiley & Sons, New York, 681 p.

Macdonald, A.J. 1985 The Lac des Iles platinum-group metals deposit, Thunder Bay District, Ontario; p.235-241 in *Summary of Field Work and Other Activities 1985*, by the Ontario Geological Survey, Ontario Geological Survey Miscellaneous paper 126, 361 p.

Macdonald, A.J., Brugmann, G.E. and Naldrett, A.J. 1989. Coeval felsic, mafic and ultramafic magmas: Magma mixing during formation of PGE-rich Ni-Cu sulphides at Lac des Iles, Ontario, Canada: Magmatic Sulphide Conference, 5th Harare, Zimbabwe, 1987. IGCC Project 161, p.139-150.

Macdonald, A.J., Brugmann, G.E. and Naldrett, A.J., 1989. Preliminary results of investigations into magma mixing, fractionation and deuteric alteration during formation of PGE-rich Ni-Cu mineralization in the Lac des Iles gabbroic complex, Ontario, Canada.

Macdonald, A.J. 1987. Ore deposit models #12: The platinum-group element deposits: classification and genesis. *Geoscience Canada*, v.14, p.155-166.

Macdonald, A.J. 1988. Platinum-group element mineralization and the relative importance of magmatic and deuteric processes: field evidence from the Lac des Iles deposit, Ontario, Canada; in *Geo-Platinum 87* Prichard H.M. et al. eds. Barking, Essex: Elsevier Applied Science, p. 215-236.

Macdonald, A.J. and Lawson, G.E. 1987. Lac des Iles (Pd-Pt-Au) deposit: geology of the mineralized zone, contact phenomena and mafic/ultramafic dikes within the gabbroic complex; p.256-264 in *Summary of Field Work and Other Activities 1987* by the Ontario Geological Survey, Ontario Geological Survey Miscellaneous Paper 137, 429 p.

McCallum, M.E., Loucks, R.R., Carlson, R.R., Cooley, E.F. and Doerge, T.A. 1976. Platinum metals associated with hydrothermal copper ores of the New Rambler mine, Medicine Bow Mountain, Wyoming. *Economic Geology*, v.71, p.1429-1450.

Morimoto, N., Fabries, J., Ferguson, A.K., Ginzburg, I.V., Ross, M., Seifert, F.A., Zussman, J., Aoki, K. and Gottardi, G. 1988. Nomenclature of pyroxenes, *American Mineralogist*, v. 73, p. 1123-1133.

Naldrett, A.J. 1979. Partitioning of Fe, Co, Ni and Cu between sulfide liquid and basaltic melts and the composition of Ni-Cu sulfide deposits - a reply and further discussion. *Economic Geology*, v.74, p.1520-1528.

Naldrett, A.J. 1981. Nickel sulphide deposits: Classification, composition and genesis; *Economic Geology*, 75th Anniversary Volume, edited by B.J. Skinner, 964 p.

Naldrett, A.J. 1981. Platinum-group element deposits; p.198-231 in *Platinum Group Elements: Mineralogy, Geology and Recovery*, edited by L.J. Cabri. Canadian Institute of Mining and Metallurgy, Special Volume 23.

Naldrett, A.J. and Cabri, L.J. 1976. Ultramafic and related mafic rocks: their classification and genesis with special reference to the concentration of nickel sulfides and platinum-group elements. *Economic Geology*, v. 71 p.1131-1158.

Naldrett, A.J. and Duke, J.M. 1980. Platinum metals in magmatic sulfide ores. *Science*, v.208, p.1417-1424.

Naldrett, A.J. Hoffman, E.L. Green, A.H., Chen-Lin Chou, Naldrett, S.R. and Alcock, A.R. 1979. The composition of Ni-sulfide ores, with particular reference to their content of PGE and Au. *Canadian Mineralogist*, v. 17, p.403-416.

Naldrett, A.J., Innes, D.G. and Sowa, J.M. 1980. Platinum-group element concentrations in some magmatic ores in Ontario; p.171 - 178 in *Geoscience Research Grant Program, Summary of Research, 1979-1980*. Ontario Geological Survey Miscellaneous Paper 93.

North American Palladium Ltd. 1997. Annual Report, p.27.

Palmer, H.C. 1987. Paleomagnetism and rock magnetism of the Mulcahy Lake Gabbro and the Lac des Iles Complex; p.126-139 in *Geoscience Research Grant Program, Summary of Research, 1986-1987*. Ontario Geological Survey Miscellaneous Paper 136, 241p.

- Platt, J.P. 1983. Secondary cleavages in ductile shear zones. *Journal of Structural Geology*, Vol. 6, No. 4, p.439.
- Pye, E.G. 1968. Geology of the Lac des Iles Area, District of Thunder Bay. Ontario Department of Mines, Geological Report 64, 47 p.
- Rowell, W.F. and Edgar, A.D. 1985. Genesis of platinum-group elements and gold in a hydrothermal sulfide occurrence in an Nipissing intrusion, northeastern Ontario (abs). *Canadian Mineralogist*, v.23, 313 p.
- Rowell, W.F. Edgar, A.D. 1986. Platinum-group element mineralization in a hydrothermal Cu-Ni sulfide occurrence, Rathbun Lake, northeastern Ontario. *Economic Geology*, v. 81, p. 1272-1277.
- Seward, T.M. 1973. Thiocomplexes of gold and the transport of gold in hydrothermal ore solutions. *Geochimica et Cosmochimica Acta.*, v.37, p. 379-399.
- Simpson, C. 1983. Strain and shape-fabric variations with ductile shear zones. *Journal of Structural Geology*, Vol. 5, No. 1, p.61.
- Smith, A.R. and Sutcliffe, R.H. 1986. Geology of the Tib Gabbro, Lac des Iles Area, District of Thunder Bay; p.76-79 In summary of Field Work and Other Activities, 1986, by the Ontario Geological Survey. Ontario Geological Survey Miscellaneous Paper 132, 435 p.
- Sparks, R.S.J. 1986. the role of crustal contamination in magma evolution through time. *Earth and Planetary Science Letters*, v. 78, p.211-223.
- Streckeisen, A. 1976. To each plutonic rock its proper name. *Earth-Science Reviews*, v.12, p.1-33.
- Stumpfl, E.F. and Ballhaus, C.G. 1986. Stratiform platinum deposits: new data and concepts. *Fortschritte der Mineralogie*, v.64, p.204-214.
- Sutcliffe, R.H. 1986. Regional geology of the Lac des Iles area, District of Thunder Bay; p.70-75 in Summary of Field Work and Other Activities 1986 by the Ontario Geological Survey. Ontario Geological Survey Miscellaneous Paper 132, 435 p.
- Sutcliffe, R.H. 1989. Magma mixing in Late Archean tonalitic and mafic rocks of the Lac des Iles area, Western Superior Province. *Precambrian Research*, v. 44, p. 81-101.
- Sutcliffe, R.H. and Sweeny, J.M. 1985. Geology of the Lac des Iles Complex, District of thunder Bay; p.47-53 in Summary of Field Work and Other Activities 1985, by the Ontario Geological Survey. Ontario Geological Survey Miscellaneous Paper 126. 361 p.
- Sutcliffe, R.H. and Sweeny, J.M. 1986. Precambrian Geology of the Lac des Iles Complex, District of Thunder Bay, Ontario. Ontario Geological Survey, Map p.3047, Geological Series-Preliminary map, scale 1:15840 or 1 inch to 1/4 mile.
- Sutcliffe, R.H., Sweeny, J.M. and Edgar, A.D. 1989. The Lac des Iles Complex, Ontario: petrology and PGE mineralization in an Archean mafic intrusion. *Canadian Journal of Earth Sciences*, v. 26, pp1408-1427.

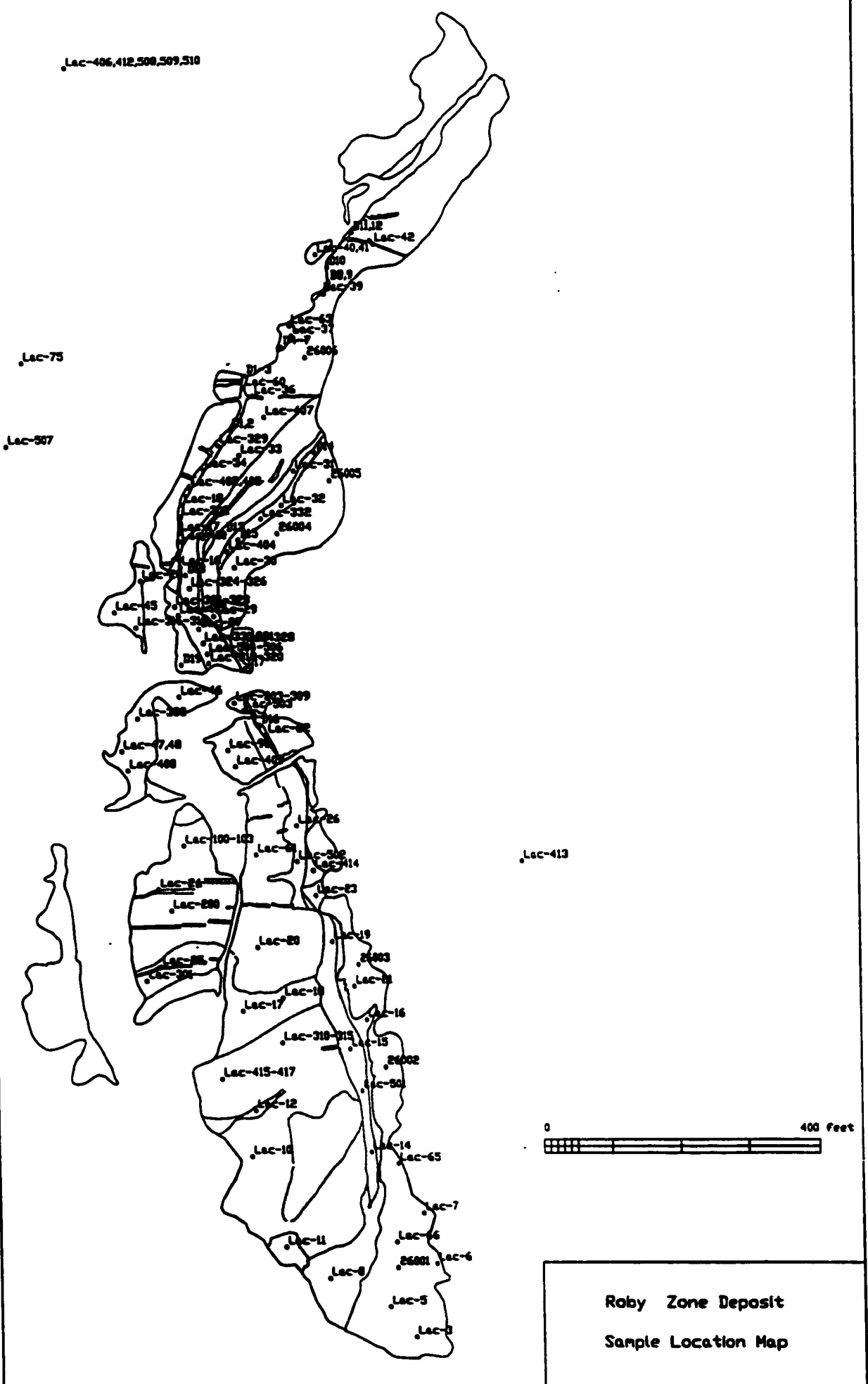
- Sutcliffe, R.H. 1990. Field Trip 1: Mafic Intrusions, Platinum-Group-Elements Mineralization and granitoid Rocks in the Lac des Iles Area; Institute on Lake Superior geology Proceedings, 36th Annual Meeting, 1990; Thunder Bay, ON, v.36, part 2, p.11-42.
- Sweeny, J.M., 1989. The geochemistry and origin of platinum group element mineralization of the hybrid zone, Lac des Iles Complex, Northwestern Ontario. Unpublished M.Sc. Thesis, University of Western Ontario, London, Ontario, 185p.
- Sweeny, J.M. and Sutcliffe, R.H. 1986. Geology and platinum-group element mineralization of the Roby Zone, Lac des Iles complex; p.82-84 in Summary of Field Work and Other Activities, 1986, by the Ontario Geological Survey. Ontario Geological Survey, Miscellaneous Paper 132, 435p.
- Sweeny, J.M. and Edgar, A.D. 1987. The geochemistry, origin and economic potential of platinum-group element bearing rocks of the Lac des Iles complex, northwestern Ontario; p.140-152 In Geoscience Research Grant Program, Summary of Research, 1986-1987. Ontario Geological Survey Miscellaneous Paper 136.
- Talkington, R.W. and Watkinson, D.H. 1984. Trends in the distribution of precious metals in the Lac des Iles complex, northwestern Ontario. Canadian Mineralogist, v.22, p.125-136.
- von Gruenewaldt, G. 1979. A review of some recent concepts of the Bushveld Complex, with particular reference to sulfide mineralization: Canadian Mineral., v. 17, p. 233-256.
- Watkinson, D.H. and Dunning, G.R. 1979. Geology and Platinum-group mineralization, Lac des Iles complex, northwestern Ontario. Canadian Mineralogist, v. 17, p.453-462.
- White, S.H., Burrows, S.E., Carreras, J., Shaw, N.P. and Humphreys, F.J. 1980. On mylonites in Ductile shear zones. Journal of Structural Geology, v. 2, No. 12, p.175.
- Wood, S.A. 1987. thermodynamic calculations of the volatility of the platinum group elements (PGE): the PGE content of fluids at magmatic temperatures. PGE content of fluids at magmatic temperatures. Geochimica et Cosmochimica Acta., v. 51, p.1041-1050.

APPENDIX 1

Sample Location Map

Approximately 200 rock grab samples were collected from altered and unaltered bedrock outcrops and drill core from each of the lithologies comprising the Roby Zone, including the northern layered sequence, heterolithic gabbro, shear zone, pegmatite gabbro dikes and the tonalitic rocks surrounding the Lac des Iles complex. The samples were collected for petrographic analysis, thin section microscopy, microprobe analysis and whole rock geochemistry. The samples collected for geochemical analyses ranged in size from several kilograms up to 4 kilograms. The samples collected for geochemical analyses were devoid of any surface weathering.

The samples are plotted on the following sample location map, which has been adapted from the detailed geological map in Figure 3.1.



APPENDIX 2

Whole Rock Analyses

Thirty-six rock grab samples were collected for whole rock major and trace element analyses. Of the thirty-six samples submitted for major element analyses, thirty samples were analysed at Activation Laboratories in Ancaster, Ontario, and six were analysed at Accurassay Laboratories in Thunder Bay, Ontario. The thirty samples analysed at Activation Laboratories were also analysed for trace elements and rare earth elements. The majority of the rock samples were analysed using fusion-inductively coupled plasma (ICP) and instrumental neutron activation analysis.

A summary of the analytical detection limits and analytical method are presented in the tables below. The analytical data is summarized in the following tables of Appendix 2. In the following tables, "nd" indicates the analyses was below the detection limit and "-" indicates that the sample was not assayed.

For all samples

Element		
All major oxides	0.01%	Fusion-ICP
Bi, Ge, Se, Te	0.2 ppm	Hydride-ICP
S	0.01%	Leco (Infrared Spectrometry)
Cu, Ni	1 ppm	Aqua regia Extraction, Atomic Absorption
Ba, Sr	2 ppm	Fusion-ICP
Y, Sr	1 ppm	Fusion-ICP

**For Samples Lac-29, 16,
330, 331, 5, 328, 332, 42,
D1**

Rb, Zn	10 ppm	Instrumental Neutron Activation Analysis
Ag, Mo, Pb	2 ppm	"
As, Sc, W, V, Cr, La, Ce, Nd	1 ppm	"
Hf	0.5 ppm	"
Co, Sb, Th, U, Sm, Eu, Gd, Dy, Er, Yb	0.1 ppm	"
Cs	0.2 ppm	"
Ta	0.3 ppm	"
Lu	0.01 ppm	"

For remaining samples

Lu	0.002 ppm	Fusion-ICP/MS
Ta, Th, U, Eu	0.005 ppm	Fusion-ICP/MS
La, Ce, Nd, Sm, Gd, Dy, Er, Yb, Sb, W, Cs, Hf, Mo, Rb	0.01 ppm	Fusion-ICP/MS
Co	0.1 ppm	Fusion-ICP/MS
As, Cr, Pb, V, Sc	1 ppm	Fusion-ICP/MS
Zn	2 ppm	Fusion-ICP/MS
Ag	0.5 ppm	Fusion-ICP/MS

Sample No.		SiO2	Al2O3	Fe2O3	MnO	MgO	CaO	Na2O	K2O	TiO2	P2O5	LOI	Total
LAC-405	schist	44.62	5.89	10.94	0.07	30.34	0.03	0.02	0.01	0.05	0.02	7.9	99.89
LAC-16	schist	51.5	4	9.52	0.13	24.51	3.25	0.07	0.02	0.09	0.01	4.62	97.72
LAC-330	schist	52.28	8.23	10.16	0.18	23.6	4.69	0.45	0.07	0.07	0.03	0.2	99.96
LAC-331	schist	48.64	6.98	9.27	0.16	23.36	4.11	0.19	0.12	0.07	0.04	5.14	98.07
D-1	gabnor	50.12	12.63	10.18	0.16	17.17	7.2	0.84	0.18	0.26	0.02	1.15	99.9
LAC-411	gabnor	50.42	13.86	10.81	0.16	14.74	7.52	1.21	0.24	0.13	0.01	1.331	100.41
LAC-415	gabnor	48.58	17.68	8.07	0.11	9.12	9.98	1.65	0.11	0.1	0.01	2.34	97.73
LAC-416	gabnor	50.99	9.38	10.32	0.15	19.55	5.11	0.56	0.21	0.09	0.01	1.33	97.68
LAC-417	gabnor	51.52	11.08	9.83	0.16	17.14	6.94	0.8	0.04	0.09	0.01	0.81	98.42
LAC-401	gabnor	50.17	14.38	8.3	0.14	16.85	7.09	0.96	0.37	0.07	0.02	1.671	100.01
LAC-402	gabnor	51.79	12.3	8.45	0.15	20.06	6.48	0.73	0.09	0.07	0.01	0.641	100.77
LAC-403	gabnor	49.51	19.69	6.28	0.1	11.63	9.95	1.37	0.12	0.05	0.01	1.24	99.95
LAC-332	pxn	44.69	6.3	17.92	0.27	17.56	8.36	0.12	0.04	0.28	0.01	5.451	100.98
LAC-414	pxn	48.48	9.92	14.53	0.2	11.32	10.19	0.77	0.22	0.22	0.01	2.78	98.63
LAC-404	pxn	46.99	9.01	17.18	0.24	13.55	7.4	0.48	0.2	0.21	0.01	3.97	99.24
LAC-412	West gab	68.81	16.19	2.93	0.04	1.01	4.23	4.74	0.59	0.28	0.06	0.79	99.67
LAC-406	West gab	51.32	18.16	7.4	0.13	10.26	10.29	1.91	0.21	0.11	0.02	0.901	100.71
LAC-11	leucogab	48.71	23.47	4.77	0.1	6.94	10.05	2.44	1.12	0.06	0.05	2.551	100.27
26006	leucogab	49.13	20.75	5.49	0.09	7.41	13.79	1.94	0.45	0.15	0.07	1.4	100.7
LAC-33	leucogab	49.18	22.83	4.75	0.09	8.09	12.3	1.65	0.17	0.06	0.03	1.091	100.24
LAC-407	leucogab	50.74	20.16	6.26	0.1	7.54	10.38	2.48	0.7	0.1	0.02	2.191	100.67
LAC-338	heter-gab	47.53	15.14	9.01	0.13	12.62	7.87	1.43	0.57	0.11	0.01	4.02	98.42
LAC-408	heter-gab	47.27	19.42	7.65	0.11	9.12	9.97	1.76	0.38	0.11	0.02	5.141	100.95
LAC-409	heter-gab	48.43	9.75	10.68	0.17	18.71	5.28	0.33	0.12	0.08	0.01	5.16	98.73
LAC-29	gabbro	50.37	16.48	9.23	0.16	8.35	9.99	2.41	0.67	0.22	0.02	1.67	99.56
LAC-23	gabbro	50.21	16.26	9.99	0.17	8.69	10.05	2.33	0.64	0.2	0.03	1.861	100.44
LAC-42	peg dike	50.36	16.98	7.22	0.13	10.6	10.1	1.91	0.7	0.09	0.01	2.151	100.24
LAC-25	peg dike	50.6	16.88	6.84	0.12	9.39	12.42	1.88	0.36	0.11	0.03	1.641	100.27
LAC-328	East gab	51.55	29.06	1.04	0.02	0.43	12.71	4.17	0.41	0.03	0.03	1.141	100.6
LAC-5	East gab	50.74	22.93	5.16	0.09	5.17	12.09	3.04	0.28	0.09	0.01	1.231	100.83
26001	East gab	49.54	20.18	6.43	0.1	5.76	12.16	2.95	0.54	0.13	0.07	1.8	99.7
26002	East gab	51.06	22.71	4.31	0.07	4.72	13.33	3.21	0.32	0.1	0.05	1.4	101.3
26003	East gab	50.56	24.11	4.44	0.07	3.37	13.53	3.51	0.46	0.08	0.05	1.6	101.8
26004	East gab	49.51	22.62	4.85	0.08	3.61	11.94	3.06	1.08	0.11	0.05	1.8	98.8
26005	East gab	49.81	21.49	6.05	0.1	4.76	10.99	3.11	1.11	0.12	0.07	2.1	99.7
LAC-413	East gab	31.79	12.57	37.15	0.15	6.26	4.56	1.21	0.54	2.8	0.01	1.09	98.12

Sample No.		Ba	Sr	Y	Zr
LAC-405	schist	8	5	1	3
LAC-16	schist	8	4	2	4
LAC-330	schist	13	53	2	3
LAC-331	schist	10	11	2	5
D-1	gabnor	45	104	3	8
LAC-411	gabnor	52	136	3	7
LAC-415	gabnor	42	173	2	5
LAC-416	gabnor	29	67	2	5
LAC-417	gabnor	15	90	1	5
LAC-401	gabnor	56	141	1	2
LAC-402	gabnor	19	95	2	5
LAC-403	gabnor	30	170	1	1
LAC-332	pxn	4	3	6	13
LAC-414	pxn	29	150	4	7
LAC-404	pxn	30	53	3	5
LAC-412	West gab	305	345	2	77
LAC-406	West gab	72	182	3	9
LAC-11	leucogab	191	278	2	7
LAC-33	leucogab	66	204	2	4
LAC-407	leucogab	136	246	2	13
LAC-338	heter-gab	85	142	2	8
LAC-408	heter-gab	55	213	3	10
LAC-409	heter-gab	16	27	2	10
LAC-29	gabbro	162	237	6	13
LAC-23	gabbro	121	247	4	7
LAC-42	peg dike	168	207	3	7
LAC-25	peg dike	99	174	3	4
LAC-328	East gab	104	396	1	2
LAC-5	East gab	82	287	2	1

Sample No.		Bi ppm	Ge ppm	Se ppm	Te ppm	S (%)
D-1	gabnor	0.2	0.2	nd	0.8	0.033
LAC-16	schist	nd	0.3	0.2	1.1	0.066
LAC-33	leucogab	nd	0.2	nd	0.6	0.003
LAC-29	gabbro	nd	nd	nd	nd	0.063
LAC-42	peg dike	nd	nd	nd	0.2	0.007
LAC-330	schist	nd	nd	nd	nd	0.013
LAC-331	schist	0.2	0.2	4	2.7	0.451
LAC-332	pxn	0.9	nd	5.1	nd	3.41
LAC-338	heter-gab	0.3	nd	8.4	3.6	1.34
LAC-328	East Gab	nd	nd	0.6	nd	0.03
LAC-401	gabnor	nd	nd	3.1	nd	0.411
LAC-402	gabnor	nd	nd	2.1	0.4	0.188
LAC-403	gabnor	nd	nd	2.9	0.2	0.31
LAC-404	pxn	nd	nd	1.3	nd	1.7
LAC-405	schist	2.2	nd	nd	nd	0.003
LAC-406	Wgab	nd	nd	nd	nd	0.033
LAC-407	leucogab	nd	nd	nd	nd	0.005
LAC-408	heter-gab	1.3	0.4	12.5	1.8	1.51
LAC-409	heter-gab	0.4	0.4	9.7	2	1.31
LAC-411	gabnor	1.5	0.7	5.9	1.8	0.803
LAC-11	leucogab	nd	nd	nd	0.2	0.003
LAC-23	gabbro	nd	nd	nd	0.2	0.061
LAC-25	peg dike	nd	nd	0.9	0.2	0.11
LAC-5	East Gab	nd	nd	nd	nd	0.022
LAC-412	West gab	nd	nd	nd	0.2	0.067
LAC-413	Magab	nd	nd	0.5	0.2	0.067
LAC-414	pxn	nd	nd	3.2	0.9	0.952
LAC-415	gabnor	nd	nd	11.4	2.5	1.5
LAC-416	gabnor	nd	0.2	10	3	1.02
LAC-417	gabnor	nd	nd	2.8	0.2	0.48

Sample		Cs	HF	MO	Rb	SB	Sc	TA	TH	U	W	LA	ND	SM	TB	YB	LU	CU	PB	ZN	AG	NI	BI	V		
		ppm	ppm	ppm	ppm	ppm	ppm	ppm	ppm	ppm	ppm	ppm	ppm	ppm	ppm	ppm	ppm	ppm	ppm	ppm	ppm	ppm	ppm	ppm		
LAC-29	gabbro	0.9	0	-2	19	0.2	35	-0.3	-0.1	0	-1	3	4	2	0.6	0.3	-0.1	0.57	0.09	130	-5	49	-0.4	314	-5	123
LAC-23	gabbro	2.13	0.2	3.27	20.6	-	42	0.01	0.03	0.01	0.25	1.28	2.81	1.8	0.52	0.25	0.11	0.5	0.08	34	-1	90	-0.5	197	-	196
LAC-405	schist	0.66	0.05	2.47	1.47	-	6	0.04	0.12	0.44	0.1	14.6	29.1	10.2	1.28	0.21	0.05	0.06	0.01	61	-1	105	-0.5	1794	2.2	70
LAC-16	schist	-0.2	0	-2	13	-0.1	41	-0.3	-0.1	0	-1	1	-1	-1	0.1	-0.1	-0.1	0.36	0.05	107	11	104	-0.4	1004	-5	97
LAC-330	schist	0.4	0	-2	-10	0.2	38	-0.3	-0.1	0	-1	1	-1	-1	0.1	0.1	-0.1	0.3	0.04	40	-5	50	-0.4	969	-5	86
LAC-331	schist	1.1	0	-2	-10	0.3	35	-0.3	-0.1	0	-1	1	-1	1	0.1	-0.1	-0.1	0.27	0.06	1610	473	927	1.8	2657	-5	82
LAC-5	East gab	0.83	0.08	3.32	9.25	-	23	0.06	0.02	0.01	0.33	0.88	1.49	0.76	0.21	0.16	0.04	0.19	0.03	71	-1	41	-0.5	145	-	93
LAC-328	East gab	2.7	0	-2	10	0.2	1	-0.3	-0.1	0	4	1	2	-1	0.1	0.2	-0.1	-	-	185	-5	9	-0.4	26	-5	7
LAC-411	gabnor	0.73	0.19	2.98	7.15	0.48	34	0.01	0.11	0.03	0.03	1.25	2.56	1.3	0.36	0.14	0.07	0.37	0.06	2076	1	68	-0.5	1878	-	130
D-1	gabnor	-0.2	0	-2	-10	-0.1	34	-0.3	-0.1	0	-1	1	2	-1	0.2	0.1	-0.1	0.33	0.05	64	-5	47	-0.4	754	-5	109
LAC-401	gabnor	1.28	0.05	3.61	14.5	1.27	29	-	0.03	0.04	0.2	0.47	0.81	0.42	0.1	0.08	0.03	0.21	0.04	1453	-1	62	-0.5	1703	-	97
LAC-415	gabnor	0.87	0.12	0.74	4.26	0.07	24	0.01	0.1	-	0.12	0.89	1.74	0.85	0.18	0.12	0.05	0.27	0.05	2245	-1	31	-0.5	614	-	79
LAC-416	gabnor	0.88	0.13	0.77	7.26	0.17	33	0.01	0.08	-	0.11	0.65	1.3	0.65	0.16	0.06	0.04	0.24	0.05	2415	-1	35	-0.5	1641	-	100
LAC-417	gabnor	0.35	0.08	0.93	1.2	0.06	34	0.01	0.07	-	0.02	0.5	0.69	0.51	0.12	0.07	0.03	0.3	0.04	996	-1	51	-0.5	1062	-	108
LAC-402	gabnor	0.63	0.08	3.9	3.45	-	33	0.01	0.02	-	0.2	0.41	0.73	0.4	0.13	0.06	0.03	0.22	0.04	654	-1	53	-0.5	1137	-	104
LAC-403	gabnor	0.79	-	3.6	5.05	-	21	-	0.02	0.01	-	0.44	0.78	0.39	0.12	0.09	0.02	0.18	0.03	835	-1	43	-0.5	1221	-	70
LAC-332	pxn	0.7	0	-2	-10	0.1	59	-0.3	-0.1	0	-1	1	2	-1	0.4	0.2	-0.1	0.75	0.11	651	-5	116	-0.4	605	-5	192
LAC-414	pxn	0.86	0.25	0.86	8.15	0.31	64	-	0.04	-	0.32	0.7	1.61	1.39	0.42	0.2	0.13	0.61	0.09	1085	-1	48	-0.5	454	0.13	235
LAC-404	pxn	0.72	0.12	2.94	5.94	0.74	50	0.01	0.02	0.01	0.17	0.58	1.18	0.9	0.28	0.11	0.07	0.48	0.08	1132	13	110	-0.5	496	-	237
LAC-412	West	0.79	2.51	1.27	12.7	0.12	3	0.18	1.94	0.57	0.27	14.8	25.3	7.93	1.12	0.71	0.09	0.28	0.04	8	1	34	-0.5	19	-	34
LAC-406	West	0.72	0.27	3.48	6.05	-	28	0.04	0.07	0.02	0.01	2.4	4.56	2.16	0.51	0.23	0.09	0.42	0.06	79	-1	66	-0.5	350	-	105
LAC-11	leucoga	2.53	0.16	2.76	35.8	-	14	0.04	0.15	0.08	0.15	1.92	3.17	1.43	0.28	0.13	0.04	0.17	0.03	20	2	45	-0.5	325	-	61
LAC-33	leucoga	-0.2	0	-2	12	-0.1	20	-0.3	-0.1	0	-1	1	2	-1	0.2	0.1	-0.1	0.24	0.03	41	-5	22	-0.4	304	-5	52
LAC-407	leucoga	2.05	0.5	3.31	25.2	-	24	0.04	0.31	0.1	0.22	2.12	3.95	1.68	0.43	0.22	0.06	0.26	0.04	30	-1	44	-0.5	239	-	98
LAC-338	heter-	3.1	0	-2	22	0.1	25	-0.3	0.2	0	-1	2	2	-1	0.2	0.1	-0.1	0.31	0.05	2862	-5	43	0.9	4241	-5	72
LAC-408	heter-	2.49	0.31	2.71	24.6	0.79	22	0.02	0.19	0.07	0.57	1.47	2.73	1.31	0.38	0.14	0.06	0.36	0.05	3600	7	66	-0.5	1230	-	93
LAC-409	heter-	1.47	0.26	2.78	6.91	0.13	32	0.01	0.15	0.05	0.03	0.97	2.06	0.93	0.23	0.09	0.05	0.32	0.05	3345	-1	87	-0.5	1605	-	106
LAC-42	peg dike	1.7	0	-2	23	0.1	33	-0.3	-0.1	0	-1	2	3	1	0.3	0.2	-0.1	0.43	0.06	25	-5	37	-0.4	426	-5	88
LAC-25	peg dike	1.29	0.19	2.84	13.8	1.61	43	0.02	0.08	0.06	0.28	1.08	2.01	1.24	0.39	0.16	0.09	0.41	0.05	564	-1	36	-0.5	444	-	146
LAC-413	East	1.77	0.22	0.88	18.3	0.13	21	0.04	0.12	0.02	0.2	1.21	1.99	0.78	0.12	0.13	0.03	0.15	0.03	450	-1	195	-0.5	473	-	2115

Sample No.		La ppm	Ce ppm	Nd ppm	Sm ppm	Eu ppm	Gd ppm	Dy ppm	Er ppm	Yb ppm	Lu ppm
LAC-29	gabbro	3	4	2	0.6	0.3	NA	NA	NA	0.57	0.09
LAC-23	gabbro	1.28	2.81	1.8	0.52	0.252	0.54	0.63	0.5	0.5	0.08
LAC-406	gabbro	2.4	4.56	2.16	0.51	0.233	0.54	0.51	0.43	0.42	0.062
LAC-507	gabbro	6.6	5.1	2.1	0.4	0.2	0.4	0.5	0.2	0.2	0.05
LAC-405	schist	14.61	29.13	10.18	1.28	0.207	0.61	0.23	0.07	0.06	0.011
LAC-16	schist	1	nd	nd	0.1	nd	NA	NA	NA	0.36	0.05
LAC-330	schist	1	nd	nd	0.1	0.1	NA	NA	NA	0.3	0.04
LAC-331	schist	1	nd	1	0.1	nd	NA	NA	NA	0.27	0.06
LAC-501	schist	0.6	0.8	0.6	0.1	0.05	0.2	0.3	0.2	0.2	0.05
LAC-502	schist	0.1	0.5	0.2	0.1	0.05	0.1	0.2	0.2	0.2	0.05
LAC-503	schist	9.9	0.7	0.4	0.1	0.05	0.1	0.2	0.1	0.1	0.05
LAC-504	schist	7.8	6.1	2.9	0.6	0.11	0.6	0.7	0.4	0.4	0.06
LAC-505	schist	10.6	4.2	2.6	0.9	0.17	1.1	1.3	0.6	0.7	0.11
LAC-5	East gab	0.88	1.49	0.76	0.21	0.158	0.24	0.21	0.18	0.19	0.026
LAC-328	East gab	1	2	nd	0.1	0.2	NA	NA	NA	0	0.01
LAC-411	gabnor	1.25	2.56	1.3	0.36	0.14	0.37	0.43	0.32	0.37	0.057
D-1	gabnor	1	2	nd	0.2	0.1	NA	NA	NA	0.33	0.05
LAC-401	gabnor	0.47	0.81	0.42	0.1	0.075	0.1	0.16	0.17	0.21	0.035
LAC-416	gabnor	0.89	1.74	0.85	0.18	0.116	0.25	0.33	0.27	0.27	0.045
LAC-416	gabnor	0.65	1.3	0.65	0.16	0.063	0.19	0.28	0.22	0.24	0.047
LAC-417	gabnor	0.5	0.89	0.51	0.12	0.072	0.18	0.25	0.21	0.3	0.042
LAC-402	gabnor	0.41	0.73	0.4	0.13	0.063	0.11	0.18	0.16	0.22	0.039
LAC-403	gabnor	0.44	0.78	0.39	0.12	0.089	0.1	0.15	0.12	0.18	0.025
LAC-332	pxn	1	2	nd	0.4	0.2	NA	NA	NA	0.75	0.11
LAC-414	pxn	0.7	1.61	1.39	0.42	0.204	0.65	0.81	0.58	0.61	0.068
LAC-404	pxn	0.58	1.18	0.9	0.26	0.106	0.37	0.43	0.43	0.48	0.075
LAC-11	leucogab	1.92	3.17	1.43	0.28	0.13	0.3	0.22	0.17	0.17	0.03
LAC-33	leucogab	1	2	nd	0.2	0.1	NA	NA	NA	0.24	0.03
LAC-407	leucogab	2.12	3.95	1.68	0.43	0.215	0.33	0.36	0.28	0.26	0.04
LAC-338	heter-gab	2	2	nd	0.2	0.1	NA	NA	NA	0.31	0.05
LAC-408	heter-gab	1.47	2.73	1.31	0.36	0.139	0.32	0.44	0.31	0.36	0.048
LAC-409	heter-gab	0.97	2.06	0.93	0.23	0.085	0.24	0.3	0.25	0.32	0.045
LAC-42	peg dike	2	3	1	0.3	0.2	NA	NA	NA	0.43	0.06
LAC-25	peg dike	1.08	2.01	1.24	0.39	0.162	0.47	0.48	0.36	0.41	0.051
LAC-413	Magab	1.21	1.99	0.78	0.12	0.128	0.12	0.18	0.15	0.15	0.028
LAC-10	Granite	53.3	31.2	9.2	1.3	0.34	1	0.9	0.4	0.5	0.08
LAC-28	Granite	27.7	20.7	6.5	1.1	0.27	0.8	0.7	0.3	0.3	0.05
LAC-75	Granite	4.6	2.4	0.8	0.1	0.35	0.1	0.1	0.1	0.1	0.05
LAC-324	Granite	15.3	11.2	5.2	1.1	0.27	0.9	0.8	0.4	0.5	0.07
LAC-325	schist	14.2	13.6	3.7	0.5	0.24	0.3	0.2	0.1	0.2	0.05
LAC-506	schist	5.4	11	4	0.8	0.2	0.7	0.6	0.3	0.3	0.05
LAC-508	tonalite	11.5	15	5.5	0.8	0.51	0.6	0.3	0.1	0.1	0.05
LAC-509	tonalite	12.6	17.7	5.6	0.7	0.54	0.4	0.2	0.1	0.1	0.05
LAC-510	tonalite	25.8	13	4.2	0.5	0.5	0.3	0.1	0.1	0.1	0.05
LAC-412	East gab	14.57	25.32	7.93	1.12	0.711	0.59	0.48	0.24	0.28	0.041

APPENDIX 3

Mineral Analyses

Plagioclase feldspar, orthopyroxene, clinopyroxene and amphibole mineral compositions were completed using the Energy Dispersive X-ray Spectrometer (EDS) attachment of the Hitachi 750 Scanning Electron Microscope (SEM) located in the Instrumentation Laboratory at Lakehead University.

Quantitative analyses of plagioclase, orthopyroxene, clinopyroxene and amphibole were completed under the following operating conditions: an accelerating voltage of 20 kV, a 30 degree take-off angle, a working distance of 28 mm, a beam current of 0.38 Na, and a spot size of approximately 2 μm . Counting time averaged 100 seconds. All spectra obtained were analysed using Tracor Northern ZAF computer programs and the SQ internal standards program. Plagioclase, pyroxene and amphibole minerals were analysed using natural minerals as reference standards, including garnet, diopside and ilmenite. All standards were acquired on a daily basis by A.D. McKenzie of the Lakehead Instrumentation Laboratory. Detection limits are approximately 0.05 weight percent oxide.

Structural formula calculations were completed using Minfile, a computer software program designed specifically for storage and manipulation of mineral chemistry analyses (Afifi and Essene, 1989). The results are presented in the immediately following pages.

Feldspar

Sample	Lac-5							
Rock type	East Gab							
Grain	2-1	2-2	2-3	2-4	2-5	2-6	1-6	1-8
Grain area	rim	rim	core	core	rim	core	rim	core
SiO₂	50.77	51.26	52.53	51.54	53.23	52.89	52.24	51.47
TiO₂	0	0	0	0	0	0	0	0
Al₂O₃	31.53	32.12	31.96	32.57	31.57	31.74	30.9	29.71
FeO	0.18	0	0	0	0	0	0.23	0
CaO	13.74	13.35	13.05	13.74	12.97	13.01	12.55	13.59
Na₂O	3.59	3.86	4.18	3.81	4.35	4.26	4.4	3.83
K₂O	0	0	0	0	0	0	0	0
Total	99.81	100.59	101.72	101.66	102.12	101.9	100.32	98.6
Si	2.313	2.312	2.34	2.303	2.361	2.351	2.361	2.37
Ti	0	0	0	0	0	0	0	0
Al	1.693	1.708	1.678	1.715	1.65	1.663	1.646	1.612
Fe	0.007	0	0	0	0	0	0.009	0
Ca	0.671	0.645	0.623	0.658	0.616	0.62	0.608	0.67
Na	0.317	0.338	0.361	0.33	0.374	0.367	0.386	0.342
K	0	0	0	0	0	0	0	0
O	8	8	8	8	8	8	8	8
Or	0.0	0.0	0.0	0.0	0.0	0.0	0.0	0.0
An	67.9	65.6	63.3	66.6	62.2	62.8	61.2	66.2
Ab	32.1	34.4	36.7	33.4	37.8	37.2	38.8	33.8

Sample	Lac-63	Lac-63	Lac-63	Lac-63	Lac-40	Lac-40	Lac-40	Lac-40
Rock type	Gabnor	Gabnor	Gabnor	Gabnor	Pyrox.	Pyrox.	Pyrox.	Pyrox.
Grain	1	2	4	5	2-1	2-2	1-1	1-2
Grain area	core	core	core	rim	rim	core	core	core
SiO ₂	48.75	47.3	48.53	49.13	53.8	46.96	52.42	53.09
TiO ₂	0	0	0	0	0	0	0	0
Al ₂ O ₃	33.8	34.55	34.36	34.1	29.94	35.17	29.37	29.66
FeO	0	0	0	0.26	0	0.2	0	0
CaO	16	17.25	15.69	16.12	11.25	17.05	11.51	11.35
Na ₂ O	2.64	2.19	2.7	2.71	5.14	1.9	4.71	5.07
K ₂ O	0	0	0	0	0.18	0.14	0.19	0.19
Total	101.19	101.29	101.28	102.32	100.31	101.42	98.2	99.36
Si	2.204	2.147	2.191	2.2	2.422	2.129	2.413	2.416
Ti	0	0	0	0	0	0	0	0
Al	1.801	1.848	1.828	1.8	1.589	1.879	1.593	1.591
Fe	0	0	0	0.01	0	0.008	0	0
Ca	0.775	0.839	0.759	0.773	0.543	0.828	0.568	0.553
Na	0.231	0.193	0.236	0.235	0.449	0.167	0.42	0.447
K	0	0	0	0	0.01	0.008	0.011	0.011
O	8	8	8	8	8	8	8	8
Or	0.0	0.0	0.0	0.0	1.0	0.8	1.1	1.1
An	77.0	81.3	76.3	76.7	54.2	82.6	56.9	54.7
Ab	23.0	18.7	23.7	23.3	44.8	16.7	42.0	44.2

Sample	D13	D13	D13	D13	D1	D1	D15	D15
Rock type	Gabnor	Gabnor	Gabnor	Gabnor	Gabnor	Gabnor	Shear	Shear
Grain	1-1	1-3	1-4	3-1	1	2	2	3
Grain area	core	core	core	core	core	core	rim	core
SiO ₂	48.65	49.26	47.29	53.23	47.21	49.54	54.15	53.63
TiO ₂	0	0	0	0	0	0	0	0
Al ₂ O ₃	32.79	32.81	32.81	29.29	32.36	34.1	27.67	31.74
FeO	0.27	0	0.27	0	0.23	0.27	2.68	0.93
CaO	15.68	15.92	15.7	11.73	15.08	15.92	6	9.98
Na ₂ O	2.88	2.86	2.42	5	2.68	2.66	5.29	3.96
K ₂ O	0	0	0	0.14	0	0	1.14	1
Total	100.27	100.85	98.49	99.39	97.56	102.49	98.87	102.17
Si	2.223	2.235	2.2	2.423	2.214	2.211	2.481	2.374
Ti	0	0	0	0	0	0	0	0
Al	1.766	1.754	1.799	1.571	1.789	1.794	1.494	1.656
Fe	0.01	0	0.011	0	0.009	0.01	0.103	0.034
Ca	0.768	0.774	0.782	0.572	0.758	0.761	0.294	0.473
Na	0.255	0.252	0.218	0.441	0.244	0.23	0.47	0.34
K	0	0	0	0.008	0	0	0.067	0.056
O	8	8	8	8	8	8	8	8
Or	0.0	0.0	0.0	0.8	0.0	0.0	8.1	6.4
An	75.1	75.4	78.2	56.0	75.6	76.8	35.4	54.4
Ab	24.9	24.6	21.8	43.2	24.4	23.2	56.6	39.1

Sample	Lac-65	Lac-65	Lac-65	Lac-65	Lac-65	Lac-65	Lac-33	Lac-98
Rock type	East Gab	Leucogab	Leucogab					
Grain	1	3	5	6	10	11	2-2	1
Grain area	core	rim	core	core	rim	core	core	core
SiO ₂	57.83	52.32	51.5	52.57	52.12	51.48	47.07	66.88
TiO ₂	0	0	0	0	0	0	0	0
Al ₂ O ₃	26	30.86	29.62	29.33	29.47	28.77	33.36	21.4
FeO	0	0	0	0	0	0	0.42	0.44
CaO	8.46	13.99	13.6	13.05	12.67	13.18	16.79	1.31
Na ₂ O	7.26	4.39	4.36	4.55	4.7	4.53	2.03	11.03
K ₂ O	0.17	0	0	0.18	0	0	0.09	0
Total	99.72	101.56	99.08	99.68	98.96	97.95	99.76	101.06
Si	2.602	2.346	2.366	2.396	2.39	2.411	2.171	2.907
Ti	0	0	0	0	0	0	0	0
Al	1.378	1.631	1.604	1.576	1.593	1.588	1.813	1.096
Fe	0	0	0	0	0	0	0.016	0.016
Ca	0.408	0.672	0.669	0.637	0.622	0.661	0.83	0.061
Na	0.633	0.382	0.388	0.402	0.418	0.27	0.182	0.93
K	0.01	0	0	0.01	0	0	0.005	0
O	8	8	8	8	8	8	8	8
Or	1.0	0.0	0.0	1.0	0.0	0.0	0.5	0.0
An	38.8	63.8	63.3	60.7	59.8	71.0	81.6	6.2
Ab	60.2	36.2	36.7	38.3	40.2	29.0	17.9	93.8

Sample	Lac-98	Lac-98	Lac-98	Lac-98	Lac-36	Lac-36	Lac-36	Lac-36
Rock type	Leucogab	Leucogab	Leucogab	Leucogab	Gab dyke	Gab dyke	Gab dyke	Gab dyke
Grain	2	4	5	6	1	2	3	4
Grain area	core	core	core	core	core	rim	core	core
SiO ₂	47.64	49.24	50.05	47.15	54.02	53.84	53.35	52.22
TiO ₂	0	0	0	0	0	0	0	0
Al ₂ O ₃	34.48	33.6	33.03	34.61	28.24	28.29	30.37	29.08
FeO	0.45	0	0.47	0	0	0	0.28	0
CaO	16.38	14.5	15.73	15.25	10.27	10.67	11.76	10.51
Na ₂ O	2.22	2.91	3.16	2.73	5.68	5.74	4.68	5.03
K ₂ O	0	0	0	0	0	0	0.13	0.77
Total	101.17	100.25	102.44	99.74	98.21	98.54	100.57	97.61
Si	2.162	2.235	2.239	2.162	2.477	2.466	2.4	2.422
Ti	0	0	0	0	0	0	0	0
Al	1.844	1.798	1.742	1.87	1.526	1.527	1.61	1.59
Fe	0.017	0	0.018	0	0	0	0.011	0
Ca	0.796	0.705	0.754	0.749	0.505	0.524	0.567	0.522
Na	0.195	0.256	0.274	0.243	0.505	0.51	0.408	0.452
K	0	0	0	0	0	0	0.007	0.046
O	8	8	8	8	8	8	8	8
Or	0.0	0.0	0.0	0.0	0.0	0.0	0.7	4.5
An	80.3	73.4	73.3	75.5	50.0	50.7	57.7	51.2
Ab	19.7	26.6	26.7	24.5	50.0	49.3	41.5	44.3

Sample	Lac-42	Lac-42	Lac-42	Lac-31	Lac-31	Lac-76	Lac-76
Rock type	Gab dyke	Gab dyke	Gab dyke	Gabbro	Gabbro	Tonalite	Tonalite
Grain	1	2	3	1	2	2	3
Grain area	core	core	core	core	core	core	core
SiO ₂	59.62	59.44	50.84	51.16	55.54	50.43	50.26
TiO ₂	0	0	0	0	0	0	0
Al ₂ O ₃	25.57	25.35	32.13	29.37	25.73	30.5	31.28
FeO	0.57	0.44	0	0	0	0.34	0.22
CaO	6.06	5.74	13.41	13.28	8.72	13.35	14
Na ₂ O	7.74	7.7	3.54	4.35	7.1	3.85	3.7
K ₂ O	0	0.09	0	0	0	0	0.17
Total	99.56	99.08	99.92	98.16	97.44	98.47	99.63
Si	2.666	2.668	2.307	2.37	2.564	2.331	2.302
Ti	0	0	0	0	0	0	0
Al	1.347	1.341	1.719	1.604	1.4	1.661	1.688
Fe	0.021	0.017	0	0	0	0.013	0.008
Ca	0.29	0.276	0.652	0.659	0.431	0.661	0.687
Na	0.671	0.67	0.311	0.391	0.635	0.345	0.329
K	0	0.005	0	0	0	0	0.01
O	8	8	8	8	8	8	8
Or	0.0	0.5	0.0	0.0	0.0	0.0	1.0
An	30.2	29.0	67.7	62.8	40.4	65.7	67.0
Ab	69.8	70.5	32.3	37.2	59.6	34.3	32.1

Orthopyroxene

Sample	Lac-63							
Rock type	Gabnor							
Grain	1-1	1-2	1-3	1-5	1-9	1-10	11	15
Grain area	core	core	rim	core	core	core	core	rim
SiO ₂	55.63	54.31	54.03	54.82	54.5	62.24	62.23	55.07
TiO ₂	0	0	0	0	0	0	0	0.28
Al ₂ O ₃	1.95	2.4	2.32	2.12	1.95	1.66	1.66	2.01
FeO	12.63	12.52	11.72	12.25	12.76	4.98	4.98	11.44
MnO	0.24	0	0.36	0.29	0	0	0	0.32
MgO	30.39	29.89	28.05	29.39	28.9	28.93	28.93	28.88
CaO	0.69	0.69	2.59	0.91	0.77	0	0	2.88
Na ₂ O	0	0	0.34	0	0.41	0.39	0.38	0
Total	101.53	99.81	99.41	99.78	99.29	98.2	98.18	101.09
Si	1.946	1.932	1.939	1.95	1.953	2.133	2.133	1.94
Ti	0	0	0	0	0	0	0	0.007
Al (IV)	0.054	0.068	0.061	0.051	0.047	0	0	0.06
Al (VI)	0.026	0.033	0.036	0.039	0.035	0.067	0.067	0.023
Fe	0.369	0.373	0.352	0.364	0.382	0.143	0.143	0.337
Mn	0.007	0	0.011	0.009	0	0	0	0.01
Mg	1.585	1.585	1.501	1.559	1.544	1.478	1.478	1.516
Ca	0.026	0.026	0.1	0.035	0.03	0	0	0.109
Na	0	0	0.024	0	0.028	0.026	0.025	0
O	6	6	6	6	6	6	6	6
Fs	18.6	18.8	18.0	18.6	19.5	8.8	8.8	17.2
Wo	1.3	1.3	5.1	1.8	1.5	0.0	0.0	5.6
En	80.1	79.9	76.9	79.6	78.9	91.2	91.2	77.3

Sample	Lac-40	Lac-40	Lac-40	Lac-40	D13	D13	D13	D13
Rock type	Pyrox	Pyrox	Pyrox	Pyrox	Gabnor	Gabnor	Gabnor	Gabnor
Grain	2-2	1-3	1-4	1-5	1-7	1-8	1-9	1-10
Grain area	core	core	core	rim	core	core	core	rim
SiO ₂	52.99	52.12	53.29	52.88	53.97	53.88	54.89	53.09
TiO ₂	0	0	0	0.28	0	0	0	0.22
Al ₂ O ₃	1.01	1.05	1.08	1.49	1.71	1.93	1.63	1.87
FeO	22.01	21.98	22.42	21.94	12.87	14.19	14	12.92
MnO	0.46	0.53	0.62	0.51	0.2	0.34	0.25	0.24
MgO	21.57	21.49	22.28	21.76	28.45	28.84	29.4	28.09
CaO	2.1	0.98	0.59	0.85	2.87	0.81	1.23	2.09
Na ₂ O	0.47	0.48	0.47	0.51	0.45	0.39	0.43	0.46
Total	100.61	98.63	100.75	100.22	100.52	100.38	101.83	98.98
Si	1.97	1.973	1.973	1.965	1.93	1.929	1.936	1.926
Ti	0	0	0	0.008	0	0	0	0.006
Al (IV)	0.03	0.027	0.027	0.035	0.07	0.071	0.064	0.074
Al (VI)	0.014	0.02	0.02	0.031	0.002	0.011	0.003	0.006
Fe	0.684	0.696	0.694	0.682	0.385	0.425	0.413	0.392
Mn	0.014	0.017	0.019	0.016	0.006	0.01	0.007	0.007
Mg	1.195	1.213	1.23	1.206	1.516	1.539	1.546	1.519
Ca	0.084	0.04	0.023	0.034	0.11	0.031	0.046	0.081
Na	0.034	0.035	0.034	0.037	0.031	0.027	0.029	0.032
O	6	6	6	6	6	6	6	6
Fs	34.8	35.7	35.6	35.5	19.1	21.3	20.6	19.7
Wo	4.3	2.1	1.2	1.8	5.5	1.6	2.3	4.1
En	60.9	62.2	63.2	62.7	75.4	77.1	77.1	76.3

Sample	D13	D13	D13	D13	D13	D13	D1	D1
Rock type	Gabnor							
Grain	1-11	3-1	3-2	3-5	3-6	3-7	1	3
Grain area	core	core	core	core	core	rim	core	core
SiO ₂	53.46	57.51	56.37	55.2	53.39	53.18	55.13	57.57
TiO ₂	0	0	0	0	0	0	0	0
Al ₂ O ₃	1.97	0.38	1.37	0.9	1.89	1.5	1.52	0
FeO	12.97	15.13	17.63	14.79	14.71	13.19	13.06	17.77
MnO	0.3	0.36	0.37	0.31	0	0.26	0	0.54
MgO	28.44	25.29	22.73	29.29	28.15	28.21	29.63	24.07
CaO	2.11	0.69	0.92	0.46	0.53	1.84	0.54	0.47
Na ₂ O	0.38	0.43	0.69	0.24	0.57	0.44	0	0
Total	99.63	99.79	100.08	101.19	99.43	98.62	99.88	100.42
Si	1.926	2.06	2.04	1.96	1.933	1.937	1.962	2.07
Ti	0	0	0	0	0	0	0	0
Al (IV)	0.074	0	0	0.04	0.067	0.065	0.038	0
Al (VI)	0.01	0.016	0.058	0	0.014	0.002	0.026	0
Fe	0.391	0.453	0.534	0.439	0.445	0.402	0.389	0.534
Mn	0.009	0.011	0.011	0.009	0	0.008	0	0.016
Mg	1.528	1.35	1.227	1.55	1.519	1.532	1.572	1.29
Ca	0.081	0.026	0.036	0.017	0.021	0.072	0.021	0.018
Na	0.027	0.03	0.048	0.017	0.04	0.031	0	0
O	6	6	6	6	6	6	6	6
Fs	19.6	24.8	29.7	21.9	22.4	20.0	19.6	29.0
Wo	4.1	1.4	2.0	0.8	1.1	3.6	1.1	1.0
En	76.4	73.8	68.3	77.3	76.5	76.4	79.3	70.0

Sample	D5	D5	D5	D5	Lac-33	Lac-33
Rock type	Pyrox.	Pyrox.	Pyrox.	Pyrox.	Leucogab	Leucogab
Grain	3-1	3-6	2-1	2-13	2-1	2-2
Grain area	core	core	core	core	rim	core
SiO ₂	52.94	53.38	51.81	57.58	56.6	54.21
TiO ₂	0	0	0	0	0.16	0
Al ₂ O ₃	1.7	1.36	1.27	1.64	1.02	2.21
FeO	19.89	21.08	21.94	13.41	16.05	13.14
MnO	0.34	0.27	0.47	0.19	0.62	0.21
MgO	24.45	23.79	22.69	24.07	22.1	29.26
CaO	0.63	1.17	0.62	0.54	3.28	1.05
Na ₂ O	0.52	0.68	0.4	0.28	0.51	0.3
Total	100.47	101.73	99.2	97.71	100.34	100.38
Si	1.944	1.948	1.949	2.079	2.044	1.93
Ti	0	0	0	0	0.004	0
Al (IV)	0.056	0.052	0.051	0	0	0.07
Al (VI)	0.017	0.007	0.005	0.07	0.043	0.023
Fe	0.611	0.643	0.69	0.405	0.485	0.391
Mn	0.011	0.008	0.015	0.006	0.019	0.006
Mg	1.338	1.294	1.273	1.296	1.19	1.553
Ca	0.025	0.046	0.025	0.021	0.127	0.04
Na	0.037	0.048	0.029	0.02	0.036	0.021
O	6	6	6	6	6	6
Fs	31.0	32.4	34.7	23.5	26.9	19.7
Wo	1.3	2.3	1.3	1.2	7.0	2.0
En	67.8	65.3	64.0	75.3	66.0	78.3

Clinopyroxene

Sample	D5	Lac-33						
Rock type	Pyrox.	Leucogab						
Grain	2-1	2-3	2-5	2-6	1-1	2-2	1-3	1-2
Grain area	rim	core	core	core	core	core	rim	core
SiO ₂	53.02	52.28	51.62	53.24	50.96	50.35	52.34	51.51
TiO ₂	0.47	0.4	0.47	0.49	0.3	0.39	0.26	0.55
Al ₂ O ₃	3.02	2.78	2.45	2.75	3.17	2.57	3.02	2.18
FeO	9.48	8.16	9.01	9.87	7.79	12.34	8.18	7.24
MnO	0	0	0.19	0.17	0	0.2	0	0.22
MgO	14.34	14.63	14.14	15.22	14.98	15.4	15.68	14.41
CaO	22.09	21.93	21.45	21.44	21.37	17.48	20.59	23.06
Na ₂ O	0.44	0.4	0.64	0.5	0.52	0.45	0.52	0.49
Total	102.86	100.58	99.97	103.68	99.09	99.18	100.59	99.66
Si	1.922	1.929	1.928	1.917	1.908	1.907	1.924	1.924
Ti	0.013	0.011	0.013	0.013	0.008	0.011	0.007	0.015
Al (IV)	0.078	0.071	0.072	0.083	0.092	0.093	0.076	0.076
Al (VI)	0.051	0.05	0.036	0.034	0.048	0.021	0.055	0.02
Fe	0.287	0.252	0.281	0.297	0.244	0.391	0.252	0.226
Mn	0	0	0.006	0.005	0	0.006	0	0.007
Mg	0.775	0.805	0.787	0.817	0.836	0.869	0.859	0.803
Ca	0.858	0.867	0.858	0.827	0.857	0.709	0.811	0.923
Na	0.031	0.029	0.046	0.035	0.038	0.033	0.037	0.035
O	6	6	6	6	6	6	6	6
Fs	14.9	13.1	14.6	15.3	12.6	19.9	13.1	11.6
Wo	44.7	45.1	44.5	42.6	44.2	36.0	42.2	47.3
En	40.4	41.8	40.9	42.1	43.2	44.1	44.7	41.1

Sample	Lac-33	Lac-40						
Rock type	Leucogab	Pyrox.						
Grain	1-3	2-2	2-4	2-5	1-6	1-7	1-8	1-9
Grain area	core	core	core	core	rim	core	rim	rim
SiO ₂	51.32	49.46	51.03	51.03	50.12	51.06	51.56	50.79
TiO ₂	0.66	0.52	0.44	0.44	0.47	0.59	0.26	0.52
Al ₂ O ₃	2.48	3.97	2.55	2.55	2.61	3.03	2.77	2.94
FeO	8.19	9.8	8.9	8.9	8.35	11.02	10.21	8.73
MnO	0.17	0.34	0.3	0.3	0.27	0.3	0.23	0
MgO	14.04	13.23	13.18	13.18	12.8	13.18	14.83	13.02
CaO	22.29	20.02	21.77	21.77	20.93	17.94	16.96	22.05
Na ₂ O	0.42	0.99	0.58	0.59	0.73	0.59	0.55	0.79
Total	99.57	98.33	98.75	98.76	96.28	97.71	97.37	98.84
Si	1.922	1.886	1.932	1.932	1.94	1.948	1.959	1.921
Ti	0.019	0.015	0.013	0.013	0.014	0.017	0.007	0.015
Al (IV)	0.078	0.114	0.068	0.068	0.06	0.052	0.041	0.079
Al (VI)	0.031	0.065	0.046	0.046	0.059	0.084	0.083	0.052
Fe	0.256	0.313	0.282	0.282	0.27	0.352	0.324	0.276
Mn	0.005	0.011	0.01	0.01	0.009	0.01	0.007	0
Mg	0.784	0.752	0.744	0.744	0.739	0.75	0.84	0.734
Ca	0.894	0.818	0.883	0.883	0.868	0.733	0.69	0.893
Na	0.03	0.073	0.043	0.043	0.055	0.044	0.041	0.058
O	6	6	6	6	6	6	6	6
Fs	13.2	16.6	14.8	14.8	14.4	19.2	17.5	14.5
Wo	46.2	43.4	46.3	46.3	46.2	39.9	37.2	46.9
En	40.5	39.9	39.0	39.0	39.4	40.9	45.3	38.6

Sample	D13	D13	D1-2	Lac-36	Lac-76	Lac-76	Lac-5	Lac-5
Rock type	Gabnor	Gabnor	Gabnor	Gab dyke	Tonalite	Tonalite	East Gab	East Gab
Grain	1-2	1-3	2	5	8	9	2-14	2-15
Grain area	core	core	rim	core	rim	core	core	core
SiO ₂	52.97	54.48	54.61	52.58	53.28	53.05	52.25	51.49
TiO ₂	0.29	0.4	0	0.41	0.46	0.38	0.42	0.57
Al ₂ O ₃	3.19	1.85	1.68	2.11	2.83	2.59	3.18	3.15
FeO	5.07	5.08	4.53	9.66	7.69	6.73	9.03	9.25
MnO	0	0	0	0.25	0.21	0	0.28	0.2
MgO	16.49	17.06	17.44	14.03	16.24	15.45	15.25	13.83
CaO	22.84	23.68	23.5	21.38	19.85	23.15	17.87	21.36
Na ₂ O	0.44	0.54	0.46	0.63	0.61	0.58	0.25	0.25
Total	101.29	103.09	102.49	101.05	101.17	101.93	98.75	100.31
Si	1.918	1.941	1.951	1.945	1.938	1.926	1.948	1.915
Ti	0.008	0.011	0	0.011	0.013	0.01	0.012	0.016
Al (IV)	0.082	0.059	0.049	0.055	0.062	0.074	0.052	0.085
Al (VI)	0.054	0.019	0.022	0.037	0.06	0.037	0.088	0.053
Fe	0.153	0.151	0.135	0.299	0.234	0.204	0.282	0.288
Mn	0	0	0	0.008	0.006	0	0.009	0.006
Mg	0.89	0.906	0.929	0.774	0.881	0.836	0.847	0.767
Ca	0.886	0.904	0.9	0.847	0.774	0.9	0.714	0.851
Na	0.031	0.037	0.032	0.045	0.043	0.041	0.018	0.018
O	6	6	6	6	6	6	6	6
Fs	7.9	7.7	6.9	15.6	12.4	10.5	15.3	15.1
Wo	45.9	46.1	45.8	44.1	41.0	46.4	38.7	44.7
En	46.1	46.2	47.3	40.3	46.6	43.1	46.0	40.2

Amphibole

Sample	D5	D5	D5	D5	D5	Lac-60	Lac-60	Lac-60
Rock Type	Pyrox.							
Grain	2-4	2-7	2-7	2-10	2-12	1	2	3
Grain Area	core	rim	rim	rim	rim	core	core	core
SiO ₂	51.75	52.4	52.4	55.44	54.85	61.42	53.85	54.44
TiO ₂	0.58	0.16	0.16	0.16	0	0	0	0
Al ₂ O ₃	5.9	1.82	1.82	2.22	2.36	3.37	1.63	2.45
FeO	10.23	20.72	20.72	13.38	12.44	11.12	11.64	10.99
MnO	0.22	0.23	0.23	0.44	0.44	0.32	0.44	0.34
MgO	17.91	23.4	23.4	18.18	17.95	14.38	16.82	17.14
CaO	11.94	0.93	0.93	9.95	11.05	10.84	12	12.45
Na ₂ O	1.24	0.66	0.66	0.37	0.48	0.98	0.35	0.4
K ₂ O	0.2	0	0	0	0	0	0	0
Total	99.97	100.32	100.32	100.14	99.57	102.43	96.73	98.21
Si	7.241	7.426	7.426	7.741	7.706	8.196	7.792	7.731
Ti	0.061	0.017	0.017	0.017	0	0	0	0
Al (IV)	0.759	0.304	0.304	0.259	0.294	0	0.208	0.269
Al (VI)	0.214	0	0	0.106	0.097	0.53	0.07	0.141
Fe	1.197	2.456	2.456	1.562	1.462	1.241	1.408	1.305
Mn	0.026	0.028	0.028	0.052	0.052	0.036	0.054	0.041
Mg	3.736	4.943	4.943	3.784	3.759	2.86	3.628	3.628
Ca	1.79	0.141	0.141	1.488	1.663	1.55	1.86	1.894
Na	0.336	0.181	0.181	0.1	0.131	0.254	0.098	0.11
K	0.036	0	0	0	0	0	0	0
O	24	24	24	24	24	24	24	24
Fs	17.8	32.6	32.6	22.9	21.2	22.0	20.4	19.1
Wo	26.6	1.9	1.9	21.8	24.2	27.4	27.0	27.7
En	55.6	65.6	65.6	55.4	54.6	50.6	52.6	53.1

Sample	Lac-60	Lac-33						
Rock Type	Pyrox.	Leucogab						
Grain	4	5	6	7	8	10	11	2-1
Grain Area	core							
SiO ₂	53.95	53.81	53.44	54.01	54.09	54.8	53.35	55.45
TiO ₂	0.21	0	0	0	0.33	0	0.31	0.37
Al ₂ O ₃	2.57	2.09	2.58	2.9	2.27	2.37	3.13	1.25
FeO	10.64	10.41	13.1	11.61	10.4	9.73	11.12	8.66
MnO	0.35	0.32	0.29	0	0	0	0	0
MgO	16.9	16.56	16.38	16.5	17.03	17.09	16.2	19.16
CaO	12.03	12.06	10.78	12.2	12.53	12.57	12.32	12.23
Na ₂ O	0.52	0.65	0.58	0.65	0.34	0.45	0.65	0.34
K ₂ O	0	0	0	0	0	0	0	0
Total	97.17	95.9	97.15	97.87	97.2	97.01	97.08	97.46
Si	7.729	7.807	7.722	7.708	7.738	7.814	7.67	7.829
Ti	0.023	0	0	0	0.036	0	0.034	0.039
Al (IV)	0.271	0.193	0.278	0.292	0.262	0.186	0.33	0.171
Al (VI)	0.163	0.164	0.161	0.196	0.121	0.212	0.2	0.037
Fe	1.275	1.263	1.583	1.386	1.244	1.16	1.337	1.023
Mn	0.042	0.039	0.035	0	0	0	0	0
Mg	3.609	3.582	3.528	3.511	3.632	3.633	3.472	4.033
Ca	1.847	1.875	1.669	1.866	1.92	1.92	1.898	1.85
Na	0.144	0.183	0.162	0.18	0.094	0.124	0.181	0.093
K	0	0	0	0	0	0	0	0
O	24	24	24	24	24	24	24	24
Fs	18.9	18.8	23.3	20.5	18.3	17.3	19.9	14.8
Wo	27.4	27.9	24.6	27.6	28.3	28.6	28.3	26.8
En	53.6	53.3	52.0	51.9	53.4	54.1	51.8	58.4

Sample	Lac-33	Lac-98	Lac-98	Lac-98	Lac-98	Lac-98	Lac-98	Lac-63
Rock Type	Leucogab	Gabnor						
Grain	1-1	1	2	3	4	6	7	17
Grain Area	core	rim						
SiO ₂	56.82	54.19	49.88	49.88	52.13	51.35	57.67	57.09
TiO ₂	0.17	0	0.74	0.74	0.23	0.47	0	0
Al ₂ O ₃	1.96	3.28	6.35	6.35	5.92	6.03	3	0.48
FeO	9.37	7.6	13.84	13.84	7.4	12.35	10.74	7.14
MnO	0	0	0	0	0.35	0	0	0.28
MgO	19.14	18.54	13.41	13.41	17.53	15.03	18.06	20.28
CaO	12.98	11.97	12.29	12.29	11.99	12.36	13.19	13.38
Na ₂ O	0.34	0.49	0.67	0.68	0.52	0.98	0	0.45
K ₂ O	0	0	0.27	0.27	0	0.27	0	0
Total	100.78	96.3	97.45	97.46	96.07	98.84	102.66	99.1
Si	7.78	7.706	7.277	7.277	7.445	7.328	7.771	7.899
Ti	0.018	0	0.081	0.081	0.025	0.05	0	0
Al (IV)	0.22	0.294	0.723	0.723	0.555	0.672	0.229	0.078
Al (VI)	0.097	0.255	0.369	0.368	0.442	0.342	0.248	0
Fe	1.073	0.904	1.689	1.688	0.884	1.474	1.21	0.826
Mn	0	0	0	0	0.042	0	0	0.033
Mg	3.907	3.93	2.916	2.916	3.732	3.198	3.628	4.183
Ca	1.904	1.824	1.921	1.921	1.835	1.89	1.904	1.983
Na	0.09	0.135	0.19	0.192	0.144	0.271	0	0.121
K	0	0	0.05	0.05	0	0.049	0	0
O	24	24	24	24	24	24	24	24
Fs	15.6	13.6	25.9	25.9	13.7	22.5	17.9	11.8
Wo	27.7	27.4	29.4	29.4	28.4	28.8	28.2	28.4
En	56.8	59.0	44.7	44.7	57.9	48.7	53.8	59.8

Sample	Lac-40	Lac-40	D13	D1	D15	D15	D15	D15
Rock Type	Pyrox.	Pyrox.	Gabnor	Gabnor	Shear	Shear	Shear	Shear
Grain	2-1	2-3	1-1	1-1	1	3	4	5
Grain Area	core	core	core	core	core	rim	rim	rim
SiO ₂	48.66	47.48	52.83	53.47	53.63	56.59	55.55	58.47
TiO ₂	1.01	1.51	0.24	0	0	0.38	0	0.4
Al ₂ O ₃	7.1	7.88	3.83	4.35	3.51	3.2	1.9	4.22
FeO	13.39	12.61	12.06	6.71	12.92	13.12	12.21	11.34
MnO	0.25	0	0.3	0	0.26	0.21	0.2	0.25
MgO	13.92	13.85	24.78	20.67	15.54	16.39	16.18	12.27
CaO	12.21	11.72	3.45	11.78	11.22	11.99	11.53	8.75
Na ₂ O	1.01	1.54	0.61	0.74	0.29	0.43	0.34	0.61
K ₂ O	0	0.42	0	0.24	0.32	0	0	0
Total	97.55	97.01	98.1	97.96	97.69	102.31	97.91	96.31
Si	7.101	6.97	7.393	7.474	7.701	7.736	7.904	8.253
Ti	0.111	0.167	0.025	0	0	0.039	0	0.042
Al (IV)	0.899	1.03	0.607	0.526	0.299	0.264	0.096	0
Al (VI)	0.322	0.334	0.025	0.19	0.296	0.251	0.223	0.702
Fe	1.634	1.548	1.411	0.784	1.552	1.5	1.453	1.339
Mn	0.031	0	0.036	0	0.032	0.024	0.024	0.03
Mg	3.028	3.031	5.169	4.307	3.327	3.34	3.432	2.582
Ca	1.909	1.843	0.517	1.764	1.726	1.756	1.758	1.323
Na	0.286	0.438	0.166	0.201	0.081	0.114	0.094	0.167
K	0	0.079	0	0.043	0.059	0	0	0
O	24	24	24	24	24	24	24	24
Fs	24.9	24.1	19.9	11.4	23.5	22.7	21.9	25.5
Wo	29.1	28.7	7.3	25.7	26.1	26.6	26.5	25.2
En	46.1	47.2	72.8	62.8	50.4	50.6	51.7	49.2

Sample	Lac-36	Lac-36	Lac-36	Lac-42	Lac-42	Lac-42	Lac-31	Lac-31
Rock Type	Gab dyke	Gabbro	Gabbro					
Grain	7	8	9	3	4	5	1	2
Grain Area	core	core	core	core	core	core	rim	rim
SiO ₂	54.52	52.77	48.97	56.6	55.55	56.59	53.31	52.32
TiO ₂	0	0	0.72	0.23	0.2	0	0	0
Al ₂ O ₃	2	2.85	5.58	3.4	3.01	3.25	3.13	3.36
FeO	13.33	12.83	13.61	7.86	9.31	8.1	14.49	11.26
MnO	0	0.37	0.21	0	0	0	0.43	0.3
MgO	16.39	15.75	14.29	18.78	18.18	18.8	14.6	17.04
CaO	12.89	12.86	12.19	11.97	11.72	11.9	12.42	11.93
Na ₂ O	0	0.58	0.81	0.5	0.53	0.36	0.56	0.67
K ₂ O	0	0	0.35	0	0.14	0	0	0
Total	99.13	98.01	96.73	99.34	98.64	99	98.94	96.88
Si	7.742	7.612	7.228	7.775	7.754	7.802	7.651	7.564
Ti	0	0	0.08	0.024	0.021	0	0	0
Al (IV)	0.258	0.388	0.772	0.225	0.246	0.198	0.349	0.436
Al (VI)	0.077	0.097	0.199	0.325	0.249	0.33	0.181	0.137
Fe	1.583	1.548	1.68	0.903	1.087	0.934	1.739	1.361
Mn	0	0.045	0.026	0	0	0	0.052	0.037
Mg	3.47	3.387	3.144	3.846	3.783	3.864	3.124	3.673
Ca	1.961	1.988	1.928	1.762	1.753	1.758	1.91	1.848
Na	0	0.162	0.232	0.133	0.143	0.096	0.156	0.188
K	0	0	0.066	0	0.025	0	0	0
O	24	24	24	24	24	24	24	24
Fs	22.6	22.4	24.9	13.9	16.4	14.2	25.7	19.8
Wo	28.0	28.7	28.6	27.1	26.5	26.8	28.2	26.9
En	49.5	48.9	46.6	59.1	57.1	58.9	46.1	53.4

Sample	Lac-31	Lac-31	Lac-31	Lac-31	Lac-31	Lac-31	Lac-76	Lac-76
Rock Type	Gabbro	Gabbro	Gabbro	Gabbro	Gabbro	Gabbro	Tonalite	Tonalite
Grain	4	5	6	7	8	9	4	5
Grain Area	rim	rim	rim	rim	rim	rim	core	core
SiO ₂	54.53	54.76	52.6	51.62	51.62	53.93	56.43	54.44
TiO ₂	0	0	0	0	0	0.21	0.36	0.32
Al ₂ O ₃	2.32	3.85	4.22	3.39	3.39	2.69	2.43	3.27
FeO	11.39	12.43	12.28	12.24	12.24	11.75	8.64	13.76
MnO	0	0	0	0.38	0.38	0.23	0	0.18
MgO	17.51	17.03	16.24	15.86	15.86	16.71	19.54	19.76
CaO	13.07	12.75	12.82	12.26	12.26	12.21	13.78	6.12
Na ₂ O	0.51	0.63	0.59	0.76	0.76	0.47	0.59	0.89
K ₂ O	0	0	0	0	0	0	0	0
Total	99.33	101.45	98.75	96.51	96.51	98.2	101.77	98.9
Si	7.681	7.57	7.493	7.547	7.547	7.685	7.662	7.641
Ti	0	0	0	0	0	0.023	0.037	0.034
Al (IV)	0.319	0.43	0.507	0.453	0.453	0.315	0.338	0.359
Al (VI)	0.066	0.197	0.202	0.132	0.132	0.137	0.051	0.182
Fe	1.342	1.437	1.463	1.497	1.497	1.4	0.981	1.615
Mn	0	0	0	0.047	0.047	0.028	0	0.021
Mg	3.677	3.51	3.449	3.457	3.457	3.55	3.955	4.135
Ca	1.972	1.888	1.957	1.921	1.921	1.864	2.005	0.92
Na	0.139	0.169	0.163	0.215	0.215	0.13	0.155	0.242
K	0	0	0	0	0	0	0	0
O	24	24	24	24	24	24	24	24
Fs	19.2	21.0	21.3	21.8	21.8	20.5	14.1	24.2
Wo	28.2	27.6	28.5	27.9	27.9	27.4	28.9	13.8
En	52.6	51.4	50.2	50.3	50.3	52.1	57.0	62.0

Sample	Lac-76	Lac-76	Lac-76	Lac-76	Lac-5	Lac-5	Lac-5	Lac-5
Rock Type	Tonalite	Tonalite	Tonalite	Tonalite	East Gab	East Gab	East Gab	East Gab
Grain	6	7	10	12	2-7	2-8	2-9	2-10
Grain Area	core	rim	rim	rim	core	core	core	rim
SiO ₂	54.76	55.24	52.57	53.74	56.21	55.38	53.55	54.5
TiO ₂	0.18	0.34	0.33	0	0.2	0	0.37	0.19
Al ₂ O ₃	2.67	2.67	4.03	4.17	3.27	3.07	3.75	3.81
FeO	12.12	14.53	13.71	10.8	11.34	12.03	12.65	12.6
MnO	0.24	0.25	0	0.41	0	0.24	0.18	0
MgO	19.37	19.34	17.81	16.6	16.94	16.93	15.78	16.04
CaO	8.74	6.09	8.53	12.78	11.79	12.16	12.5	12.44
Na ₂ O	0.46	0.6	0.56	0.37	0.65	0.51	0.65	0.58
K ₂ O	0	0	0	0	0	0.13	0.16	0
Total	98.54	99.06	97.54	98.87	100.4	100.45	99.59	100.16
Si	7.702	7.746	7.535	7.582	7.765	7.706	7.572	7.627
Ti	0.019	0.036	0.036	0	0.021	0	0.039	0.02
Al (IV)	0.298	0.254	0.465	0.418	0.235	0.294	0.428	0.373
Al (VI)	0.144	0.188	0.216	0.275	0.297	0.209	0.197	0.255
Fe	1.426	1.704	1.643	1.274	1.31	1.4	1.496	1.475
Mn	0.029	0.03	0	0.049	0	0.028	0.022	0
Mg	4.061	4.043	3.806	3.491	3.488	3.512	3.326	3.346
Ca	1.317	0.915	1.31	1.932	1.745	1.813	1.894	1.865
Na	0.125	0.163	0.156	0.101	0.174	0.138	0.178	0.157
K	0	0	0	0	0	0.023	0.029	0
O	24	24	24	24	24	24	24	24
Fs	21.0	25.6	24.3	19.0	20.0	20.8	22.3	22.1
Wo	19.4	13.7	19.4	28.8	26.7	27.0	28.2	27.9
En	59.7	60.7	56.3	52.1	53.3	52.2	49.5	50.0

Sample	Lac-5	Lac-5	Lac-5	Lac-5	Lac-5
Rock Type	East Gab				
Grain	1-1	1-2	1-3	1-4	1-5
Grain Area	core	rim	core	core	rim
SiO₂	51.87	54.98	54.14	54.85	53.88
TiO₂	0.41	0.19	0.21	0.16	0.18
Al₂O₃	6.53	2.44	3.45	2.8	4.07
FeO	13.63	11.36	12.4	11.54	11.31
MnO	0.26	0.19	0.18	0	0.21
MgO	15.13	16.65	16.07	17.1	17.17
CaO	11.33	12.5	12.12	12.11	11.82
Na₂O	1.16	0.5	0.52	0.52	0.95
K₂O	0.36	0	0.1	0	0
Total	100.68	98.81	99.19	99.08	99.59
Si	7.294	7.762	7.652	7.715	7.554
Ti	0.043	0.02	0.022	0.017	0.019
Al (IV)	0.706	0.238	0.348	0.285	0.446
Al (VI)	0.376	0.168	0.227	0.18	0.227
Fe	1.603	1.341	1.466	1.357	1.326
Mn	0.031	0.023	0.022	0	0.025
Mg	3.172	3.504	3.386	3.586	3.589
Ca	1.707	1.891	1.835	1.825	1.776
Na	0.316	0.137	0.143	0.142	0.258
K	0.065	0	0.018	0	0
O	24	24	24	24	24
Fs	24.7	19.9	21.9	20.1	19.8
Wo	26.3	28.1	27.4	27.0	26.5
En	48.9	52.0	50.6	53.0	53.6

APPENDIX 4**Platinum Group Element-Gold Analyses**

A total of 35 samples were collected from the various rocks of the Roby Zone and were analysed at Activation Laboratories using nickel sulphide fire assay - INAA. The detection limits are as follows:

Element	Detection Limit
Rh, Ir	0.10 ppb
Au	0.50 ppb
Pd, Os	2.0 ppb
Pt, Ru, Re	5.0 ppb

Sample No.		Os ppb	Ir ppb	Ru ppb	Rh ppb	Pt ppb	Pd ppb	Re ppb	Au ppb
LAC-29	Gabbro	nd	0.2	nd	1	68	703	nd	22
LAC-25	Peg dike	nd	nd	nd	1	37	295	nd	150
LAC-42	Peg dike	nd	0.2	nd	0	17	60	nd	7.4
LAC-330	Schist	nd	0.7	7	3	291	5370	nd	44
LAC-331	Schist	nd	0.7	nd	3	578	14174	nd	798
LAC-405	Schist	4	3.9	nd	2	7	22	nd	4.5
LAC-401	Gabnor	nd	0.3	nd	3	290	1760	nd	450
LAC-402	Gabnor	nd	nd	nd	1	126	900	nd	117
LAC-403	Gabnor	nd	0.2	nd	2	224	1570	nd	180
LAC-411	Gabnor	nd	0.4	nd	17	1100	11300	nd	950
d-1	Gabnor	<2	0.2	<5	0.6	316	7100	<5	272
LAC-415	Gabnor	nd	0.4	nd	5	533	3868	nd	980
LAC-418	Gabnor	nd	0.3	nd	3	370	2888	nd	1000
LAC-417	gabnor	3	0.3	nd	3	360	3274	nd	460
d-6	gabnor	<2	0.2	10	0.2	129	3120	<5	35
d-13	gabnor	2	0.2	5	0.3	276	3700	<5	36
LAC-338	heter-gab	nd	3	nd	8	953	7490	nd	1026
LAC-408	heter-gab	nd	0.8	nd	11	1277	20500	nd	1510
LAC-409	heter-gab	nd	nd	nd	10	15	30	nd	9.8
Lac-306	heter-gab	<2	0.8	<5	2.9	1180	18800	<5	1280
d-19	heter-gab	<2	1.2	<5	2.5	720	4500	<5	1500
LAC-404	pxn	nd	0.1	nd	0	43	153	nd	80
LAC-332	pxn	nd	0.3	nd	1	129	950	nd	46
d-5	pxn	3	0.3	5	0.2	216	1350	<5	244
d-12	Pxn	<2	0.1	<5	0.6	71	600	<5	40
d-15	Pxn	<2	0.5	<5	0.2	56	269	<5	57
d-16	Pxn	<2	0.1	<5	0.4	226	920	<5	280
LAC-414	Pxn	nd	0.2	nd	1	110	413	nd	140
Lac-16	Pxn	<2	0.9	8	3.1	668	6640	<5	110
Lac-27	Pxn	<2	0.7	16	5.8	1330	22000	<5	268
LAC-328	East Gab	6	7.2	5	2	14	2	nd	5.3
LAC-33	Leucogab	nd	nd	nd	0	13	55	nd	6.3
Lac-324	IG/opn	<2	3.2	<5	0.3	1500	29000	<5	1080
LAC-412	Wgab	nd	0.3	nd	1	19	14	nd	4
LAC-413	Magab	nd	nd	nd	1	30	244	nd	13

NOTE TO USERS

Oversize maps and charts are microfilmed in sections in the following manner:

**LEFT TO RIGHT, TOP TO BOTTOM, WITH
SMALL OVERLAPS**

This reproduction is the best copy available.

UMI

300W

200W

100W

52700N

52600N

52500N

52400N

100W

OE

100E

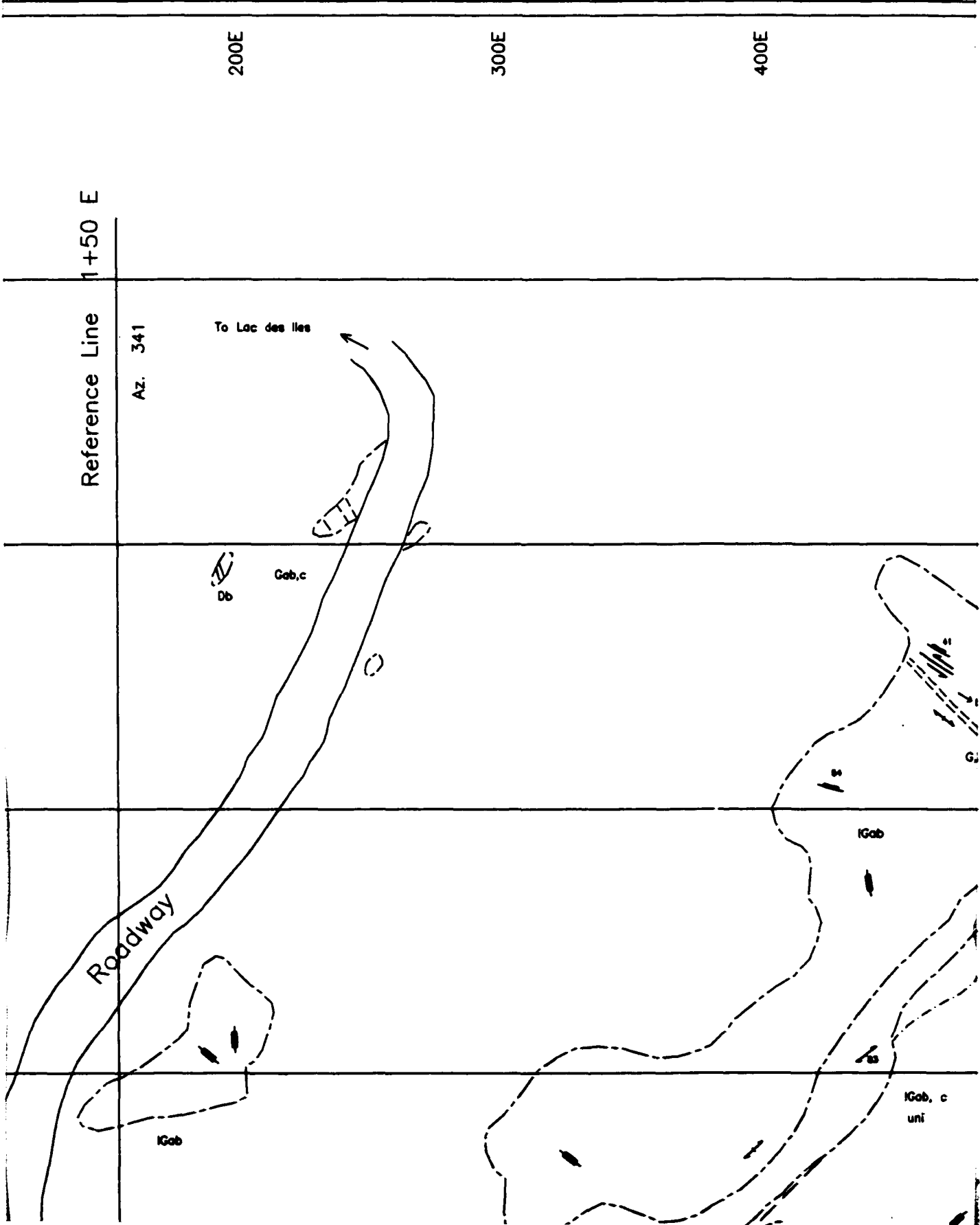
Reference Line 1+50 E

Az. 341

Roadway

100





200E

300E

400E

Reference Line 1+50 E

Az. 341

To Lac des Iles

Roadway

IGob

IGob, c

IGob

IGob

IGob, c
uni

400E

500E

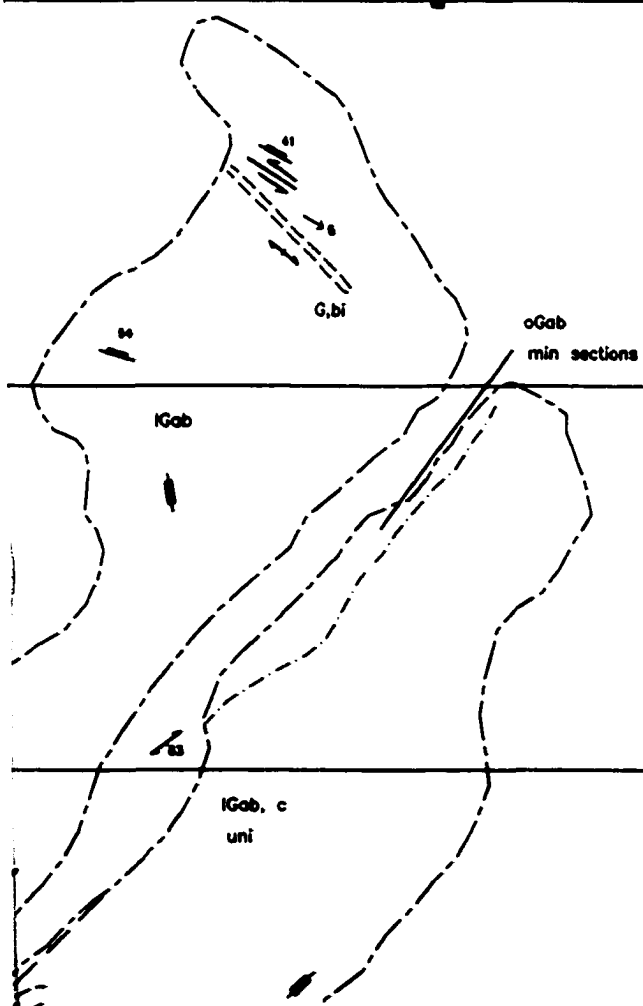
600E

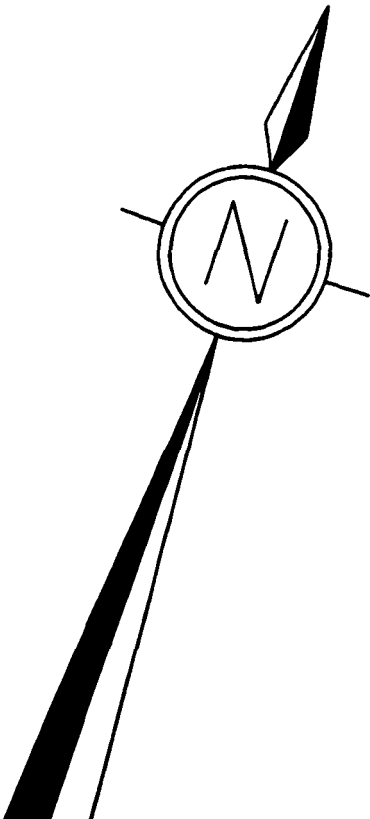
52700N

52600N

52500N

52400N





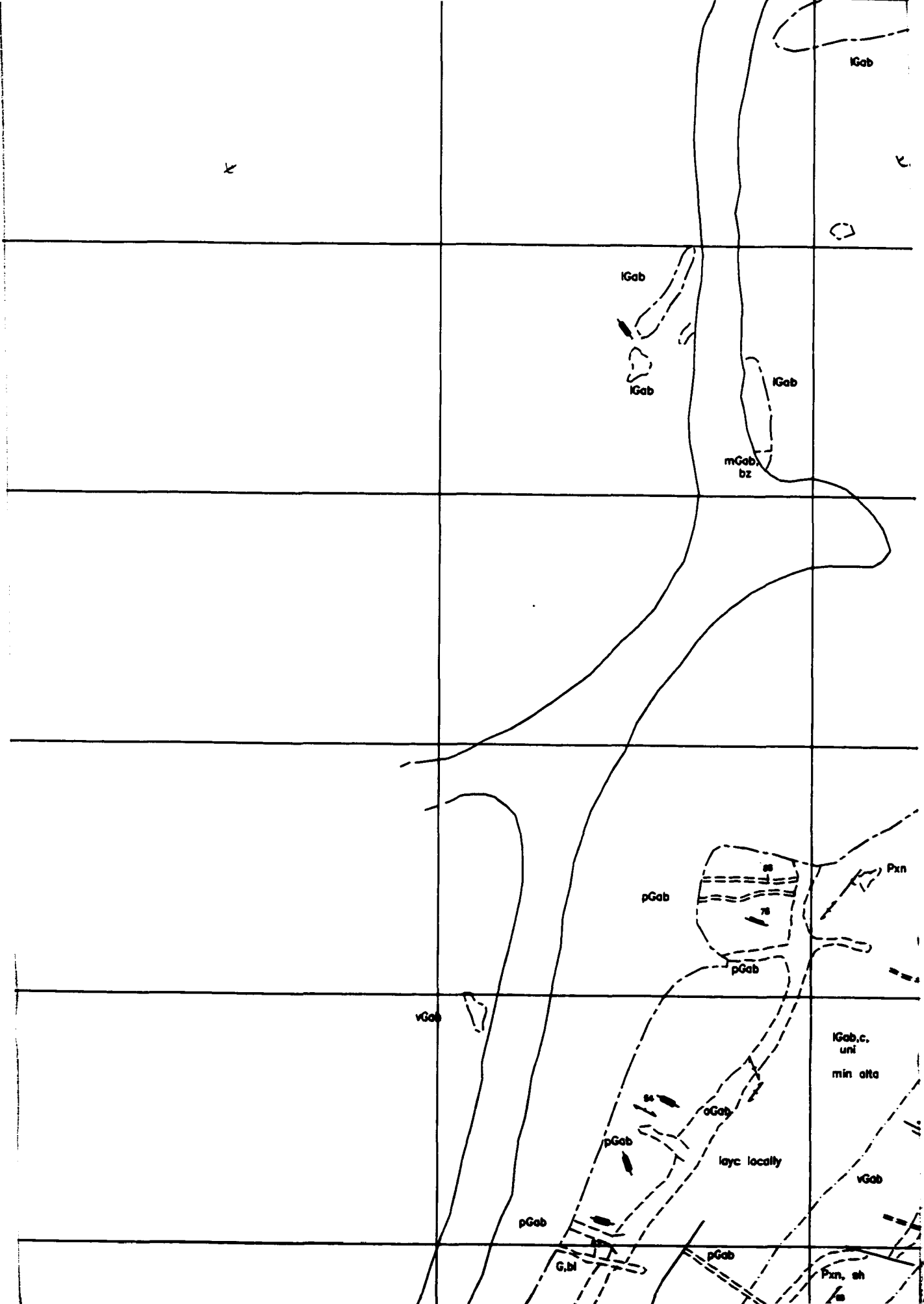
52300N

52200N

52100N

52000N

51900N



IGab, c
uni

Pxn

IGab, c
abn oGab, h sections

oGab
layc

52300N

52200N

52100N

52000N

51900N



An

lGab

Gab

pGab

vGab

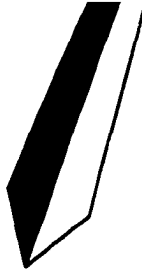
mGab

oGab

Am

Pxn

C



+

Legend

An	Anorthosite
lGab	Leucogabbro
Gab	Gabbro
pGab	Pegmatitic Gabbro Dike
vGab	Heterolithic Gabbro
mGab	Melagabbro
oGab	Gabbronorite
Am	Shear Zone
Pxn	Clinopyroxenite
G	Undifferentiated Granites

51900N

51800N

51700N

51600N

51500N

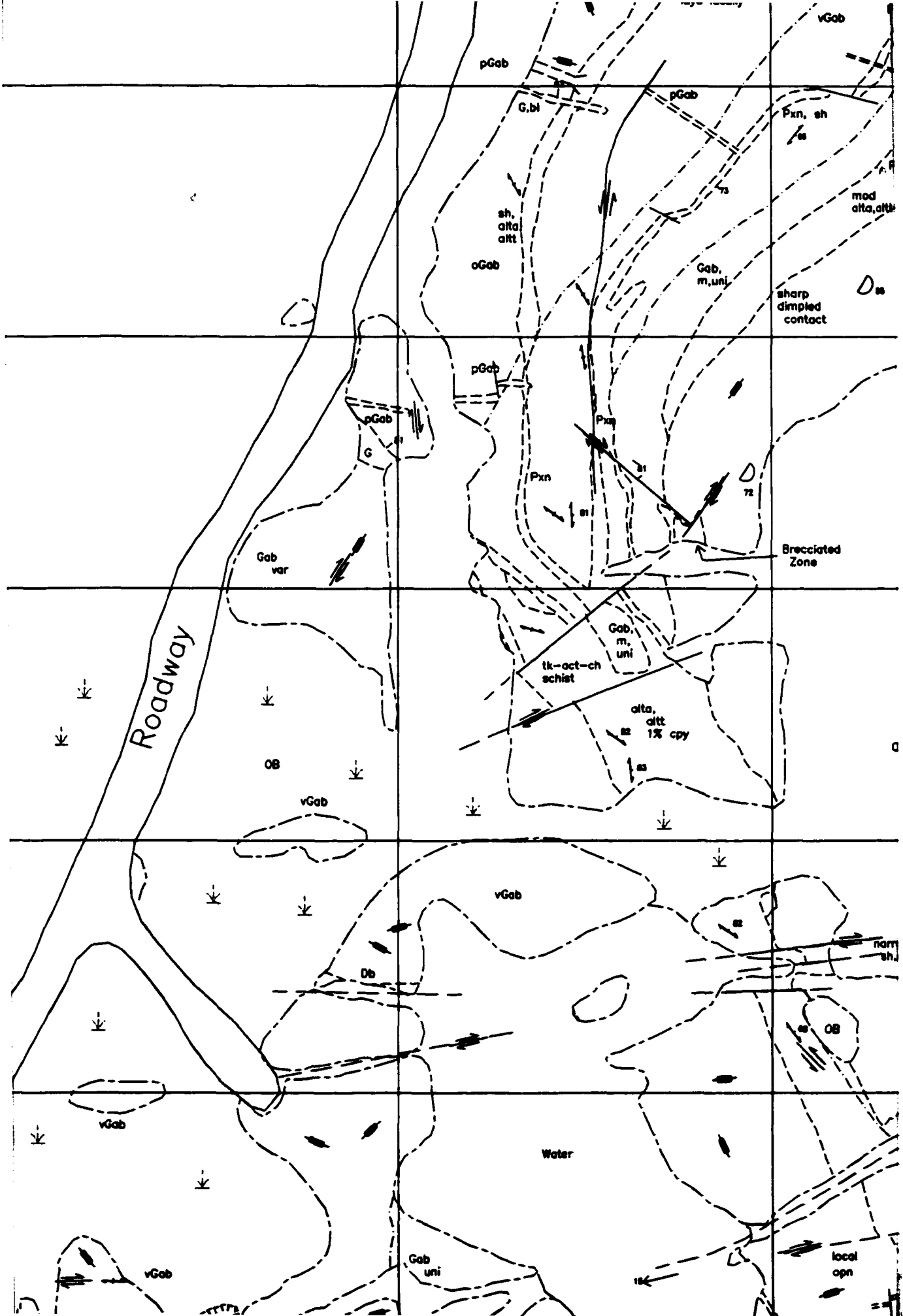
Roadway

vGab

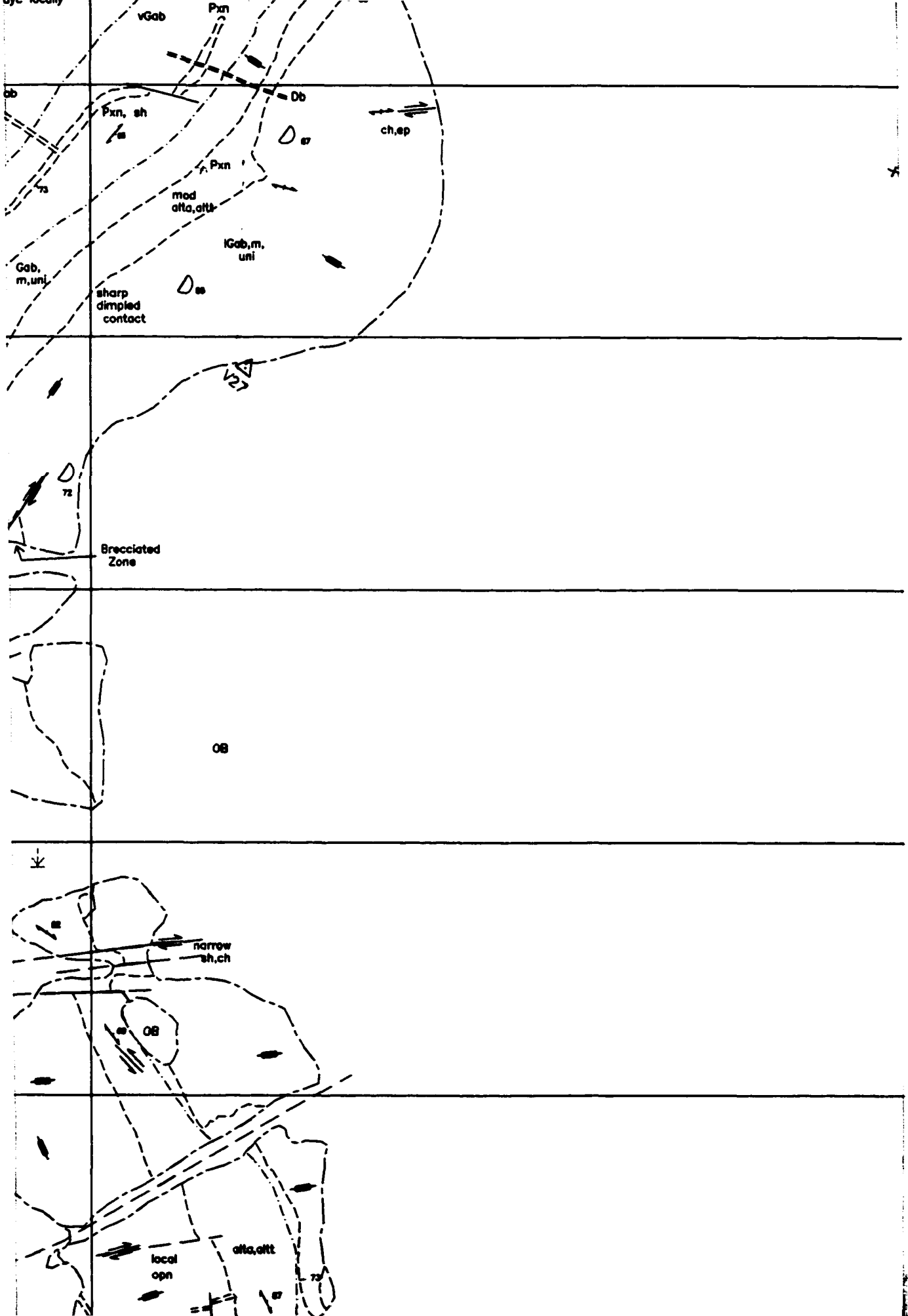
vGab

vGab





Reproduced with permission of the copyright owner. Further reproduction prohibited without permission.



Reproduced with permission of the copyright owner. Further reproduction prohibited without permission.

51900N

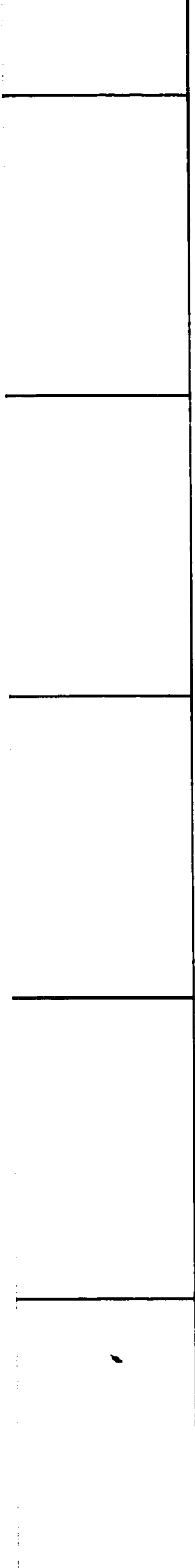
*

51800N

51700N

51600N

51500N



x

Am

Pxn

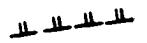
G

Db

x



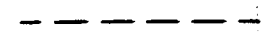
OB



↓



•

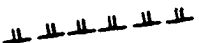


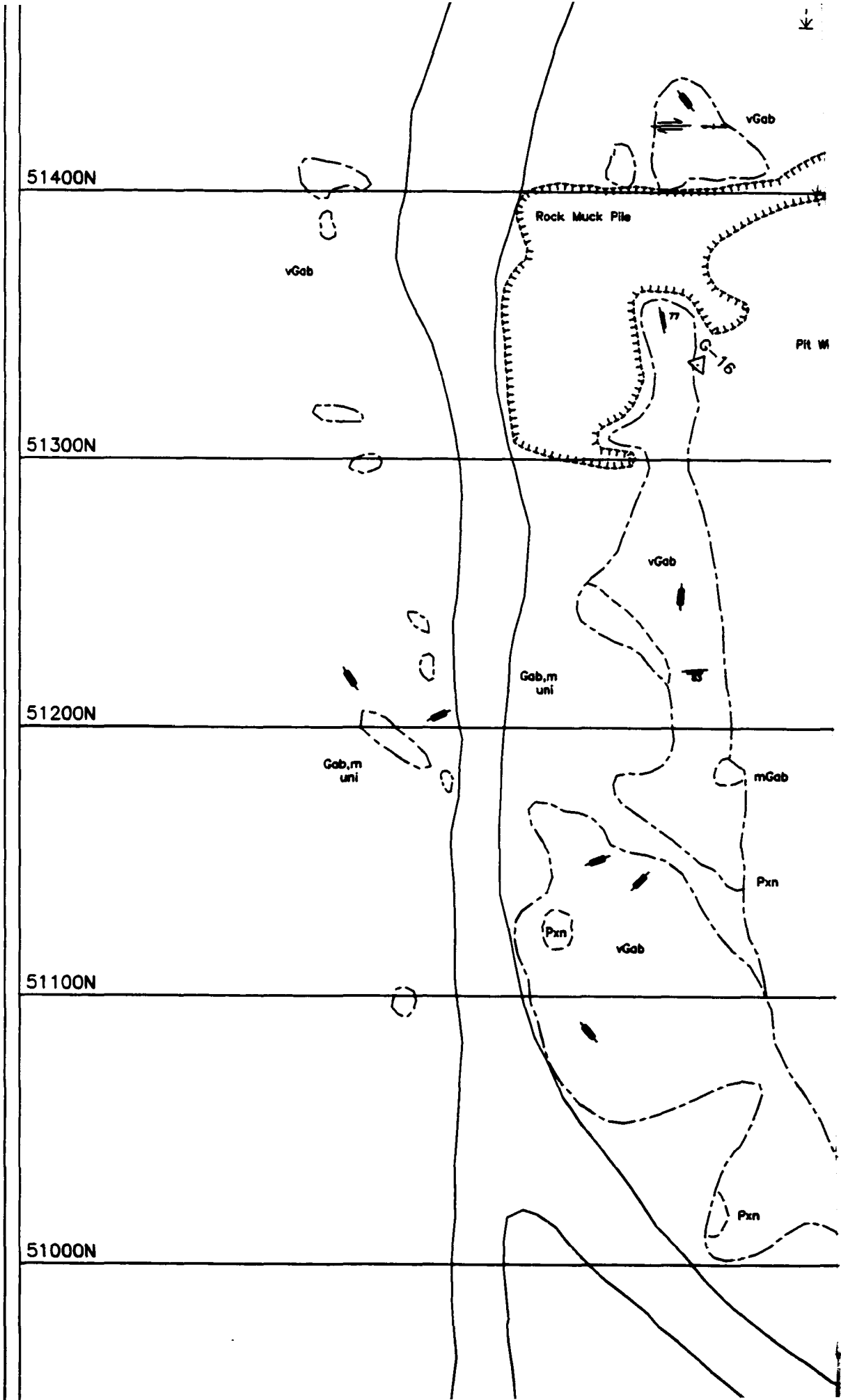
D

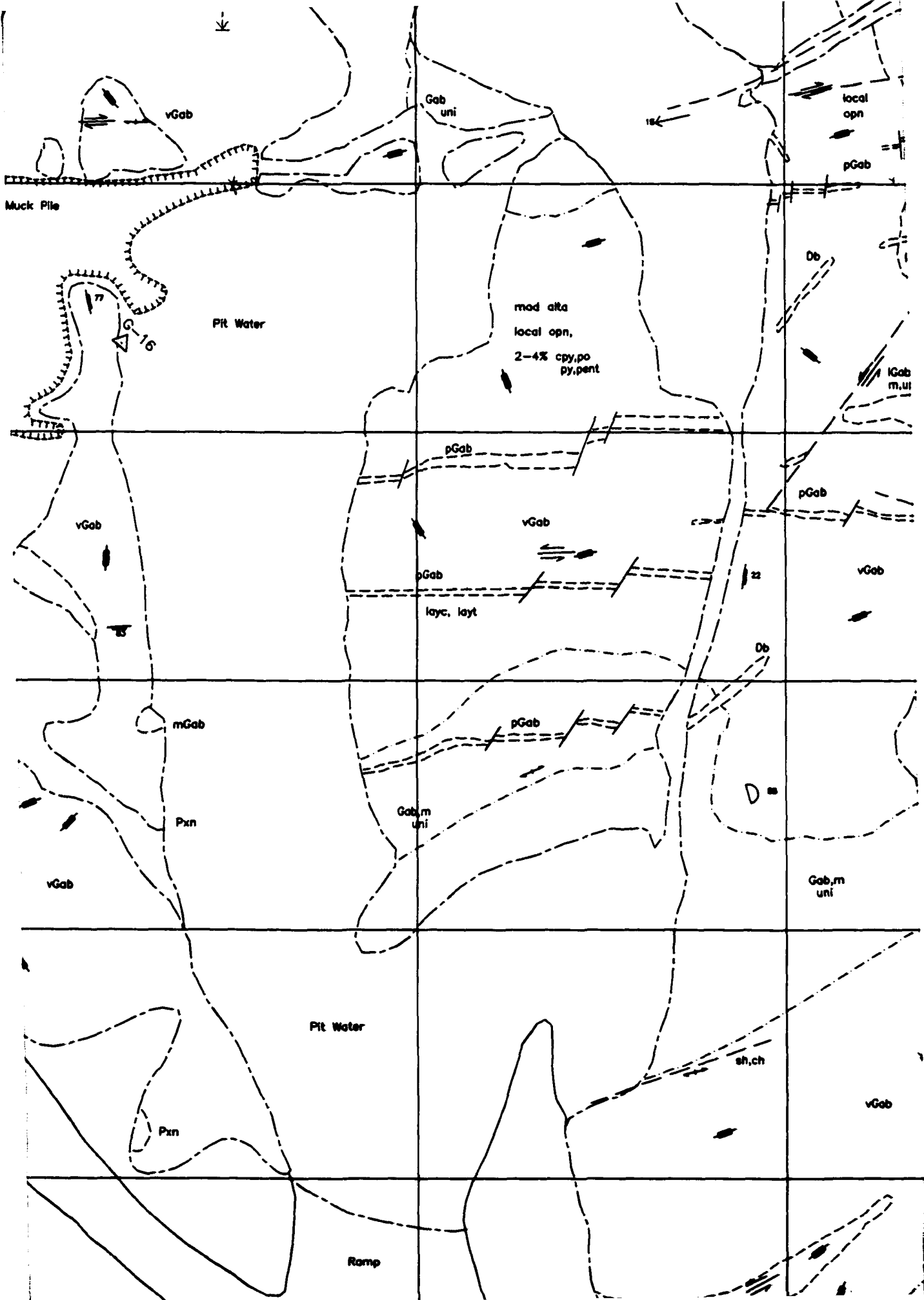


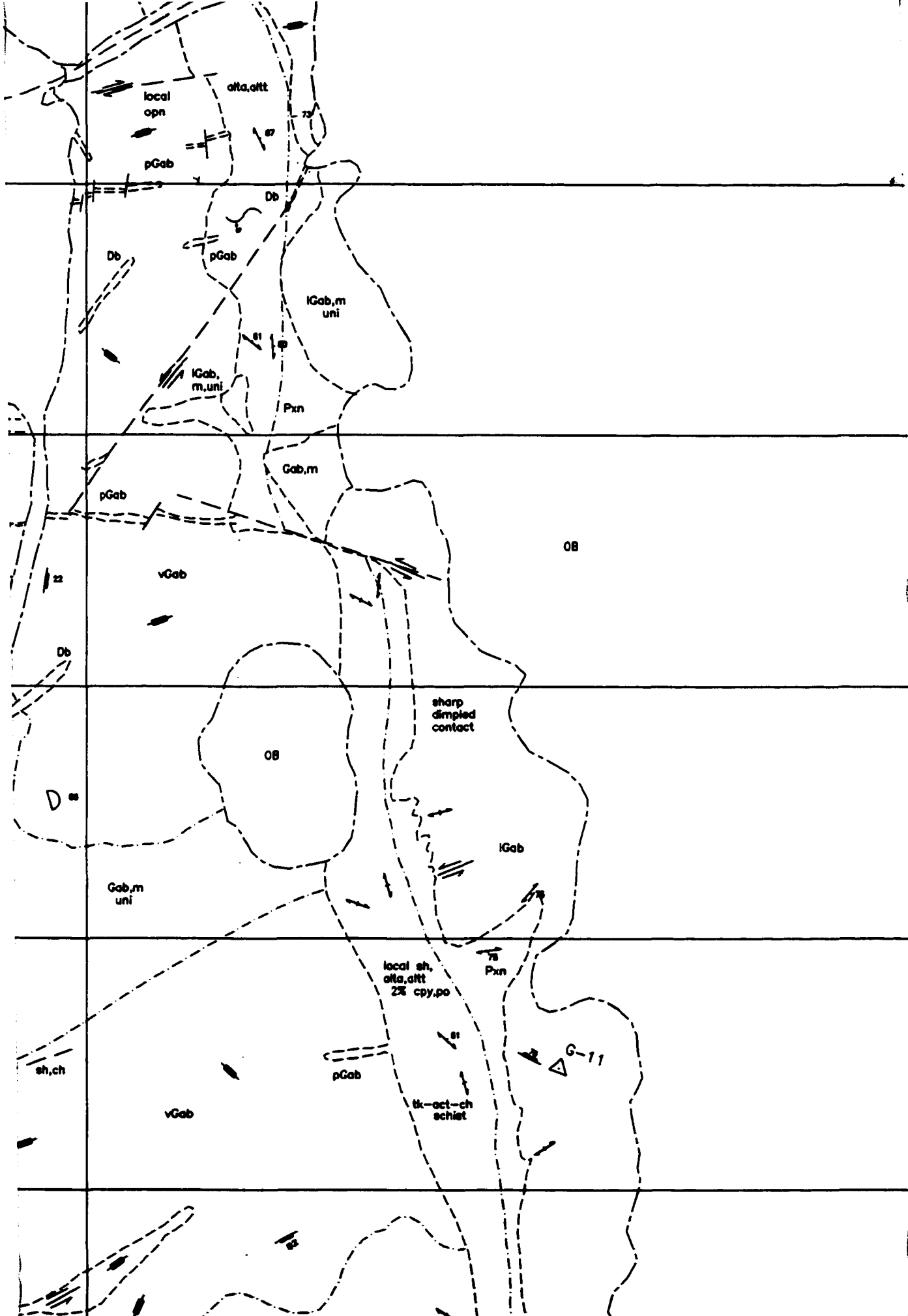
- Am Shear Zone
- Pxn Clinopyroxenite
- G Undifferentiated Granites
- Db * Diabase

Symbols

-  Roadway
-  Extent of Bedrock Exposure
-  Overburden
-  Bedrock Cliff
-  Marsh Area
-  Rock Muck Pile
-  Survey Iron Bar
-  Geological Contact (Defined)
-  Geological Contact (Gradational)
-  Geological Fault (Defined)
-  Geological Fault (Assumed)
-  Intrusive Layering
-  Foliation







51400N

51300N

51200N

51100N

51000N

D



cpn	clinopyroxene
opn	orthopyroxene
pn	pyroxene
h	hornblende
ov	olivine
bz	bronzite
sep	serpentine
aug	augite
bi	biotite
ch	chlorite
ep	epidote
tk	talc
mag	magnetite
hem	hematite

D	Intrusive Layering
	Foliation
	Fracture
	Mineral Lineation
	Fold (Direction and Plunge)
	Sense of Movement

Abbreviations

n	clinopyroxene	f	fine grained
n	orthopyroxene	m	medium grained
	pyroxene	c	coarse grained
	hornblende	v	very coarse grained
	olivine	uni	uniform textured
	bronzite	var	variable textured
b	serpentine	gntx	gneissic textured
g	augite	layc	compositional layers
	biotite	layt	texturally layered
	chlorite	fol	foliated
	epidote	sh	sheared
	talc	fr	fractured
g	magnetite	min	minor
n	hematite	mod	moderate

51000N

50900N

To Primary Crusher

50800N

50700N

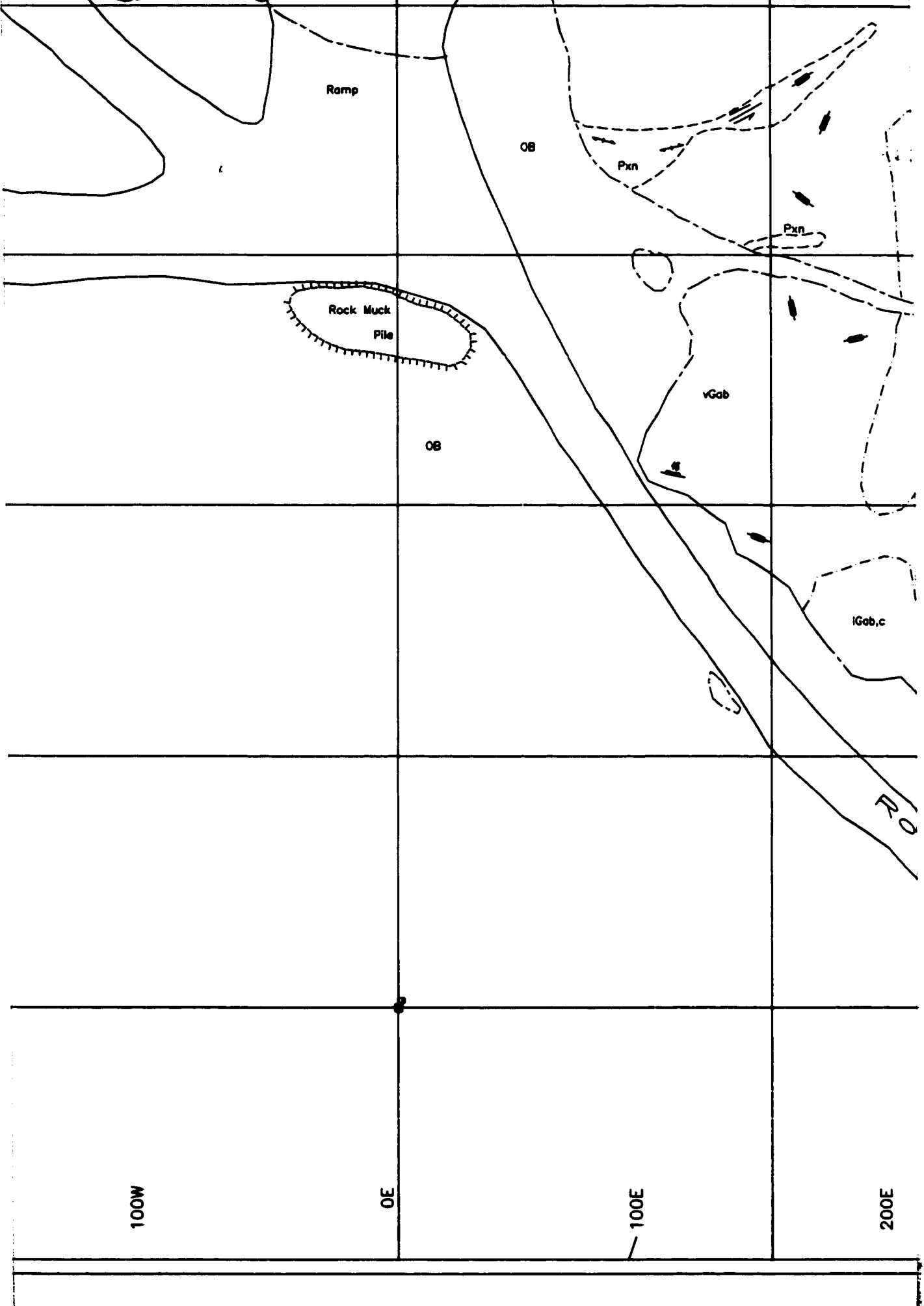
50600N

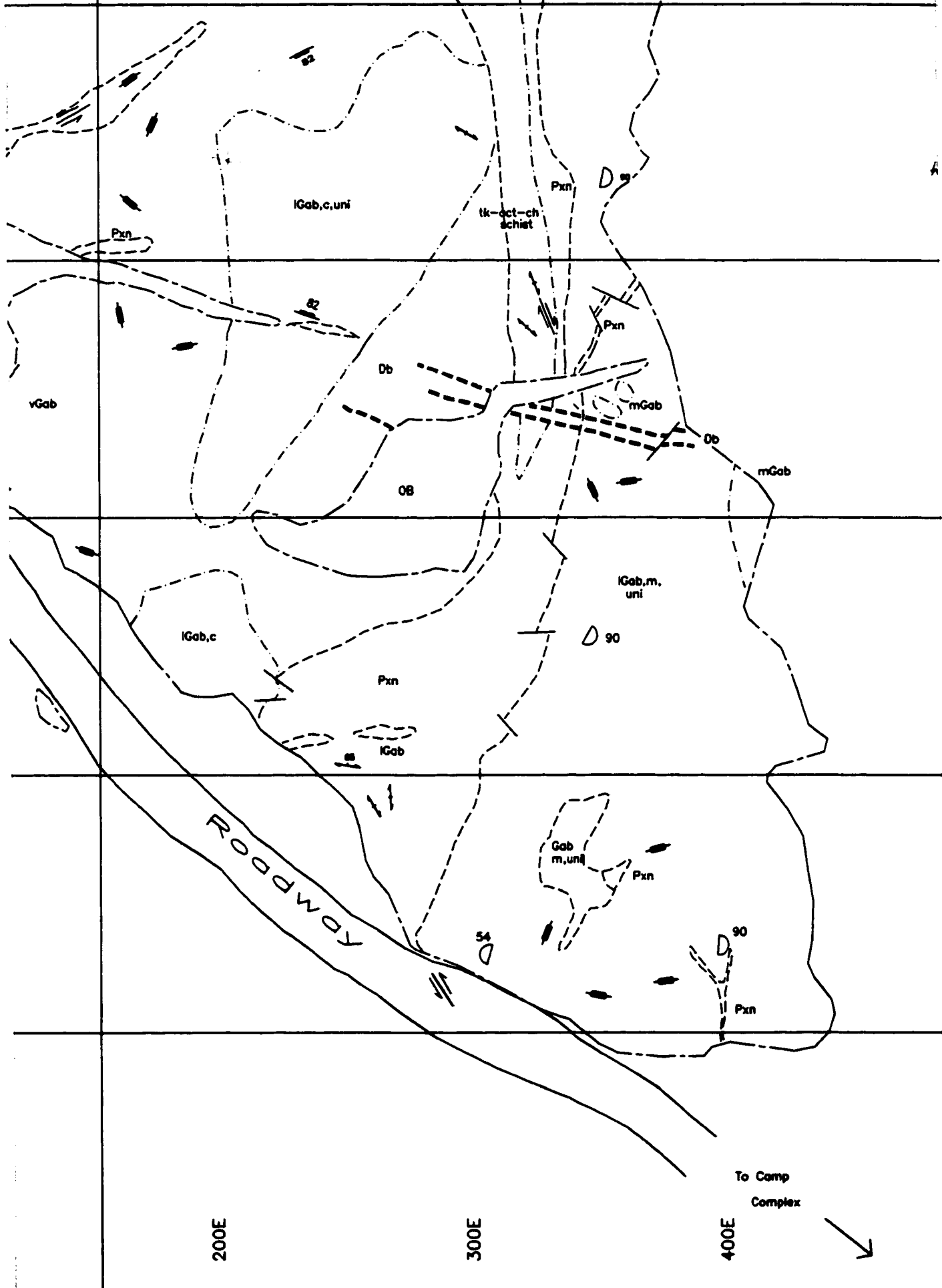
300W

200W

100W







51000N

A

50900N

mGob

50800N

50700N

90

Pxn

50600N

To Camp
Complex



500E

600E

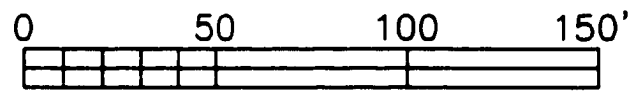
700E

ep	epidot
tk	talc
mag	magn
hem	hemat
ur	uralite
Pt	platinu
Pd	palladi
Au	gold
py	pyrite
cpy	chalcop
po	pyrrhot
pent	pentlan
mo	molybi
fel	feldspc

700E

SC
N.T

k	talc	fr	fractured
mag	magnetite	min	minor
em	hematite	mod	moderate
r	uralite	abn	abundant
t	platinum	alts	serpentinized
d	palladium	altc	chloritized
u	gold	alte	epidotized
y	pyrite	altt	talc altered
py	chalcopyrite	altu	uralized
p	pyrrhotite	alta	amphibolitized
ent	pentlandite	qv	quartz vein
io	molybdenite	act	actinolite
il	feldspar		



ROBY ZONE

Bedrock Geology Map

Theses
M.Sc.
1998
M63
C.1

SCALE: 1" = 50'	DRAWING NO: G92-2	DATE: MAR 7, 1994
N.T.S. 52 H/4 N.E.	DRAWN BY: M.M.	